ORE GENESIS OF GRANITE-RELATED Sn-W DEPOSIT IN TAGU AREA, MYEIK REGION, SOUTHERN MYANMAR

チョウ, トゥ, トゥン

https://doi.org/10.15017/4060151

出版情報：Kyushu University, 2019, 博士（工学）, 課程博士
バージョン：
権利関係：

ORE GENESIS OF GRANITE-RELATED Sn-W DEPOSIT IN TAGU AREA, MYEIK REGION, SOUTHERN MYANMAR

A dissertation submitted in partial fulfilment of the requirements

for the degree of

DOCTOR OF ENGINEERING

By

KYAW THU HTUN

Department of Earth Resources Engineering,

Kyushu University

January 2020

Fukuoka, Japan

This work is dedicated to my beloved parents,

U Khin Mya and Daw San Yee,

For a lifetime of love

With love and respect.....

ABSTRACT

Most granite-related tin-tungsten deposits in Myanmar are located in the Western Granitoid Province (WGP) of Southeast Asia. The majority of tin-tungsten deposits in Myanmar are situated in the Tanintharyi (Tennanserim Division) region, especially in the Dawei (Tavoy Township) and Myeik (Mergui Township) districts except the largest deposit at Mawchi (Kayah State). The mineralization style of the Tagu deposit in the Myeik district is vein type tin-tungsten deposit in both biotite granite and Carboniferous to Lower Permian metasedimentary rocks (Mergui Group). This dissertation describes the characteristics of tin-tungsten mineralization of the Tagu deposit on the basis of field observation, whole-rock geochemistry of granitic rocks, ore mineralogy and fluid inclusion study and discusses the origin of the ore-forming fluid as well as tectonic setting of the granitic magmatism in the Tagu area. This dissertation consists of the following six chapters.

Chapter I delivers location of the research area, history and previous works on the mine, objectives of this dissertation, methodology of research and expected outcome from this study.

Chapter II reviews the geologic background including tectonic evolution of Southeast Asia and Tethys Ocean and granitoid belts of Southeast Asia and Myanmar. Three granite belts of Southeast Asia represent one of the greatest metallogenic province of the world. Their metallogenic endowment is dominated by tin-tungsten, and the province is called as Southeast Asian Tin Belt. The three granite belts of Southeast Asia are Eastern Granite Province, Central Granite Province and Western Granite Province (WGP). The Central Granitoid Belt of Myanmar approximately corresponds to WGP of the Southeast Asian Granitoid Belt.

Chapter III describes the regional geology, deposit geology and nature of tin-tungsten mineralization of the Tagu area. The Mergui Group, which is variably deformed clastic sedimentary strata consisting mainly of pebbly mudstone (diamictite), pebbly sandstone and minor pyroclastic rocks, regionally metamorphosed to phyllites, argillites and quartzites, is widely distributed throughout the Tanintharyi region. The intrusive igneous rocks, very important for the tin-tungsten mineralization, are distributed in this region. Tin-tungsten mineralization was primarily associated with the intrusion of these granitoid rocks. The major mineralization style of the Tagu deposit is represented by cassiterite-wolframite bearing quartz veins that are hosted by the granitic rocks and metasedimentary rocks.

Chapter IV demonstrates the petrography and whole-rock geochemistry of the granitic rocks in Tagu deposit. The biotite granite of the Tagu deposit is composed of quartz, feldspars (plagioclase, orthoclase, and microcline), and micas (muscovite and biotite) and is classified as S-type and peraluminous characterized by the A/CNK [molar Al_2O_3/ ($CaO+Na_2O+K_2O$)] value ranging from 1.17 to 1.41. Enrichment in LILEs (Large Ion Lithophile Elements) such as Rb, K and Pb together with negative anomalies of HFSEs (High Field Strength Elements) such as Nb, P and Ti indicate that the magma was formed by partial melting of metasedimentary rocks.

Chapter V delivers the ore mineralogy and fluid inclusion studies of the Tagu deposit. In the mineralized veins, early-formed minerals are characterized by oxide ore minerals such as cassiterite and wolframite which were followed by the formation of sulfide minerals such as arsenopyrite, pyrite, chalcopyrite, molybdenite, pyrrhotite, sphalerite, galena and covellite in the later stage. Three main types of fluid inclusions were distinguished from the mineralized quartz veins hosted by granite and metasedimentary rocks: type-A—two phases, liquid + vapor liquid-rich aqueous inclusions; type-B—two phases, vapor + liquid vapor-rich inclusions; and type-C—three phases, aqueous liquid + CO_2-liquid + CO_2-vapor inclusions. The homogenization temperatures of type-A inclusions range from 140 °C to 330 °C (mode at 230 °C), with corresponding salinities from 1.1 wt.% to 8.9 wt.% NaCl equivalent for quartz veins hosted in metasedimentary rocks, and from 230 °C to 370 °C (mode at 280 °C), with corresponding salinities from 2.9 wt.% to 10.6 wt.% NaCl equivalents for quartz veins hosted in granite. The homogenization temperatures of type-B vapor-rich inclusions in quartz veins in granite range from 310 °C to 390 °C (mode at 350 °C), with corresponding salinities from 6.7 wt.% to 12.2 wt.% NaCl equivalent. The homogenization temperatures of type-C three-phase inclusions vary from 270 °C to 405 °C (mode at 330 °C), with corresponding salinities from 1.8 wt.% to 5.6 wt.% NaCl equivalent. The original ascending ore fluid was probably CO_2-bearing fluid which was evolved into two phase fluids by immiscibility due to pressure drop in the mineralization channels. Furthermore, the temperature and salinities of two-phase aqueous fluids were later most likely decreased by the mixing with meteoric water.

Chapter VI discusses the petrogenesis of granitic rocks, tectonic setting of the research area and mechanism of ore formation based on the study of fluid inclusions, and concludes that the granite-related Tagu tin-tungsten deposit was formed at a collision zone.

ACKNOWLEDGEMENTS

First and foremost, I would like to give my gratitude to the members of my dissertation committee, Professor Dr. Koichiro Watanabe, Professor Dr. Akira Imai, Associate Professor Dr. Kotaro Yonezu, Assistant Professor Dr. Thomas Tindell and Lecturer Dr. Aung Zaw Myint for their valuable annotations, comments, suggestions, advive, encouragement and support to complete my dissertation.

I would like to express my gratitude to the Japan International Cooperation Agency (JICA), Shigen No Kizuna Program, for the PhD scholarship and their financial support.

I would like to express my sincere grateful to Professor Dr. Koichiro Watanabe, Department of Earth Resources Engineering, Kyushu University in Japan for his kind helps, encouragement and support to carry out the research work and giving good advice and facilities in various ways.

I am deeply grateful to Professor Dr. Akira Imai, Department of Earth Resources Engineering, Kyushu University in Japan for his valuable annotations, suggestions, close supervision, and crucial reading repeatedly during the preparations of my thesis and manuscript.

My deepest gratitude goes to my supervisor to Associate Professor Dr. Kotaro Yonezu, Department of Earth Resources Engineering, Kyushu University in Japan to give me opportunity to travel around the world to get good experiences in geology industry and thanks for his guidance, kindly help, encouragement, support and critical reading during the preparation of this thesis.

I am deeply thankful to Assistant Professor Dr. Thomas Tindell, Department of Earth Resources Engineering, Kyushu University in Japan for his guidance, advice, suggestions, encouragement and critical reading during the preparation of this thesis.

My special thanks goes to Lecturer Dr. Aung Zaw Myint, Department of Geology, University of Yangon in Myanmar for his valuable suggestions, comments, annotations and crucial reading during the preparation of my manuscript.

I also express my appreciation to Professor Dr. Khin Zaw, CODES Centre of Ore Deposits and Earth Sciences, University of Tasmania, Australia for his valuable suggestions, advice and critical reading which had substantially improved the earlier versions of the manuscript.

I would like to give special thanks to Diamond Shark Co. Ltd for generously providing to work in mine site smoothly and safely.

My special thanks go to all of my friends and lab members from Economic Geology Laboratory, Department of Earth Resources Engineering for their helping hand assistances with analyses, sharing knowledge and encouragement during this PhD period.

Eventually, I would like to express my deepest thankful and gratitude to my parents and all members of my family for their encouragement and patience during away from them.

CONTENTS

LIST OF FIGURES

LIST OF TABLES

CHAPTER I: GENERAL INTRODUCTION

1.1 Location of the research area

The research area, Tagu mine is situated in Myeik, Tanintharyi Region, Southern Myanmar (Figure 1.1). The Tagu mine is the one of the largest Sn-W mines in the Myeik area, located in the southeast of the Myeik Township, situated about 59 km southeast of Myeik. It lies between latitude 12° 13′ to 12° 15 ′ 30 ′′ N and longitude between 98° 58 ′ to 99 ° E.

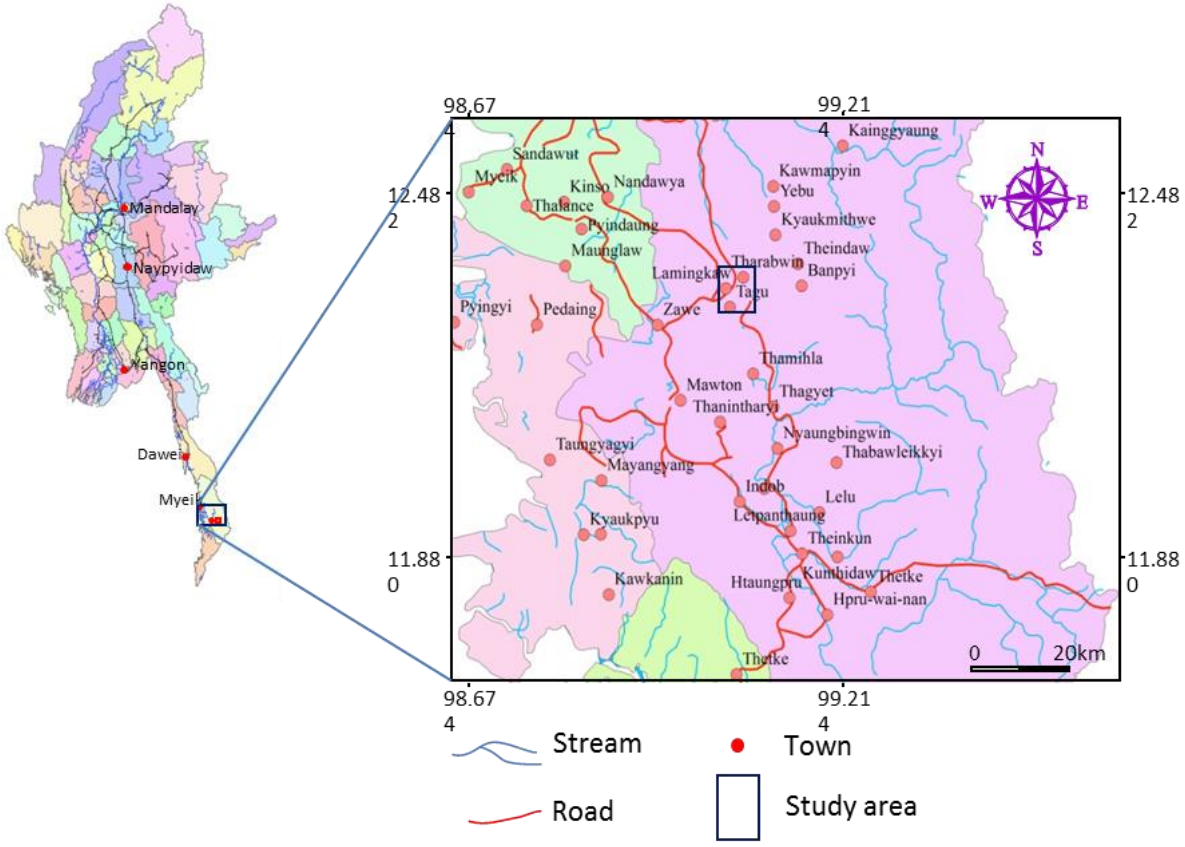

Figure 1.1. Location map of research area (after Htun Linn, 2013).

1.2 History and previous works at the mine

According to the report of Geological Surveys of India (GSI) (Clegg, 1944), ore explorations began in the 1st Century. At the end of 1838, geologists surveyed this area for

mineral exploration. In 1904, Thai and Chinese geologists conducted ore exploration. From 1956 to 1964, U War and local people explored the area for their domestic exploration. After 1984, Mining Enterprise (2) explored for domestic industry exploration. In September 2008, 24 Hour Services Co. Ltd. made geological observation for the appropriate area of Diamond Sharp Mining Co. Ltd. at Inn-Shi-Kon area of Tagu Taung. Diamond Sharp Mining Co. Ltd. is currently operating for production of tin-tungsten ore in this area. Previous work related to the study area are reviewed below;

- Granite related tin-tungsten deposits, hosted by the metasedimentary rocks of Mergui Group, in Myeik district, Southern Myanmar were described by Chhibber (1934).
- The tin and tungsten belt in Tanintharyi Region of south Burma was expressed by Clegg (1944).
- In 1966, Tin Aye and Kyaw Nyein (1966) reviewed the history of the tin and tungsten mining industry in Burma.
- In 1980-1982, Department of Geological Survey and Mineral Exploration (DGSE) surveyed the regional geological mapping and mineral exploration, Aung Gyi and other geologists made detailed a geological survey and extrapolated tonnage of tin-tungsten deposits around Tagu Taung area in August, 1984.

1.3 Objectives of dissertation

The research attempts to constrain the geological, mineralogical and geochemical conditions of tin-tungsten deposit at Tagu mine, Myeik, Tanintharyi Region, Myanmar. The main objectives are as follows;

- To improve the geological understanding of the tin-tungsten mineralization in the Tagu area.
- To document the style and genetic aspects of tin-tungsten mineralization, characteristics of the mineralizing fluids in terms of fluid source and precipitation mechanisms.
- To understand the relationship of the mineralization to the regional geology and tectonic setting.
- To make systematic mineralogical, geochemical and petrographical studies on mineralized zone and host rocks.
- To compare the nature of the deposits in Myanmar and throughout the world.

The ultimate aim of the research is to develop an ore deposit model, and to establish exploration criteria for vein type tin-tungsten deposits.

1.4 Methodology

1.4.1 Field work and sample collection

Geological field work was conducted in October 2016, April-May 2017, May-June 2018 and October-November 2018. In this thesis, most of the data were collected during these four field works. Rock samples and geological data were collected during the field works to make a detailed geological map, to investigate the structural and lithological controls on tin-tungsten mineralization and to collect the systematic samples from the surface and subsurface outcrops for geochemical analyses, and mineralogical studies to fulfill the objectives mentioned above.

1.4.2 Laboratory works

In the laboratory work, mineralogical analysis, petrographic study, ore microscopy, fluid inclusion studies and XRF (X-ray fluorescence spectroscopy) are the main experimental analysis employed in this research. Polished sections were analyzed for ore mineralogy using a scanning electron microscope (SEM) with energy-dispersive X-ray spectroscopy (EDS) of HITACHI-SU3500 at the Center of Advanced Instrumental Analysis, Kyushu University, to provide quantitative and semi-quantitative compositional information.

Petrographic analyses were carried out on thin sections and polished sections using transmitted and reflected light optical microscopes. For polished sections of ore and gangue minerals from the Tagu tin-tungsten deposit, 35 ore samples were selected to investigate for transmitted and reflected light petrographic and mineralogical properties with a NIKON ECLIPSE LV100N POL petrographic microscope to establish mineral paragenesis and textural relationship of ore minerals. In addition, diagnostic hydrothermal minerals are recognized which typically occur in the alteration zone.

For mineralogical analyses, over 95 samples were selected and a total of 30 samples of granitic rocks were collected from the Tagu area for geochemical studies. Representative 10 samples of granitic rocks selected for whole-rock geochemistry were prepared by crushing to small pieces with a hammer and then by powdering to 200-mesh using an alumina disk mill. Loss on ignition (LOI) was determined by heating the samples at 1000 ^{o}C for 2 h to determine relative weight loss. The sample pellets XRF analysis were prepared by pressing at 20t about 2 minutes in a vinyl chloride ring. The measurement conditions of analysis were 30kV and 70mA and the standard JA-3 andesite (Imai et al., 1995) was used

to monitor the precision, yielding an error of less than ± 5%. The concentration of major and minor elements of 10 fresh granitic rocks was determined by X-ray fluorescence (XRF) analysis using a RIGAKU RIX-3100 manufactured by Rigaku Corporation, at the Department of Earth Resources Engineering, Kyushu University.

The concentration of trace elements and rare earth elements (REE) of the samples collected from the ore zones, granitic rocks and host rocks were determined by Inductively Coupled Plasma-Mass Spectrometer (ICP-MS) at the Center of Advanced Instrument Analysis, Kyushu University, Japan. The 0.1 gram of bulk samples were emplaced in Teflon tubes and 1 ml of pure water was added with 5 ml HF (46-48% mass/mass) and 0.5 ml $HClO_4$ (60-62)%. The solution was heated once more at 120^{o}C for 320 minutes until it dried and then, it was diluted by 0.1 M HNO_3 in measuring flask up to 50 ml in total. Subsequently, solution was filtrated by 0.45 μm membrane filter. Dilution rate is 5000 and added 5 ppb indium as an internal standard. Eventually, solution was examined by ICP-MS.

For fluid inclusion studies, doubly polished thin sections were prepared from the 7 mineralized quartz samples to figure out the ore forming mechanism of tin-tungsten mineralization of Tagu area. Fluid inclusion microthermometry on doubly polished sections was conducted at the Department of Earth Resources Engineering, Kyushu University, Japan. Microthermometric analyses were carried out using a Linkam LK600 heating–freezing stage with a Nikon Y-IM microscope. The errors for the temperature of measurements are ±0.5, ±0.2 and ±2.0^{o}C for runs in the range of -120 to -70^{o}C, -70 to 100^{o}C, and 100 to 600^{o}C, respectively. The final ice-melting temperatures were measured at the heating rate of less than 0.1^{o}C/min and the homogenization temperatures at the rate of ≤1^{o}C/min.

Total salinities for NaCl-H_2O fluid inclusions were calculated from the final ice melting temperatures by using the equation of wt% NaCl= 1.78 T - 0.0442 T_2 + 0.000557 T_3 where T is depression temperature in ^oC (Bodnar 1993), and are expressed as wt. % NaCl equivalent. The salinities of the CO_2–H_2O inclusions were calculated from the melting temperature of clathrate using the equation wt% NaCl= 15.52022 – 1.02342T – 0.05286T_2 where T is the clathrate melting temperature expressed in ^oC (Bozzo et al., 1973; Collins, 1979).

1.5 Expected Outcome

This study will establish the source of magma of granitoids and their corresponding tectonic setting and mechanism of ore formation. Geochemical characteristics of I- and S-type granites (illmenite series and magnetite series) of the Central Granitoid Belt of Myanmar will be differentiated. The REE content of these rocks will be determined and the REE mineralization potential of this belt will be established.

In mining activities, lack of understanding of geology of ore deposits sometimes will cause heavy losses amounting to millions of dollars. In this regard, this research project will prevent these losses by using all the geological data related to tin-tungsten deposits. As there is a higher demand for tin and tungsten in this century, this research can bring new geological context to tin-tungsten mineralization in Myanmar for future exploration.

This research will also help design a regional strategy for tin-tungsten mineral exploration and add a new interpretation and solid geological, mineralogical and geochemical knowledge of the deposits, petrogenesis and their ore forming mechanisms based on geochemical and fluid inclusion studies to the scientific community in Myanmar.

In addition, it will provide new data or ideas with reference to the ore forming processes that will attract and enhance mineral exploration in the Central Granitoid Belt of Myanmar corresponding to Western Granite Province of Southeast Asia.

CHAPTER II: REGIOINAL GEOLOGIC SETTING

2.1 Geological background

Myanmar is endowed with gemstones and ore deposits of tin, tungsten, copper, gold, zinc, lead, nickel and silver. It has one of the most diverse natural and mineral resources in Southeast Asia, largely reflecting its geological history (Khin Zaw, 2017). There are at least three world class deposits including Bawdwin (lead–zinc–silver), Monywa (copper) and Mawchi (tin–tungsten). Myanmar can be divided into four principal metallogenic provinces from west to east (Figure 2.1): the Indo-Myanmar Ranges; the Wuntho-Popa Arc, comprising subduction-related granites with associated porphyry-type copper-gold and epithermal gold mineralization including the Monywa deposit, the Mogok-Mandalay-Mergui Belt hosting both significant tin–tungsten mineralization associated with crustal melt granites including the Mawchi deposit, and major orogenic gold resources; and the Shan Plateau with massive sulfide-type lead–zinc deposits including the Bawdwin deposit (e.g., Gardiner et al., 2014 and 2016a).

In the far west, the Indo-Myanmar Ranges comprise Triassic–Eocene flyschoid sedimentary rocks and obducted ophiolites which contain chromite, nickel, PGE and precious metals, and have potential for discovery of Cyprus-type Cu (Au) deposits outcropping both within the Mount Victoria Belt and elsewhere (Khin Zaw, 2017; Brunnschweiler, 1966; Mitchell, 1993). West of the Indo-Myanmar Ranges lies the effective margin of Asian continent (Ghose et al., 2014; Mitchell, 1993; Mitchell et al., 2012).

The 500 km-long arcuate N-S Central Volcanic Belt formed as a magmatic–volcanic arc of Late Cretaceous–Tertiary age defines the Wuntho-Popa Arc (WPA) and hosts the

Monywa high sulphidation Cu–(Au) deposit (Mitchell et al. 2011; Khin Zaw et al. 2017), the Shangalon porphyry Cu–Au–Mo deposits (Hammarstrom et al. 2013; Khin Zaw et al. 2017) and a variety of epithermal- to mesothermal-style gold–silver veins (e.g. the Kyaukpahto deposit). The WPA is a continental magmatic arc (Mitchell and McKerrow, 1975; United Nations Development Programme (UNDP), 1978), and comprises major Cretaceous-Eocene granodiorite intrusions with associated volcanic rocks, and middle Miocene rhyolites and dacites, principally outcropping in Mount Popa and outliers to the south (Barley et al., 2003; Khin Zaw, 1990; Mitchell andMcKerrow, 1975; Mitchell et al., 2012).

The Mogok-Mandalay-Mergui Belt (MMMB) comprises the Slate Belt and the Mogok Metamorphic Belt. The Slate Belt, running broadly north-south from Mandalay towards Myeik (Mergui), is dominated by Carboniferous to early Permian interbedded slaty mudstone and pebbly wacke, with rare quartzite and calcareous beds (Mitchell et al., 2012). The Mogok area is known for its famous gemstone tract and lies within a series of undifferentiated high-grade metamorphic rocks; the dominant unit is banded gneiss with biotite, garnet, sillimanite and oligoclase and is interspersed with quartzite and bands and lenses of marble (Khin Zaw et al. 2014; Kyaw Thu and Khin Zaw 2017). Low-grade metamorphism is locally recognised in biotite schist at Yesin Dam near Tatkon, and also north of Mandalay. Both hornblende and biotite I-type and two-mica, sporadic tourmaline-hosting S-type crustal melt granite punctuate the MMMB. The S-type granites, where hosted by the Slate Belt, are associated with significant tin-tungsten mineralization such as Mawchi (tin–tungsten), Hermyingyi (tin-tungsten), Yadanabon (tin-tungsten) and Tagu mine (tin-tungsten) (Aung Zaw Myint et al., 2018; Brown and Heron, 1923; Khin Zaw, 1990;

Gardiner et al., 2014, 2016a). Extensive, unrelated, orogenic-type gold deposits also occur within the Slate Belt (Mitchell et al., 1999), making this a highly prospective unit.

The Shan Plateau in eastern Myanmar, consists of Cambrian-Ordovician sedimentary sequences with localized Ordovician volcanic rocks and volcaniclastics (Aye Ko Aung, 2012), unconformably overlain by thick Middle-Upper Permian limestone sequences. These latter sequences may represent the protolith carbonates of the high-grade Mogok marbles. The boundary between the MMMB and the Shan Plateau sequences is marked by the Shan Scarps and the Paung Laung-Mawchi Fault Zone (Garson et al., 1976). The Shan Plateau is a component of the Sibumasu microplate, containing significant base-metal mineralization. The richest base metal mineralization in the Eastern Shan Highlands was the largest polymetallic VHMS deposit mined in the world before War World II (the Bawdwin Mine) (Khin Zaw, 2017).

Myanmar has more than 120 Sn–W occurrences, including the world-class Sn–W deposits of the Hermyingyi Mine (the largest tungsten–tin vein system mined before World War I) and the Mawchi Mine (the largest tungsten–tin vein system mined before World War II) (Khin Zaw, 2017). Tin-tungsten mineralization in Myanmar is found as cassiterite and wolframite bearing pegmatites and greisen-bordered quartz veins. These are hosted both by the granites, and also by country rocks of the Slate Belt (Aung Zaw Myint et al., 2018). The majority of tin-tungsten deposits are situated in the Tanintharyi (Tennanserim) region, especially in the Dawei (Tavoy) and Myeik (Mergui) districts except for the largest deposit at Mawchi (Kayah State). The Dawei district has the largest and more important tin–tungsten mines, whereas more tin-rich tin–tungsten mines, tin mines and alluvial tin deposits occur in the Myeik district (Figure. 2.2 and Table 2.1) (Than Htun et al., 2017).

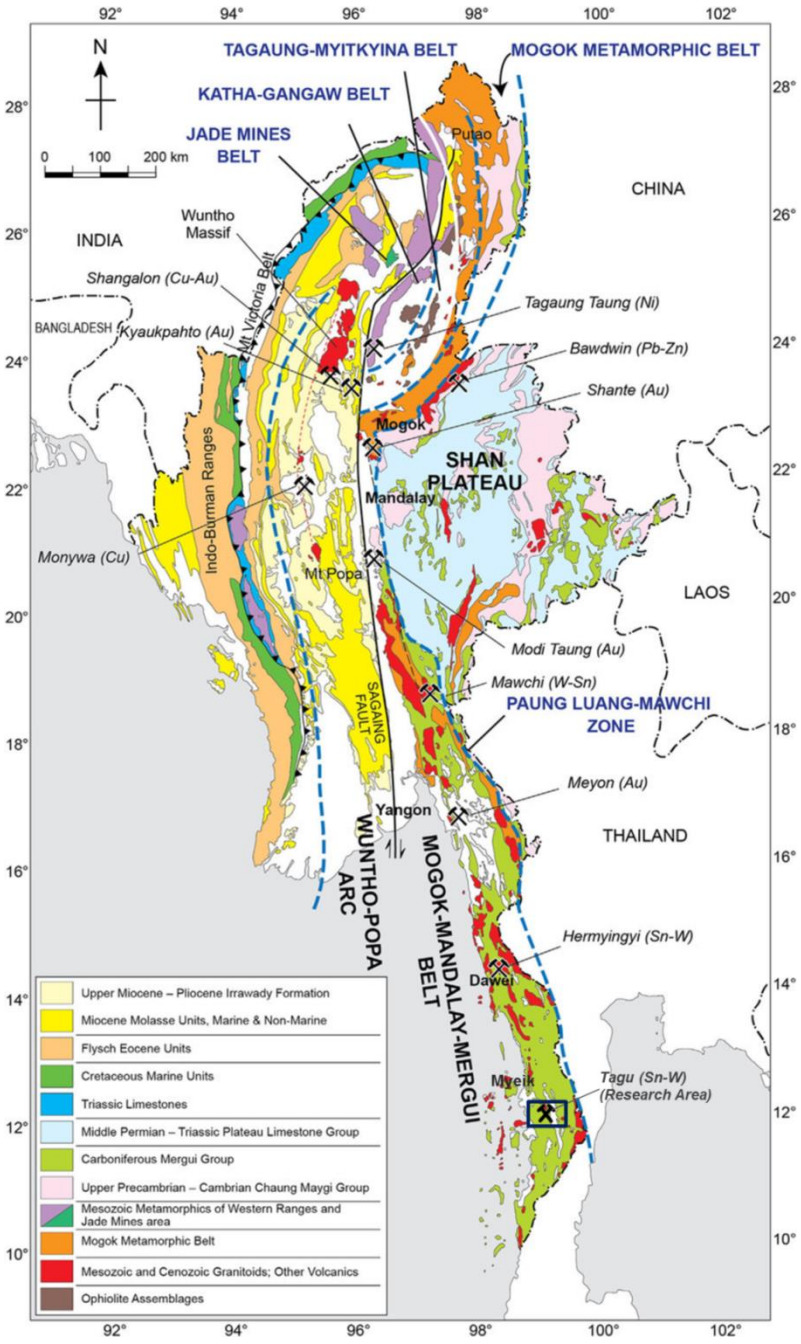

Figure 2.1 Main metallogenic provinces of Myanmar (Myanmar Geosciences Society (MGS), 2013; Gardiner et al., 2014)

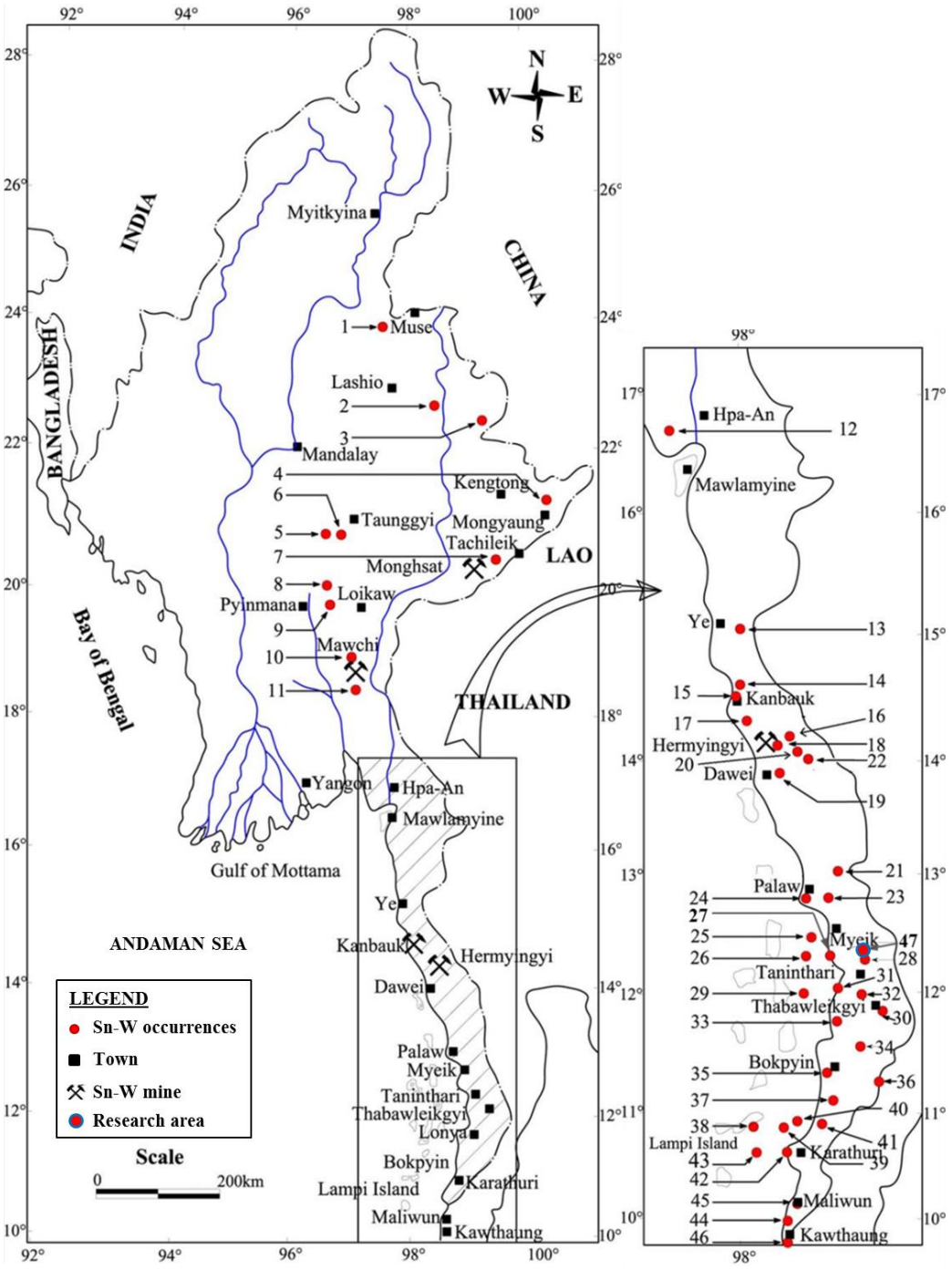

Figure 2.2. Tin–tungsten occurrences in Myanmar (after Tin Aye and Kyaw Nyein 1966; Ye Myint Swe (pers. comm. 2012); Than Htun et al., 2017; Kyaw Thu Htun et al., 2019. 1, Nam Kham; 2, Pansan–Pankhan; 3, Walinkhunmar; 4, Wan Pon; 5, Chaungnibauk; 6, Palamaw; 7, Mong Hsat; 8, Peinnedaik; 9, Myinmati; 10, Mawchi; 11, Mawday; 12, Natkyigyaung;

13, Natkyizin; 14, Ohnbinkwin; 15, Kanbauk; 16, Widnes; 17, Pha Chaung; 18, Hermyingyi; 19, Pagaye; 20, Mwehauk Chaung; 21, Nanthila; 22, Phachaung; 23, Thanbaya Chaung; 24, Palaw; 25, Yemyintkyi; 26, Yamon-kazat; 27, Zegami; 28, Gahan; 29, Dongyi; 30, Thabawleik; 31, Kadebyin; 32, Zalun; 33, Khe Chaung; 34, Yengan; 35, Bokpyin; 36, Yadanabon; 37, Kyaukhtanaung; 38, Lampi Island; 39, Harkapru; 40, Kyaukpan Chaung; 41, Chaungnagpi; 42, Karathuri; 43, Palau Bada; 44, Chockling; 45, Maliwun; 46, Pakchan River; 47, Tagu.

Table 2.1 Details of the major tin–tungsten-producing mines in Myanmar;

Source: Tin Aye & Kyaw Nyein (1966), Than Htun (2017), Kyaw Thu Htun et al., 2019.

No. in Figure 2.2	Name	Township, region, state	Latitude (N)/ longitude (E)	Metal	Deposit type	Brief geological description	Ore reserve (metric tonne)	Remarks
3	Man Maw Mining District	Wa region, northen Shan State	22° 55′, 99°	Sn	Veins, stockworks and alluvial			Current production 10 000–20 000 ore t/year
10	Mawchi	Pasawng, Kayah	18° 45′, 97° 10′	Sn–W	Veins and stockworks	En echelon quartz veins and stockworks in both tourmalinized biotite granite and Mawchi Formation metasediments	102,022	A world-class deposit in the pre-war period
20	Heinda	Dawei, Tanintharyi	14° 7′ 98° 27′	Sn	Fossil placer	Uplifted fossilized placer deposit with large granite boulders and gravels	12,464	Largest tin placer deposit
18	Hermyingyi	Dawei, Tanintharyi	14° 15′ 98° 35′	Sn–W	Veins and stockworks	En echelon quartz veins stockworks in biotite granite and Mergui metasediments	2,636	One of the major tin–tungsten mines; in 1917 it produced 1051 long tons
19	Pagaye	Dawei, Tanintharyi	14° 6′ 98° 19′	Sn–W	Stockwork pegmatite and quartz veins	Stockwork quartz veins and pegmatites in biotite granite	6,050	One of the major W-producing mines
15	Kanbauk	Yebyu, Tanintharyi	14° 35′ 98° 3′	Sn, Sn–W	Alluvial flats and quartz veins	Alluvial tin placers and quartz veins in granite at Home Hill	1,323	Major tin–tungsten producer
30	Thabawleik	Myeik, Tanintharyi	12° 1′ 99° 12′	Sn	Alluvial flats	A huge alluvial tin deposit underlain by Mergui Group metasediments; no granite outcrop	160	Alluvial mining by dredgers in the past
16	Widnes (Wazun-chaung)	Dawei, Tanintharyi	14° 3′ 98° 28′	Sn–W	Quartz veins	Sn–W-bearing quartz veins in both granite and argillites of Mergui Group	927	One of the big W-producing mines in pre-war days
22	Paungdaw	Dawei, Tanintharyi	14° 2′ 98° 33′	Sn–W	Quartz veins	Parallel veins containing wolframite, cassiterite, sulphides and fluorite	90	Major tungsten mine
36	Yadanabon (Namyen)	Bokpyin, Tanintharyi	11° 17′ 05″ 99° 17′	Sn–W	Quartz veins eluvial and alluvial deposits	Sn–W-bearing quartz-sulphide veins and eluvial deposits in weathered granite and also Sn alluvial deposits	43	Sn–W mine developed in postwar period close to Thai–Myanmar border
21	Nanthilar (Muntet)	Palaw, Tanintharyi	13° 22′ 40″ 98° 41′ 30″	Sn	Cassiterite-sulphidequartz vein (lode type) deposit	Single large quartz lode carrying cassiterite and base metal sulphides in slates and quartzites of Mergui Group	233	Tin lode underground mine
47	Tagu (Lathar Taung)	Myeik, Tanintharyi	12° 14′ 05″, 98° 59′54″	Sn-W	Quartz veins	Quartz veins in both pophyritic biotite granite and metasedimentary rocks (Mergui Group)	2,157	One of the largest Sn-W deposits in Myeik area.

2.2 Tectonic evolution

Mainland Southeast Asia is endowed with a diversity of mineral resources and consists of a collage of continental blocks or fragments, together with accreted volcanic arcs and backarc basins. Major fragments, such as Indochina, Sibumasu and West Myanmar terranes, rifted away from the northwestern Gondwana margin at different periods in the Phanerozoic, and led to the opening of the Palaeo-, Meso- and Neotethyan (or Cenotethys) Oceans (Metcalfe, 2011, 2012 and 2013) and drifted north to progressively assemble during the Late Paleozoic to Cenozoic (Metcalfe, 2011 and 2013; Barber and Crow, 2003). Following the separation of the South China Block and Indochina Block from Gondwana (Figure 2.3), the Paleothethys Ocean opened in the Middle Devonian, in response to a period of Early Devonian rifting on the NE margin of Gondwana (Metcalfe, 2011 and 2013).

Southeast Asia is geographically located south and south-west of China, east of India, and north of Australia (Figure 2.3). It lies on the intersection of the Eurasian, Indian-Australian and Philippine Sea plates, and is located in the easternmost segment of the Tethyan tectonic domain and much of the region can now be regarded as part of the Eurassian Plate (Metcalfe, 2011; Simons et al., 2007). It consists of a collage of continental blocks or fragments, together with accreted volcanic arcs and back-arc basins and suture zones that have recorded a long-term convergence history between multiple tectonic domains induced by subduction (Figure. 1.2). The long and complex tectonic evolutionary history, diversity of plutonic magmatism, volcanic eruption, and a wealth of mineral deposits are developed in Southeast Asia (Hall and Spakman, 2015; Khin Zaw et al., 2014; Metcalfe, 2011), in particular the tin-tungsten deposits occurring in this area constitute one of the most important tin-tungsten metallogenic belts in the world (Schwartz et al., 1995).

The continental rifting and subsequent development of Paleotethys Ocean Basin led to the formation of sediment-hosted/orogenic gold deposits in Peninsular Malaysia (Makoundi et al., 2014; Khin Zaw et al, 2014). The Sibumasu Block was rifted from Gondwana in the Early Permian and collided with the Indochina Block by the Late Triassic (Metcalfe, 2013). Continuous subduction of the Paleotethys beneath the Indochina Block resulted in the Indosinian orogeny in SE Asia during the Triassic and Jurassic, which in turn closed the Paleotethys Ocean (Metcalfe, 2011 and 2013; Sengör, 1987). Many sediment-hosted/orogenic gold deposits formed throughout this period along or adjacent to major suture zones (Khin Zaw et al., 2014).

Myanmar has been affected by at least two major Tethyan plate collisions related to the closure of the Palaeo-Tethys and the Neo-Tethys oceans, represented by the Triassic-Early Jurassic Indosinian and Cenozoic Himalayan orogenies, respectively, resulting in several major Tethyan-related metamorphic belts extending from the Eastern Syntaxis southwards across Myanmar, and which may be correlated with those lying further west along the main India-Asia collision zone (Searle et al., 2016).

The Mesozoic-Recent geology of Southeast Asia is dominated by the accretion of several continental micro-plates and island arc terranes that were rifted from Gondwana, migrated and eventually sutured onto the South China Craton (Figure 2.3) (reviews in Hall, 2012, and Metcalfe, 2013). The Late Triassic closure of Palaeo-Tethys and the collision of Sibumasu with the mainland (Asia) Indochina terrane resulted in the Indosinian Orogeny. During the collision between Sibumasu and the Sukhothai Arc and Indochina, Sibumasu continental crust (Figure 2.3) was thickened and melted to produce voluminous S-type granites of mainly Late Triassic (but also including minor earliest Jurassic) age (Searle et al.,

2012; Ng et al., 2015). The Palaeo-Tethyan suture zone is interpreted to lie in a north-south band cutting through Yunnan, eastern Myanmar, central-western Thailand and the central Malay Peninsula (Barr and Macdonald, 1991; Gardiner et al., 2015a; Metcalfe, 2000 and 2002; Mitchell, 1977; Ng et al., 2015; Sone and Metcalfe, 2008; Zi et al., 2012). This suture zone forms the boundary between two major north-south Mesozoic-age granite provinces that run across much of Southeast Asia (Cobbing et al., 1986).

The Meso-Tethys was a wide ocean basin and the collision between Sibumasu and the Sukhothai Arc and Indochina initiated northwards subduction of Meso-Tethys beneath Sibumasu (Figure 2.3) (Searle et al., 2012; Metcalfe, 2013; Ng et al., 2015). Southward subduction of Meso-Tethys beneath SE Pangea initiated rifting of the India-Australia Pangea margin and led to separation of the Lhasa, East Java-West Sulawesi and SW Borneo blocks from Gondwana and opening of the Ceno- Tethys ocean in the Jurassic, and their accretion to Sundaland and mainland Asia by the Late Cretaceous (Figure 2.3) (Metcalfe., 2017).

The Neotethys Ocean opened in the Mid-Late Permian as a result of rifting of the Cimmerian Continental fragments from Gondwana (Figure 2.3) (Hou and Zhang, 2015). The West Myanmar Block and other small continental fragments now located in SW Sumatra were developed within the Neotethys Ocean Basin during the Late Triassic to Late Jurassic (Metcalfe, 2011 and 2013). The northward shift of the Lhasa Block and West Myanmar Block (Figure 2.3) led to the formation of some branches of the Neotethys Ocean, as represented by the eastern ophiolite belt in northern Myanmar (Liu et al., 2016). The early Eocene closure of the Neo-Tethys resulted in the collision of the Indian Plate with Asia along the main convergent margin, and the subsequent onset of the Himalayan Orogeny.

The amalgamation of the West Myanmar Block with the Subumasu Block to form the Shan Boundary Suture in Myanmar and the Woyla Suture in Indonesia took place during the Jurassic and Early Cretaceous (Figure 2.3) (Metcalfe, 2011 and 2013; Morley, 2012). Subduction of the Neotethys Ocean Plate beneath the Cimmerian Continent not only led to the formation of typical subduction-related porphyry copper-gold deposits in western Myanmar (Gardiner et al., 2015b), but also accounted for the formation of many magmatic-hydrothermal W-Sn deposits in the central and southern part of Myanmar (Jiang et al., 2017; Gardiner et al., 2015b; Khin Zaw et al., 2014). The collision of Arabian and Indian Continents with the Eurasian Continent led to the closure of the main branch of the Neotethys Ocean during the Late Cretaceous to Paleogene (Hou and Zhang, 2015). The Neogene epithermal deposits in central Myanmar and northwestern Sumatra formed as a result of the oblique subduction of the Sunda Trench (Figure 2.3) (Khin Zaw et al., 2014).

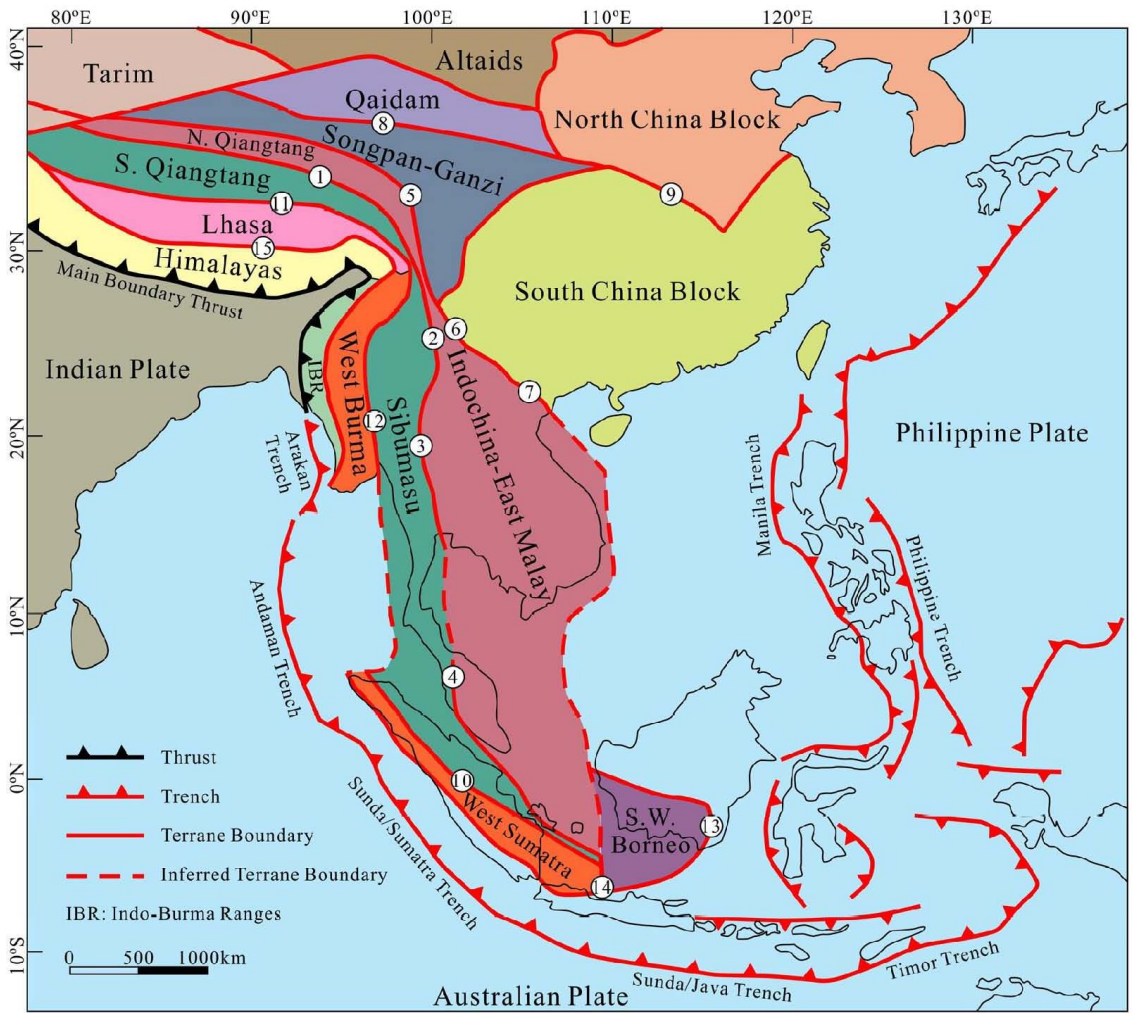

Figure 2.3 Distribution of principal continental blocks and sutures of Southeast Asia and adjacent regions (after Liu et al., 2018; Liu et al., 2016; Hou and Zhang, 2015; Metcalfe, 2013). Paleo-Tethyan sutures: 1: Longmucuo-Shuanghu, 2: Changning-Menglian, 3: Chiang Mai/Inthanon, 4: Bentong-Raub, 5: Jinshajiang, 6: Ailaoshan, 7: Song Ma, 8: Kunlun, 9: Qinling-Dabie, 10: Median Sumatr. Meso-Tethyan sutures, 11: Bangonghu-Nujiang, 12: Shan Boundary, 13: Meratus, 14: Lok Ulo. Neo-Tethyan sutures and 15: Indus Yarlung-Zangbo.

2.3 Granitoid belts of Southeast Asia

The Southeast Asia Granitoid Belt is a north-south elongate zone of 2800 km length and 400 km width, extending from Burma (Myanmar) and Thailand, to Peninsular Malaysia and the Indonesian Tin Islands. Altogether 9.6 million tonnes of tin, equivalent to 54% of the world tin production have been derived from this region (Schwartz et al., 1995). Firstly, the granites of Southeast Asia were classified by Hutchison (1973) into three fold division as Eastern, Central and Western Belts. The term Central Belt is replaced by Main Range Belt (Hutchison, 1977 and 1978) and Central Belt is used for a subdivision of the Eastern Belt. In that study, granites from northern Thailand was defined as "other granites". Mitchell (1977) grouped these granites of north Thailand with the tin granites of Peninsular Thailand and Malaysia as the Central Belt.

Cobbing et al. (1986 and 1992) followed the most of the features of Hutchison's classification but they used the term "Province" instead of "Belt". Cobbing et al. (1986 and 1992) supposed that the granite occurrences did not conform to geographical belts and consequentially replaced the term Eastern Province, Main Range Province, Western Province for Eastern Belt, Main Range Belt, and Western Belt, respectively. They used the term North Thai Province for the "other granites" of Hutchison (1977 and 1978) and introduced the Central Valley Terrain of Myanmar. The granite subdivision of Hutchison (1978 and 1983) is more detailed than those of made by others but the classification of Cobbing et al. (1992) is more simplified than Hutchison (1978; 1983). As such, Cobbing et al. (1992) is used for the classification of Southeast Asia Granitoids.

The Eastern Province Terrain can be supposed as Cathaysian affinity (Metcalfe, 1988), emerging from the Tin Islands of Indonesia northwards through Peninsular Malaysia and Thailand to the north of Thailand and continues eventually into the Yunnan Province of China. At the Tin Islands of Indonesia these granitoids are geographically intermingled with S-type plutons similar to those of the Main Range Province.

In Thailand this province is bounded by the Khotat Plateau to the east and Indochina massif to the west. The break between terrains of Lower Paleozoic and Upper Paleozioc to Mesozoic age is characterized by the occurrences of sporadic ultrabasic bodies along the Bentong-Raub Line (Hutchison, 1975 and 1977). However, this line is not defined in northern Thailand and the Tin Islands of Indonesia. Along the Nan-Uttaradit Line, this situation is particularly anomalous and is characterized by ultramafic bodies and glucophane schists (Barr et al., 1985) and it forms a major suture which is flanked by Permo-Triassic volcanic rocks and typical Eastern Province granitoids.

In Peninsular Malaysia along the boundary between the Eastern Province terrain and Main Range terrain, Na-rich granitoids and metamorphic rocks are supposed to belong to Central Belt (Hutchison, 1977, 1983 and 2007). This terrain is mainly composed of Carboniferous and Permian shelf strata and Triassic flysch with locally very low grade regional metamorphic rocks and volcanic rocks. The age of these granitoids varies from Permian to Triassic (Bignell and Snelling, 1977; Beckinsale, 1979; Liew, 1983). Later granitic rocks of Cretaceous age are also present within the Easterm Province. I-type granitoids with gabbroic to monzogranitic composition are predominant. Biotite granite and biotite-hornblende granite are common rock types of this province. Base metals with some gold and uranium occurrences are principal mineralization of the Eastern Province and they

are located in or within the periphery of certain plutons. Alluvial Tin deposits and cassiterite-magnetite skarn deposits also occurred.

Main Range and North Thai Province Terrain is paleontologically of Gondwana land affinity (Metcalfe, 1988) and it stretches from the eastern part of South Sumatra and the Tin Islands northwards through Peninsular Malaysia and Thailand to the easternmost part of Myanmar and Yunnan Province of China. It is bounded to the east by the Bentung-Raub Line and, to the west by the Khlong Maru (Ban Kham) Fault and the Three Pagodas Fault. This terrain consists of Lower Paleozoic sedimentary rocks and metasedimentary rocks.

In northern Thailand the geology is complicated by the presence of nappe structures. The majority of the granitoids of the Main Range Province are concentrated in the Main Range Batholith of Peninsular Malaysia. These Triassic age granitoids (Bignell and Snelling, 1977; Beckinsale, 1979; Liew, 1983) extend northwards through Peninsular Thailand as discontinuous intrusive bodies and southwards through the Tin Island as geographic overlapping terrain with the granitoids of the Eastern Province. The Main Range Batholith is composed of biotite granite and biotite-muscovite granite which have xenoliths of metasedimentary origin.

The plutons in the Main Range Province are generally undeformed apart from cataclasis clearly related to fault zones. They are unmineralized but cassiterite bearing endogenous greisen-bordered quartz veins or tourmaline quartz veins and massive greisens and pegmatites of disseminated ore are accompanied. North Thai Province is geographically continuous with the Main Range Province. Its southern limit is poorly defined and the Phanerozoic which envelops the granitoids consists of Cambrian to Permian sedimentary

rocks and low grade metasedimentary rocks. The central part comprises foliated granites and metasedimentary rocks (Chakkaphak and Veeraburus, 1982).

The granites of the North Thai Province are distinguished from those of the Main Range Province by their greater textural and compositional uniformity. They have higher biotite content, equant shaped K-feldspar megacrysts and blue-gray colour. They have usually monzogranitic composition but vary from syenogranitic to grandioritic. They are of Permo-Triassic age (Teggin, 1975) and all have field characteristics of S-type granites (Pitcher, 1983). A number of relatively small tin deposits are associated with the coarse megacrystic granite batholiths. Scheelite deposits are found as either replacements at granite-limestone contacts or endogenous.

The Western Province Terrain lies to the west of the Ban Kram and Three Pagodas Faults. It occupies most of the Thai-Myanmar Peninsula north of Phuket and probably forms much of Tanintharyi and westernmost part of the Shan Plateau in Myanmar. It stretches southward into Sumatra and forms a large part of that island. This terrain is principally characterized by pebbly units of Carboniferous age which may be the origin of marine tillites formed along the border of Gondwana land (Stauffer, 1983; Stauffer and Lee, 1986; Metcalfe, 1988) or mass flow deposits formed on a continental margin. Minor tin-tungsten mineralization is associated with the S-type granites of this province and it occurs as the endogenous mineralized pegmatites and greisen veins swarms which are accompanied with a pervasive kaolinisation. Granitoids from Tanintharyi and Shan Scarp region of Myanmar are mainly medium-to coarse-grained megacrystic biotite granites and tourmaline granites of both I-type and S-type origins. Major tin-tungsten deposits of Myanmar all lie in this Province (Figure 2.4).

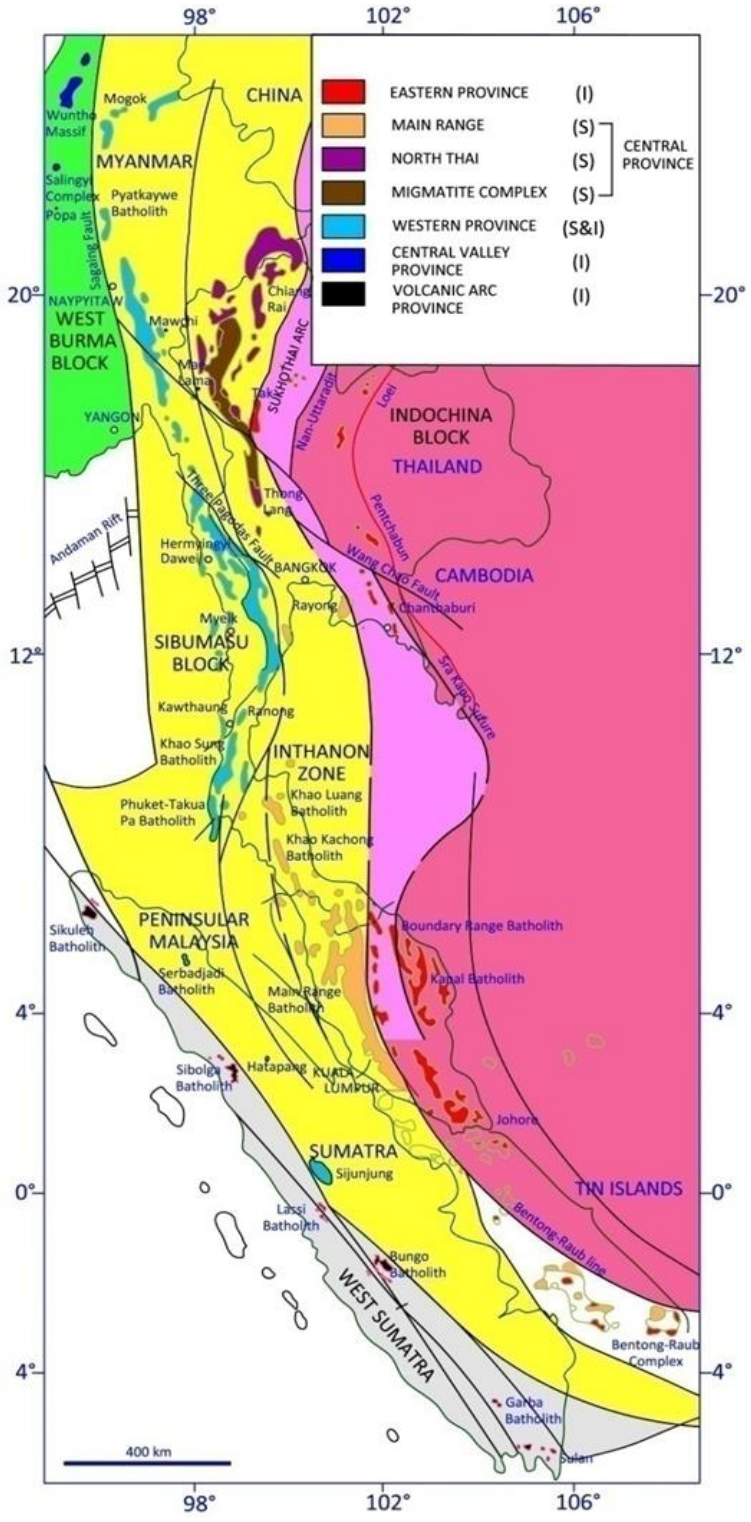

Figure 2.4. Granite provinces of Southeast Asia (after Cobbing et al.,1986 and 1992; Khin Zaw, 1990; Hutchison, 2007; Cobbing, 2005, 2011; Sone and Metcalfe, 2008).

2.4 Granitoid belts of Myanmar

Granitic rocks of Myanmar occur as the N-S trending linear belts along a distance of over 1450 km from Kachin State in the north to Tanintharyi Region in the South. Chhibber (1934) delineated the five igneous lines in Myanmar from west to east such as the Western Igneous Line, Igneous Line of Central belt, Edge of Shan Plateau, two igneous lines in Shan Plateau. He described two Igneous Lines which were passed the Shan Plateau. On the former line, siliceous tuffs near the Lagwi Pass situated on the northeastern frontier of Myanmar, the Bawdwin lavas and tuffs, and the siliceous volcanic rocks of the Myeik (Mergui) Archipelago.

The later comprises the Loi Han Hun volcano in the Northern Shan States and some of the volcanoes of the Myeik Archipelago, including the basaltic lava flows of Medaw Island. This line passes further southwards to the Malay Peninsula. The igneous line of Edge of Shan Plateau consists of lavas and dolerites of the Kabwet, Mandalay and Shwebo areas, rhyolites and rhyolite tuffs of the Thaton district, etc. The igneous line of the central belt connected with the folding of the Pegu Roma and their continuation in to the northern hill ranges, those of the Jade Mines area, Wuntho, Shinmadaung, Mount Popa, Pyay and Irrawaddy. Western Igneous Line connected with the upheaval of the western hill ranges is the belt of serpentinized peridotite, which runs from Java and Sumatra through the Andaman and Nicobar Islands in the south. Bender (1983) classified the granites of Myanmar as (i) pre-Mesozoic igneous rocks and (ii) Mesozoic and Cenozoic igneous rocks. Khin Zaw (1990) divided the granitoids of Myanmar as three major belts: namely Western Granitoid Belt, Central Granitoid Belt and Eastern Granitoid Belt (Figure 2.5).

2.4.1 Western Granitoid Belt of Myanmar

Various sizes of intrusive bodies of granitoids with younger volcanics (which are principle components of Central Volcanic Arc of Myanmar) belong to this belt. It stretches from the south of Taungthonlon southwards through Wuntho and Salingyi areas and to Popa area. Existence of younger volcanic rocks (e.g. Mt Popa) along this belt suggests a shallow-level (epizonal) emplacement of these granites. Porphyry copper-gold mineralization (e.g. Monywa) is associated with younger volcanic rocks in this belt.

At Salingyi, the granitic rocks occur as marginal differentiates of predominantly dioritic plutons with minor gabbros and are associated with the volcanic rocks of trachyte and rhyolite. K/Ar dating of the igneous rocks of the Salingyi area has yielded 103±4 Ma for granites, and 106±7 Ma and 91±11.8 Ma for diorites and gabbros respectively (Ahad, 1980). The Salingyi Granite is grey to pink, locally leucocratic and mostly medium-grained. It is essentially composed of quartz, orthoclase, plagioclase, biotite and very minor hornblende. The granitoid intrusions in the Wuntho and Pinlebu areas were thought to be contemporaneous with granites in the Salingyi area. The volcanic and intrusive rocks in the Western Belt are considered to have been emplaced in a magmatic volcanic arc above an east-dipping subduction zone during the Upper Mesozoic-Cenozoic (Khin Zaw, 1990).

2.4.2 Central Granitoid Belt of Myanmar

This belt approximately corresponds to the most Western Granitic Belt of Southeast Asian tin-bearing granitic belts (Mitchell, 1977), the back-arc tin granitoid belt (Mitchell, 1981), and the Mogok Belt of Searle and Ba Than Haq (1964) and lies also in the Western Province Terrain of Southeast Asia Granitoid Tin Belt (Cobbing et al., 1992). The Central

Granitoid Belt of Myanmar emerges from Putao and the jade mine areas in Myitkyina in the north, through Mogok, Mandalay, Kyaukse, Yamethin, Pyinmana, Taungoo, Loikaw, Dawei and Myeik areas to Kawthaung (Victoria Point) in the south forming as a narrow linear belt of 1450 km in length and 50 km in width. Tin-tungsten mineralization is closely related and spatially associated with the plutons of S-type granitoid rocks in this belt.

According to the Rb/Sr chronological data the age of the major episode of granitoid emplacement in the Central Granitoid Belt of Myanmar is interpreted to be Upper Cretaceous and Lower Eocene. The significant tungsten-tin deposits are the Mawchi mine and Hermyingyi mine. The granitic rocks in the Central Belt of Myanmar were possibly emplaced during continent-arc collision at the early stage of westward migrating, east-dipping subduction zone during the Upper Mesozoic and Lower Eocene. The tin-tungsten related, Central Belt Granitoids of Myanmar and porphyry copper-gold related, Western Belt granitoids were considered to have been emplaced during the Upper Mesozoic and Lower Cenozoic interval but might not have been strictly comtemporaneous (Khin Zaw, 1990).

2.4.3 Eastern Granitoid Belt of Myanmar

Granitoid intrusions in the areas of Namhsan, Mong Tung, south Hsenwi, Kyaington and Tachileik belong to the Eastern Granitoid Belt of Myanmar. A series of granitoid plutons east of Bhamo and Myitkyina probably belongs to this belt and it possibly extends northward into the Yunnan Province of China. It can be supposed as the northern continuation of the granitoid rocks of the North Thai Province of Cobbing et al. (1992).

The Tawngpeng Granitoid (La Touche, 1913) in the northern Shan State occurs as a very large intrusion in north-east of Burma. It lies along the Eastern Granitoid Belt covering

the ranges west of Bawdwin mine, a volcanic-hosted, silver-rich, polymetallic (Pb-Zn-Cu-Ag-Ba) massive sulfide deposit (Khin Zaw, 1990). The Tawngpeng Granitoid is also exposed in the high country around Loi Mong and can be traced to the vicinity of Loi Lem Ridge and as far north as the Myanmar-China border and it extends northwards into Yunnan. The Tawngpeng Granitoid in the Eastern Granitoid Belt demonstrably intruded the Chaung Magyi Group of Upper Precambrian age in the main area of Tawngpeng, on the north side of Loi Pan and along the southern slope of Loi Ling in south Hsenwi. Thus, stratigraphic data indicates that the Tawngpeng Granitoid was emplaced during the Phanerozoic.

Mitchell et al. (1977) reported a Rb/Sr whole-rock age of 340 ± 34 Ma for the Tawnpeng Granitoid exposed along the Kyaukme-Namhsan road, and accordingly Bender (1983) regarded the Tawnpeng Granitoid as a Carboniferous intrusive rock, but Mitchell et al. (1977) pointed out that this age data must be treated with caution because of the divergence in the initial Rb/Sr ratios. Similar Rb/Sr whole rock analysis indicates a Paleozoic (Cambro- Ordovician) age for the Tawngpeng granitoid. K/Ar dating of biotites and feldspars suggests that the Tawngpeng Granitoid has suffered significant thermal disturbances in relatively recent time (Brook and Snelling, 1976).

The Tawngpeng Granitoid consists of quartz, plagioclase, orthoclase (sometimes microcline), muscovite and biotite and usually exhibits evidence of intense fracturing. It is generally coarse-grained, often porphyritic, with phenocrysts up to 3 cm across. Sphene, apatite, and zircon are found as accessories. Passcoe (1959) reported sporadic tourmaline and pyrite as accessory constituents. These phases were not observed in the few Tawngpeng granitoid samples studied by the author.

The Tawngpeng Granitoid suffered from some sericitization and saussuritization. The Tawngpeng Granitoid in the main area differs from the adjacent Kabaing (Mogok) Granitoid of the tin-tungsten related Central Granitoid Belt of Myanmar. The Tawngpeng Granitoid is coarse grained and does not contain tourmaline. The intrusion of the Tawngpeng Granitoid also gave a limited metamorphic aureole in the Chaung Magyi country rocks which have been converted into quartzites, and sometimes into feldspathic, and micaceous slates and phyllites.

Pascoe (1959) also reported that in places, the Tawngpeng Granitoid is associated with muscovite granite and quartz feldspar porphyry and the Tawngpeng Granitoid of these parts was intruded by dolerites. The granitoids exposed along Kyaington-Tachileik road are medium-to coarse-grained with biotite and locally abundant hornblende. The minor importance of Sn-W mineralization has been found in association with the granitoid of the Eastern Granitoid Belt of Myanmar. Moreover recently economic importance of manganese mining in this belt has become of interest to the Myanmar mining industry.

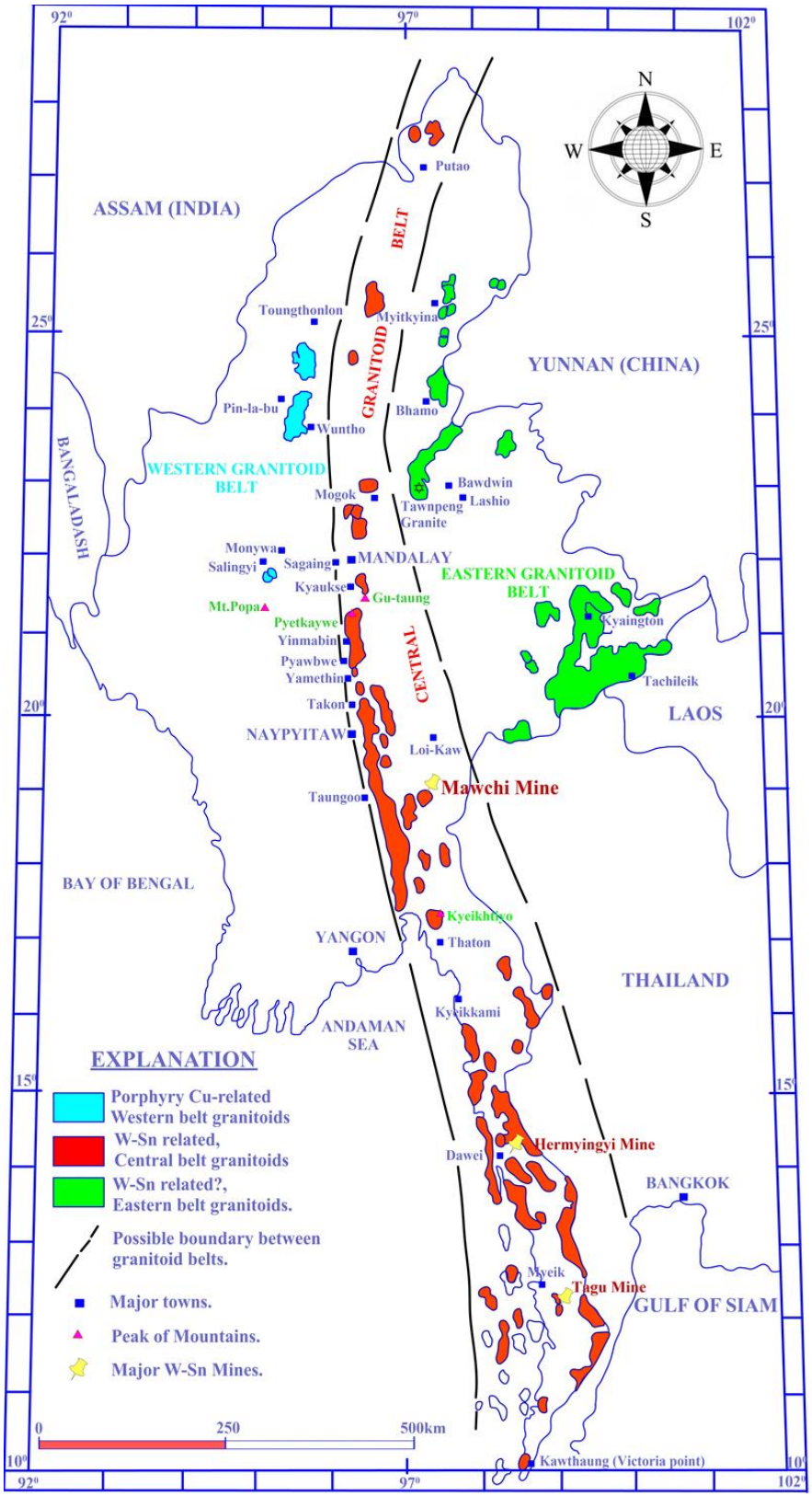

Figure 2.5. Granitoid Belts of Myanmar (modified after Khin Zaw, 1990).

CHAPTER III: REGIONAL AND DEPOSIT GEOLOGY OF TAGU AREA

3.1 Regional geology

Primary tin-tungsten deposits are commonly associated with the intrusion of Late Cretaceous-Eocene granites of the Mogok Mandalay Mergui Belt (MMMB) which emplaced into metasedimentary rocks of the Slate Belt (Chhibber, 1934; Hutchison and Taylor, 1978; Khin Zaw, 1990 and 2017). The principal tin-producing area is located around the port town of Dawei. Much historical production was elluvial / alluvial, and these deposit types are particularly focused around Myeik in the far south. This metallogenic province is also rich in tungsten, commonly as wolframite, and more rarely as scheelite found spatially associated with the tin mineralization. Greisen-bordered tin-tungsten quartz veins are sometimes associated with pegmatites, sub-vertical veins are found in parallel groups, mostly trending NE-SW or sometimes E- W with steep dips. Notable tin-tungsten vein type deposits occur at Tagu, Maliwun, Palauk, and Yadanabon (Khin Zaw, 1990). The veins frequently strike parallel to the trend of the elongated granite bodies with a general NNW–SSE strike except for the E–W-striking vein system of the Kanbauk mine in the Dawei tin-tungsten district (Bender, 1983).

The Mergui Group is mostly composed of interbedded pebbly mudstones or diamictites, with minor turbidite wackes, thin limestones, and local white quartzites (Hobson, 1941). The tin-tungsten mineralization is predominantly associated with granites, granitic pegmatites and aplite dykes of the WGP which intruded into Carboniferous to Early Permian metasedimentary and sedimentary sequences of Mergui Group (e.g., Bender, 1983; Mitchell et al., 2004; Aung Zaw Myint et al., 2013 and 2017b). Granitoids in the Mergui area form into three distinct ranges; Eastern Frontier Range along the Myanmar-Thai border,

the Central Range, and the Western (Coastal) Range (Figure 3.1) (Rao, 1930). Most of the areas are covered by intensely deformed Mergui Group metasedimentary rocks; the age is regarded as Carboniferous based on paleontological evidencs (Brown and Heron, 1923).

The Mergui Group trends roughly NS to NNW–SSE and is extensively intruded by granitic intrusions of various sizes (from 32 to 64 km in length and up to 16 km in width) (Li et al., 2018). Plutons in the Mergui district are elongated NNW-SSE parallel to the trend of the country rocks. In Mergui tin-tungsten district, there are many primary and placer tin-tungsten deposits. The major tin-tungsten deposits are Yamon-Kazet, Tagu (Kuntabin), Theindaw, Thabawleik and Yadanabon (Figure 3.1). Only the deposits at Theindaw and Thabawleik are placer deposits and the deposits at Yamon-Kazet, Tagu (Kuntabin) and Yadanabon are vein-type primary deposits.

The Tagu Mine is one of the major tin-tungsten deposits in the Myeik District. It is located near Tagu village and right bank of Tanintharyi River in north-east of Tanintharyi Township. This area is mainly composed of coarse-grained porphyritic granite and greywacke of the Mergui Group. The mineralized quartz veins and veinlets are observed not only in the metasedimentary rocks but also in granitoids. Aditting is the common method used for the ore production and gravel pumping method is used for weathered exposure.

The Yamon-kazet mine is located near Thinkanshaunt village in south-east of Myeik Township. This mine is a vein-type deposit. A major source of ore mineralization comes from granite intrusion with tourmaline-muscovite-quartz pegmatite veins. This area produces tin more than that of tungsten. Open cut and gravel pump mining methods are used for ore production (Tin Aye and Kyaw Nyein, 1966).

Thabawleik mine is located about 20 km southeast of Thabawleik Village in Tanintharyi Township. The huge alluvial tin-tungsten deposit occurs at the Thabawleik mine. This area contains more cassiterite rather than wolframite. Greisen is developed in the granite wall of the quartz veins. Generally, more mineralization can be found in narrow veins rather than in wide veins. Pegmatite veins are found in the upper Namron Chaung. Molybdenite, bismuthinite, pyrite, chalcopyrite, tourmaline, fluorite and lepidolite are found as accessory minerals (Tin Aye and Kyaw Nyein, 1966).

More than 50 tin-tungsten workings have been recorded in the Mergui area and the adjacent islands. The residual and detrital tin deposits frequently resulted from decomposition and weathering of pegmatites and tin-tungsten quartz veins. Although eluvial and alluvial cassiterite occurrences are widely scattered in the Mergui area, only some localities are important for tin-tungsten bearing pegmatites and quartz veins which penetrated both granitoids and surrounding metasedimentary country rocks. Workable mineralized tourmaline muscovite pegmatites are noted at Kazat, Zegami, Palaw, Te-Twe, and Yengnan.

The texture of the Mergui Biotite Granite varies from coarsely porphyritic to equigranular. The biotite granite consists of quartz, microcline partly sericitized, a little plagioclase, biotite and minor muscovite. Tourmaline and muscovite are usual accessories found at the margins of the plutons where biotite becomes scarce. The tin-tungsten bearing quartz veins with greisen borders and pegmatites are notably associated with the Mergui Biotite Granite. The medium-grained, biotite granite appears to be a more favorable host than the coarse-grained porphyritic granite. Pegmatites occur as disconnected, lenticular

veins but trend in a regular direction parallel to the strike of the country rocks (NNW-SSE) (Khin Zaw, 1990).

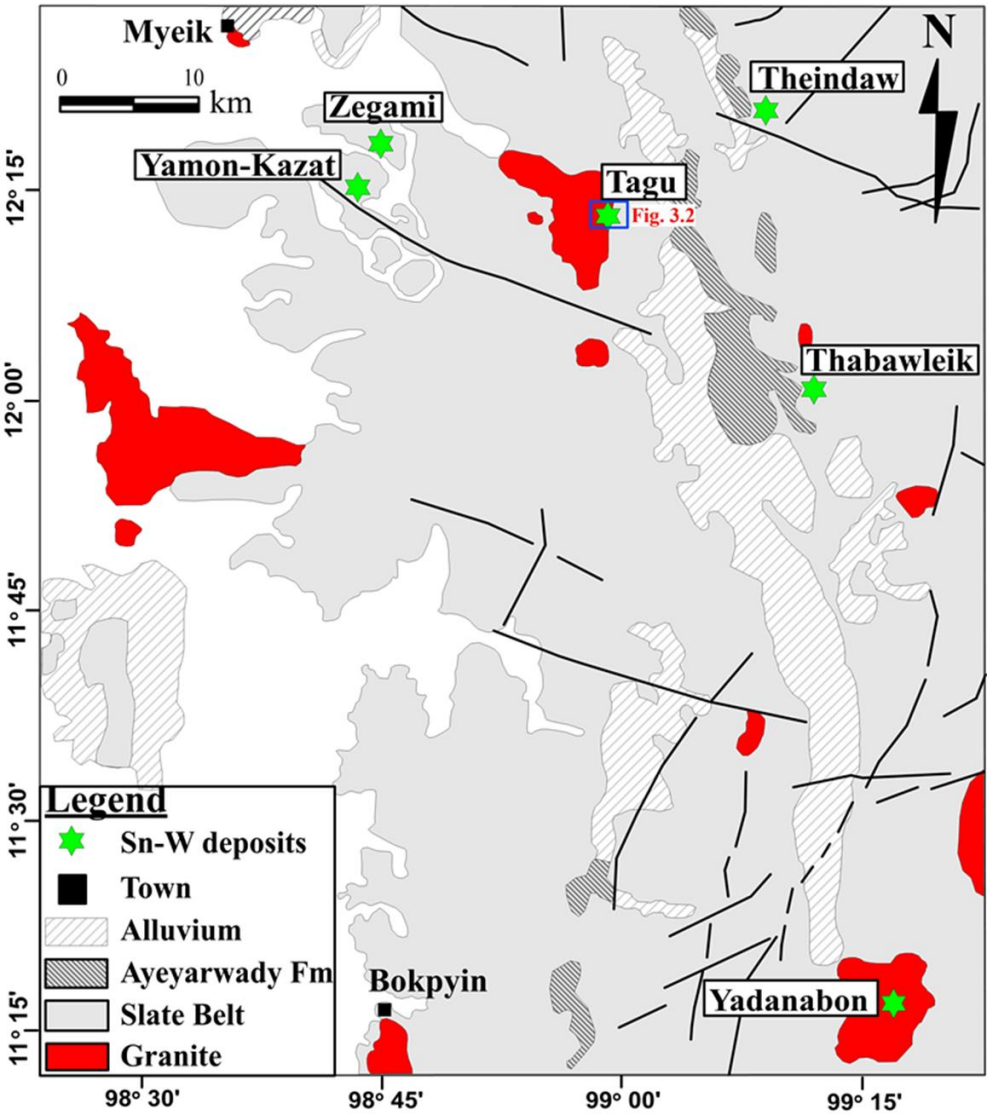

Figure 3.1. Regional geology of Mergui District, Southern Myanmar (modified after Aung Zaw Myint, 2016).

3.2 Deposit geology

The Tagu tin-tungsten deposit, hosted in the granite and Carboniferous-Permian Mergui Group metasedimentary rocks (Figure 3.2) is one of the largest tin-tungsten deposits in the Myeik area. It is located near Tagu village and right bank of Tanintharyi River in the north-east of Tanintharyi township. The Mergui Pluton is elongated NNW-SSE parallel to the trend of the metasedimentary rocks of Mergui Group which are affected by greenschist to lower amphibolite facies metamorphism. The metasedimentary country rocks also exhibit contact aureoles but not so pronounced over a large area.

Biotite granites together with two mica (biotite and muscovite) granites are the most abundant rock types with a subordinate amount of porphyritic biotite granites. The coarse-grained porphyritic biotite granite and metasedimentary rocks (greywacke) of the Mergui Group are the main lithological units in this area (Figure 3.2).

The oldest lithologic unit is metasedimentary rock of the Mergui Group (Carboniferous-Permian) as a country rock unit which is widely distributed in the study area. It is composed of a thick sequence of folded, crushed phyllites, argillites, greywackes and shales, with subordinate amount of conglomerates, sandstones, quartzites, limestone, and agglomerates. The coarse-grained porphyritic biotite granite consists of quartz, microcline, plagioclase (partly sericitized), biotite and minor muscovite.

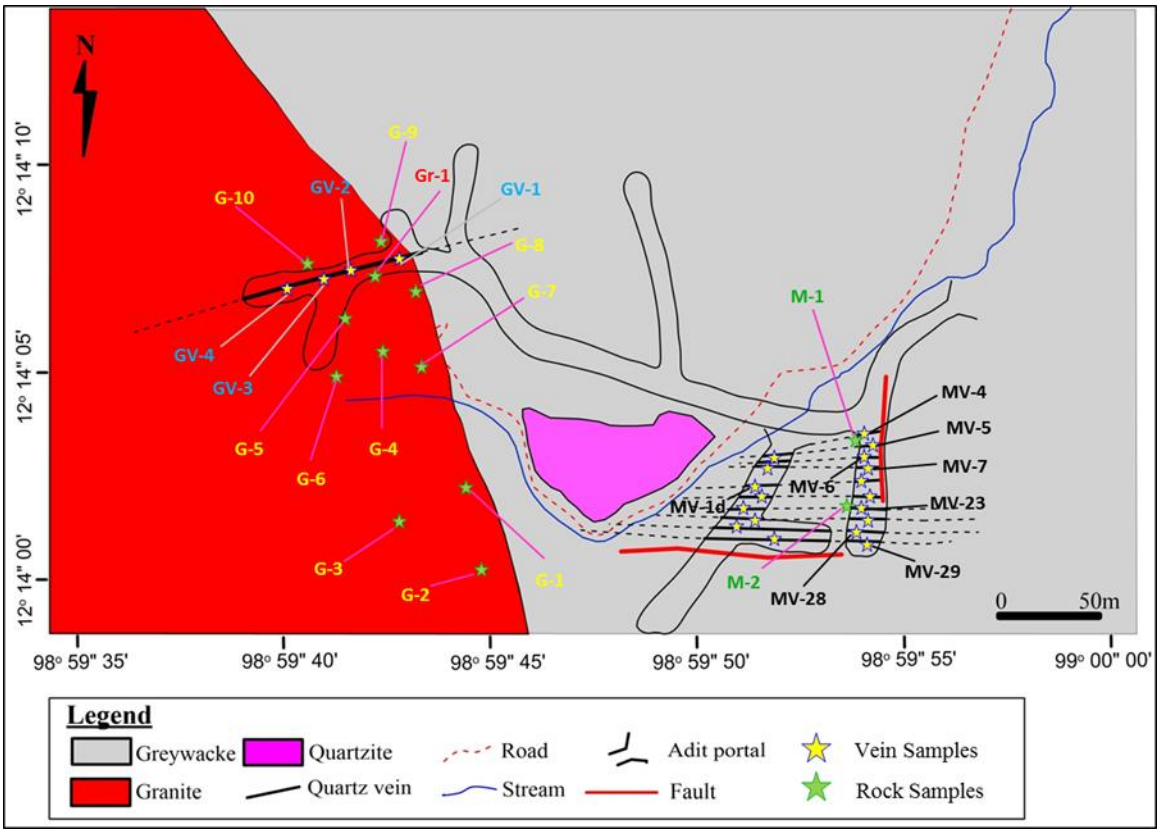

Figure 3.2. Geological map with sample locations of the Tagu mine area (modified after Tagu mine project map).

3.3 Mineralization of Tagu Sn-W deposit

The major mineralization style of the Tagu deposit is represented by cassiterite-wolframite bearing quartz veins that are hosted in the granitic rocks and metasedimentary rocks. The mineralized quartz veins occur as steeply dipping veins that contain oxide ore minerals such as cassiterite and wolframite which are associated with sulfide minerals. The mineralized quartz veins and veinlets can be observed not only in the metasedimentary rocks but also in the granitic rocks.

The width of some quartz veins in the granite varies from 1m to 5m across (Figure 3.3A). Underground mining methods (Figure 3.3B) are used for the ore production, with the gravel pumping method used for weathered exposures. Some mineralized quartz veins parallel to each other and trending approximately E-W directions exhibit pinch and swell structures, quartz veins are displaced by the faults (Figure 3.3C and D).

The mineralized quartz veins are pinched out and branched upwards. Subsequently, these veins are terminated as small parallel and branched veins into the metasedimentary rocks (Figures 3.4A, B and C). Most of mineralized quartz veinlets are small with the exception of MV-28 vein which is the biggest mineralized vein in the metasedimentary rocks (Figure 3.4D). The ore minerals are mostly associated with quartz and muscovite. Almost all of the quartz veinlets are parallel to each other. More than 30 mineralized quartz veinlets trending nearly E-W are observed in metasedimentary rocks which are discordant to the direction of host rocks, whereas in the granite, the mineralized massive quartz veins which are 1m to 5m across and trend nearly NEE-SWW (Figure 3.5A and B).

Wolframite occurs in swarms of quartz veins trending from NE-SW and E-W, which are hosted by the porphyritic biotite granite and metasedimentary rocks (greywacke), occurring especially within the outermost zones of the veins, and is associated with cassiterite. Cassiterite appears as micrometer- to centimeter-sized (up to 1 cm long) subhedral to euhedral crystals at the margin of quartz vein (Figure 3.5C and D) , as well as anhedral aggregates of more than 2 cm (Figure 3.6A). Sometimes, wolframite is associated with cassiterite at the margin of quartz vein (Figure 3.6B). Cassiterite is the main ore mineral in quartz veins of the Tagu deposit together with wolframite at the margin of quartz

vein. Some sulfide rich quartz veins are also found in the Tagu tin-tungsten deposit (Figure 3.6C, D).

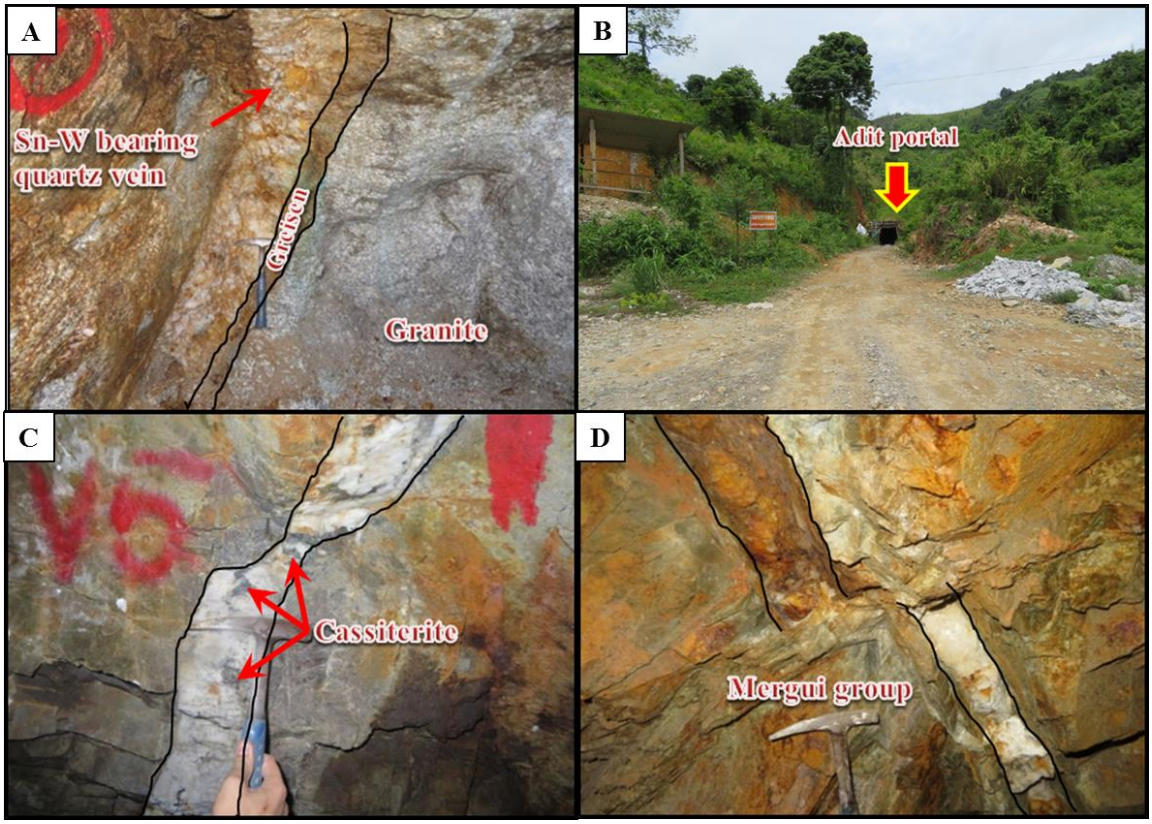

Figure 3.3. Field photos for lithologic units in the Tagu area. A. Tin-tungsten bearing quartz vein within the granite with greisen border (GV-1), B. the portal of underground adit at the Tagu tin-tungsten deposit, C. Cassiterite-bearing quartz vein which exhibits pinch and swell structure (MV-5) and D. Mineralized quartz vein which was displaced by a fault (MV-1d).

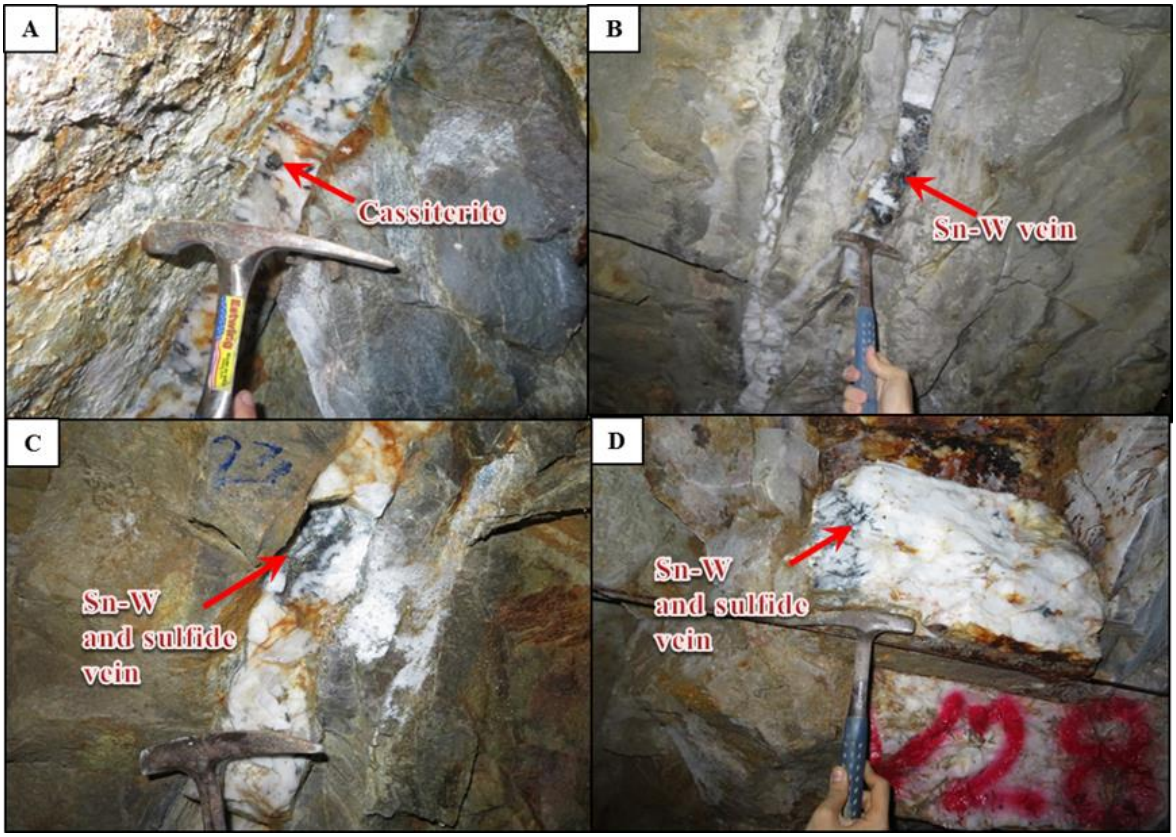

Figure 3.4. Field photos for lithologic units in the Tagu area. A. Cassiterite bearing quartz vein in metasedimentary rock (Mergui group) (MV-29), B. Cassiterite and wolframite in quartz vein within the metasedimentary rock (MV-4). C. Tin-tungsten and sulfide-bearing quartz vein in metasedimentary rock (MV-23) and D. Tin-tungsten and sulfide-bearing quartz vein, the widest of which is amongst the metasediment-hosted quartz veins (MV-28).

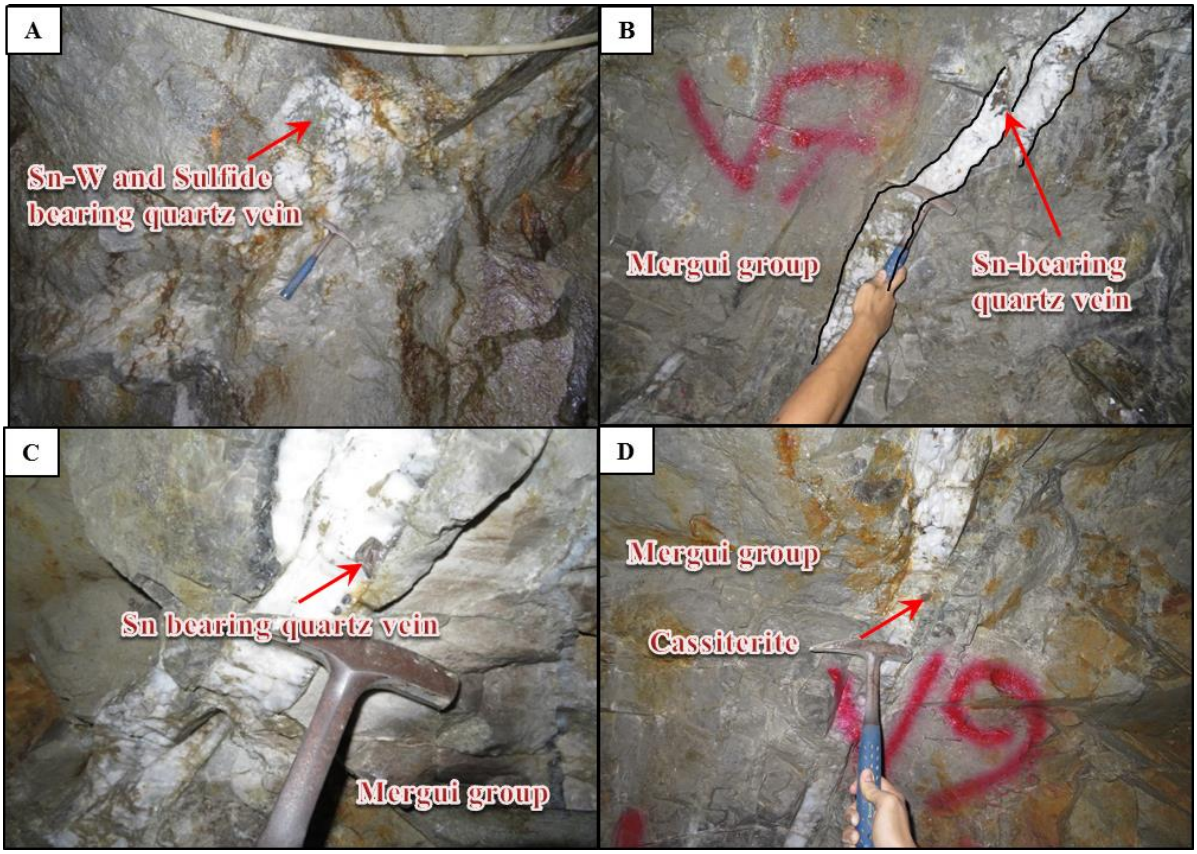

Figure 3.5. The nature of mineralized quartz veins and granitic rocks at the Tagu area. A. Tin-tungsten and sulfide-bearing quartz vein in granite (GV-2). B. Sn bearing quartz vein within the metasedimentary rock (MV-7). C. Sn-bearing quartz vein within the metasedimentary rock (MV-6). D. Sn-bearing quartz vein within the metasedimentary rock (MV-9).

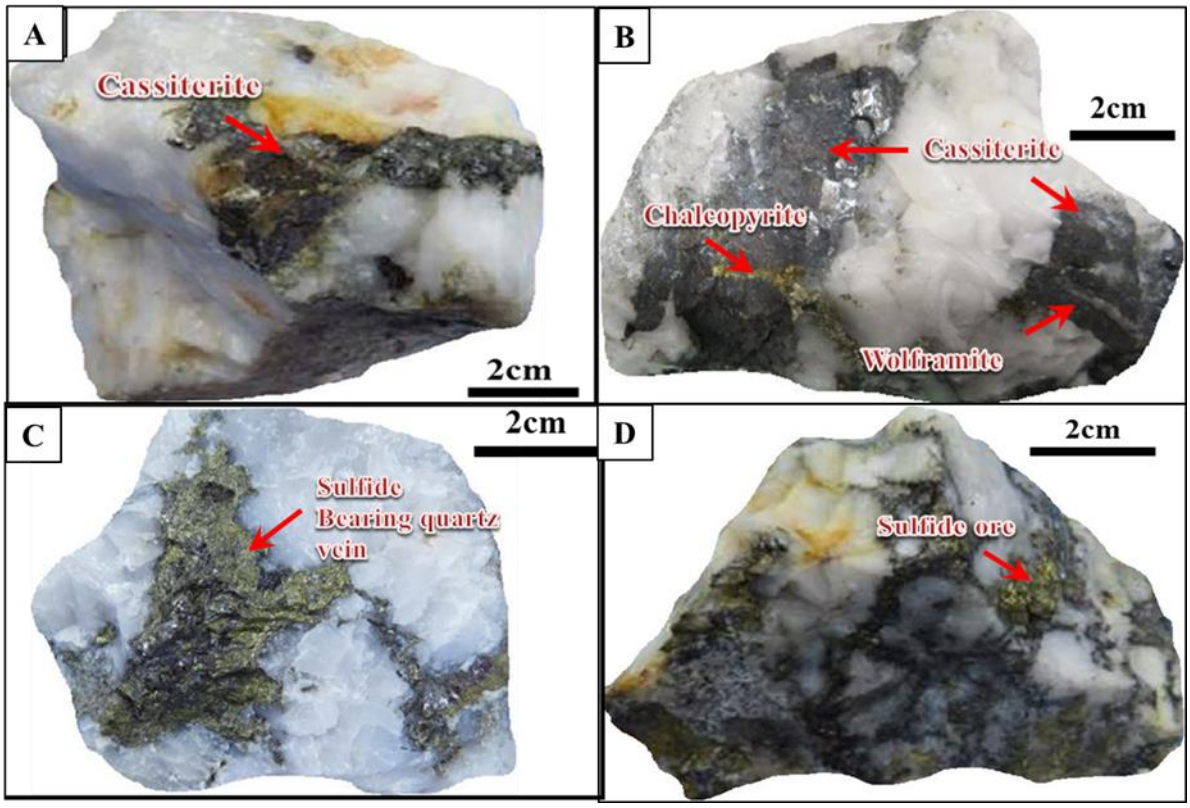

Figure 3.6. Hand specimen photos for the mineralized quartz veins from Tagu mine. A. Sn-mineralized quartz vein at the Tagu tin-tungsten deposit (GV-2), B. Wolframite and cassiterite disseminated ore in quartz vein (GV-1), C. Sulfide bearing quartz vein (MV-23) and D. Sulfide bearing quartz vein (MV-28)

CHAPTER IV. PETROGRAPHY AND GEOCHEMISTRY OF INTRUSIVE ROCKS

4.1 Petrography of granitic rocks

The texture of the biotite granite in the Mergui district varies from coarsely porphyritic to medium-grained. The biotite granite consists of quartz, microcline partly sericitized, plagioclase, biotite and minor muscovite. Zoned K-feldspar phenocrysts occur as in the porphyritic granite (Figures 4.1A and B). The prominent rock unit of the Mergui Group is greywacke which is well exposed along this area as well as quartzite. Graywacke is commonly dark grey in color, fine-grained, compact and highly jointed (Figures 4.1D).

The granitic rocks are coarse-grained, porphyritic and massive in places and secondary muscovite is present as an alteration product of K-feldspar (Figures 4.2A and B). The essential constituents are quartz, K-feldspar (orthoclase, microcline), plagioclase; minor amount of biotite and opaques (Figures 4.2 A,B,C,D,E,F and Figure 4.3 A,B). Microcline is predominant over orthoclase. The microcline phenocrysts have inclusions of quartz and twinned plagioclase. The groundmass is composed of quartz, alkali feldspar, plagioclase and biotite with K-feldspars partially sericitized (Figures 4.3C,D,E and F). Most of the quartz grains exhibit undulose extinction and plagioclase is highly sericitised. Greywacke of the metasedimentary sequence is fine- to medium-grained. It is mainly composed of quartz, muscovite and iron oxide minerals. Quartz shows wavy extinction and they are anhedral to polycrystalline and poorly sorted (Figure 4.3G and H).

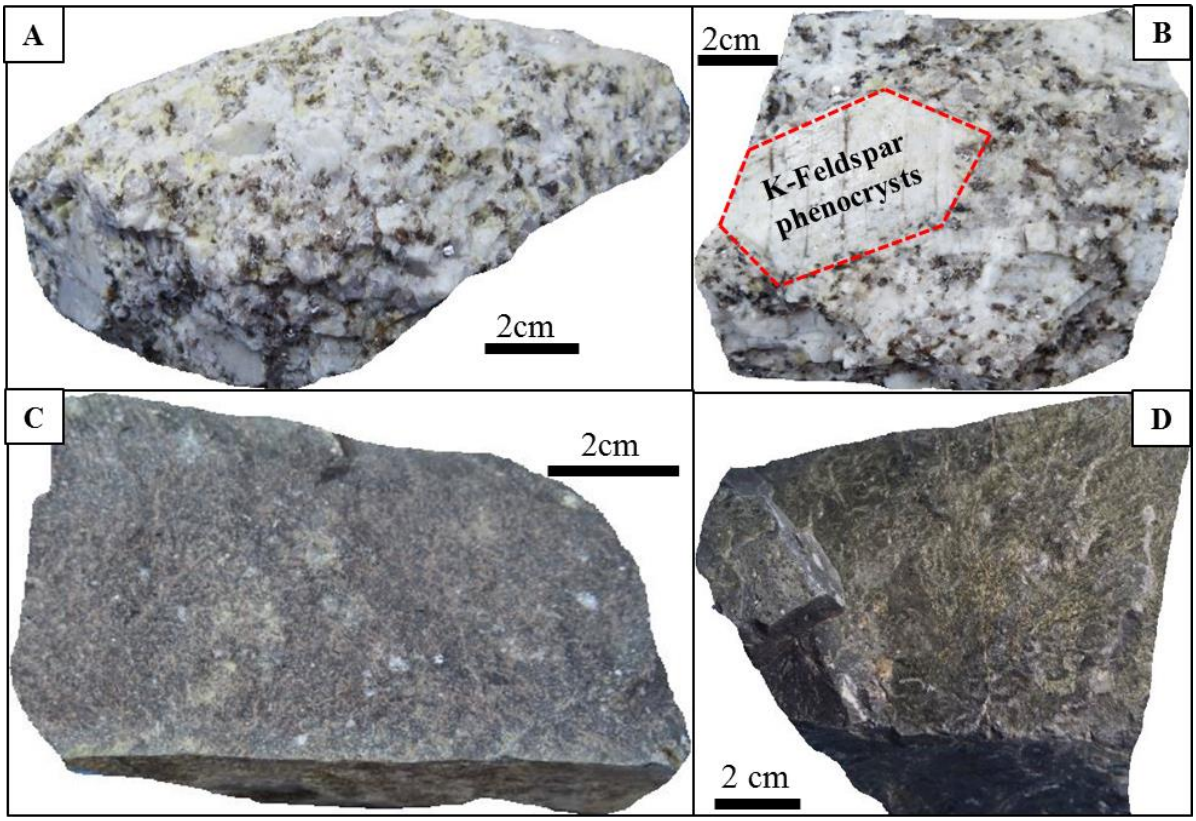

Figure 4.1. Photographs showing hand specimens from the Tagu deposit. A. Pophyritic biotite granite at the Tagu tin-tungsten deposit (G-1); B. Porphyritic biotite granite rock including K-feldspar phenocrysts (G-3); C. Metasedimentary rock (greywacke) of Mergui Group (M-2); D. Metasedimentary rock (greywacke) at the Tagu tin-tungsten deposit (M-1).

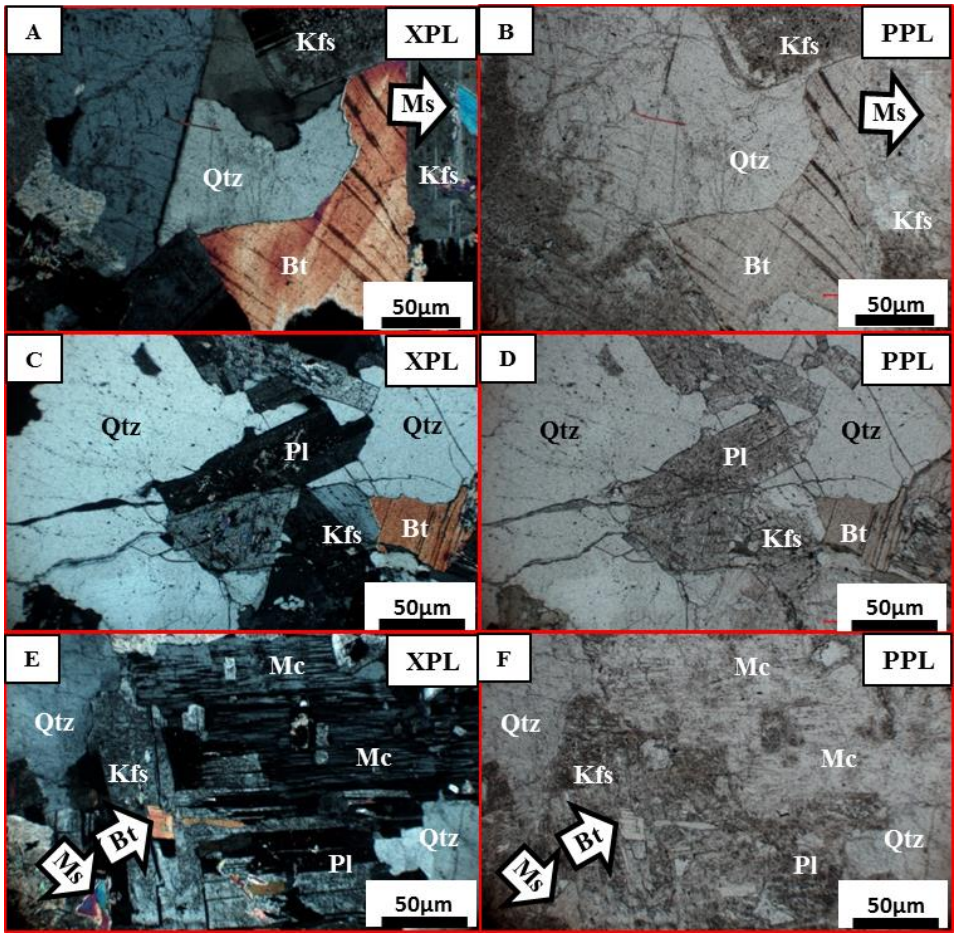

Figure 4.2. Photomicrographs of granite. A. Granitic rocks under cross-polarized light showing the biotite and secondary muscovite resulting from the alteration of K-feldspar (G-7); B. Same as A under plane-polarized light (G-7); C. Biotite associated with quartz and plagioclase which was altered to sericite (G-5); D. Same as C under plane-polarized light (G-5); E. Microcline associated with plagioclase, K-feldspar and quartz with minor amount of biotite and muscovite (G-8); F. Same as E under plane-polarized light (G-8); Abbreviations: Qtz=quartz, Pl=plagioclase, Kfs=K-feldspar, Bt=Biotite, Ms=muscovite, Mc=microcline.

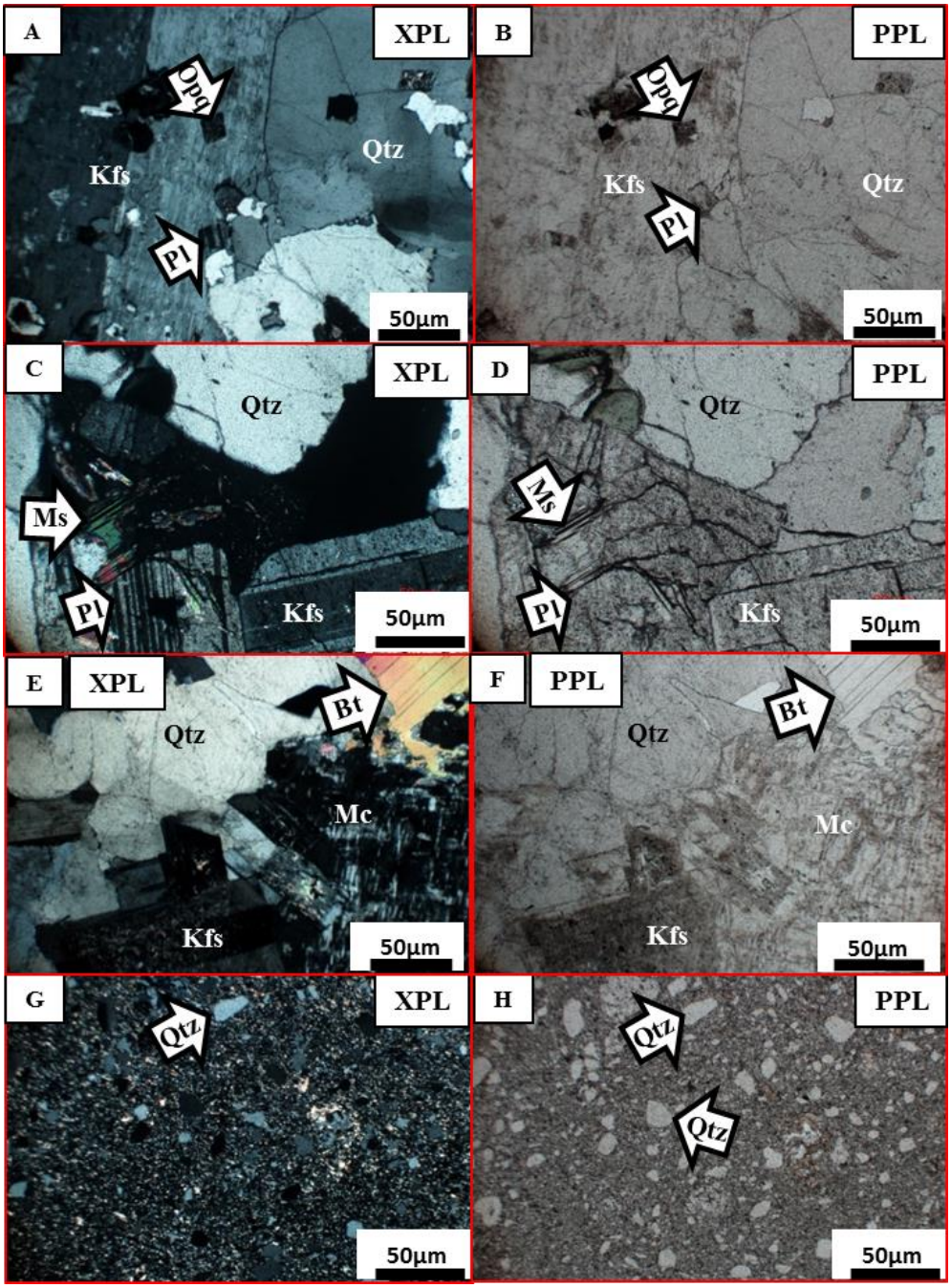

Figure 4.3. Photomicrographs of granitic rocks and metasedimentary rocks. A. Quartz associated with plagioclase and K-feldspar which has opaque mineral inclusions (G-9); B. Same as A under plane-polarized light (G-9); C. K-feldspar associated with plagioclase and minor amount of muscovite in granitic rock (G-10); D. Same as C under plane-polarized

light (G-10); E. Biotite associated with microcline and K-feldspar which is altered to sericite partly in granitic rock (G-4); F. Same as E under plane-polarized light (G-4); G. Microscopic thin section of metasedimentary rock (greywacke) undert cross-polarized light (M-1); H. Same as G under plane-polarized light (M-1). Abbreviations: Qtz=quartz, Pl=plagioclase, Kfs=K-feldspar, Bt=Biotite, Ms=muscovite, Mc=microcline, Opq=opaque mineral.

4.2 Geochemical characteristics of granitic rocks

4.2.1 Major elements oxide

The concentration of major element oxides of granitic rocks from the Tagu area include SiO_2, Al_2O_3, FeO, MnO, MgO, CaO, K_2O, Na_2O, TiO_2 and P_2O_5 are presented in Table 4.1. The SiO_2 contents range between 69.4 and 75.9 wt. % corresponding to a felsic composition. The contents of Al_2O_3, K_2O and Na_2O varies from 12.8 to 15.8 wt. %, 4.4 to 7.3 wt. % and 1.6 to 2.5 wt. %, respectively. Total alkali contents ($Na_2O + K_2O$) ranges from 6.5 to 9.6 wt. %. MnO and P_2O_5 concentrations are less than 0.5 wt. %, and LOI values range from 0.8 to 1.7 wt. % (Table 4.1).

These data are applied to construct several discrimination and variation diagrams to distinguish the rocks types, to identify their geochemical characters and to constrain the tectonic setting of the granitic magmatism. Harker diagrams (Figure 4.4) are used for some major elements relative to SiO_2. Most of the major elements are negatively correlated with SiO_2 (Figures 4.4A, B, C, D, E and F) with the exception of the P_2O_5 contents which are slightly positively correlated (Figure 4.4G). Classification of the rock with SiO_2 vs

(K_2O+Na_2O) geochemical rock classification diagram of Middlemost (1994) for plutonic rocks shows that they plot in the granite field (Figure 4.5).

Table 4.1. Concentration of major (in wt. %) and trace elements (in ppm) by XRF and rare earth elements (in ppm) by ICP-MS for the Tagu Granite samples, Southern Myanmar.

Sample No.	G1	G2	G3	G4	G5	G6	G7	G8	G9	G10
Major elements (wt%)										
SiO_2	71.53	73.56	71.65	71.79	72.34	71.15	71.15	69.48	71.68	75.98
TiO_2	0.31	0.38	0.32	0.36	0.30	0.27	0.31	0.31	0.36	0.30
Al_2O_3	13.67	13.68	14.95	14.72	14.45	15.06	15.09	15.88	14.36	12.83
FeO	2.08	2.27	2.07	2.08	2.06	1.82	1.88	1.58	2.18	1.68
MnO	0.04	0.04	0.04	0.04	0.03	0.03	0.06	0.02	0.04	0.06
MgO	0.71	0.79	0.77	0.78	0.67	0.61	0.65	0.64	0.72	0.57
CaO	1.23	1.25	1.11	1.00	1.05	1.04	1.16	0.71	1.18	0.61
Na_2O	1.62	2.19	2.28	2.07	2.50	2.39	2.37	2.30	2.24	1.89
K_2O	6.70	4.61	5.01	5.02	4.46	5.92	5.49	7.37	5.59	4.62
P_2O_5	0.16	0.20	0.18	0.17	0.17	0.14	0.15	0.18	0.17	0.15
LOI	1.74	0.86	1.42	1.78	1.51	1.35	1.51	1.30	1.27	1.09
Total	99.79	99.83	99.80	99.81	99.54	99.79	99.81	99.78	99.78	99.77
Trace elements (ppm)										
Sc	1.3	0.8	1	2.2	1.7	2.1	2.1	1.8	1.7	1.9
V	31	36	24	25	28	17	25	27	31	21
Co	45	30	40	46	38	30	38	41	29	26
Ni	15	15	11	12	15	13	16	15	14	13
Cu	23	n.d	6	64	34	14	11	3	4	97
Zn	91	12	203	154	81	74	n.d	23	153	61
Pb	44	24	34	65	31	57	52	98	70	109
As	1	9	7	n.d	7	n.d	n.d	n.d	95	148
Mo	12	16	18	15	13	11	11	14	18	15
Rb	911	633	634	621	680	801	846	757	727	835
Sr	32	31	35	36	26	40	46	66	49	25
Ba	349	202	250	264	159	257	318	437	320	234
Y	31	30	29	29	28	33	33	31	31	35
Zr	188	204	197	200	154	158	181	192	210	217
Nb	28	32	27	29	32	27	36	23	29	27
Th	56	61	58	58	47	44	46	49	58	53
U	15	38	44	21	31	19	22	21	13	15
Sb	18	20	14	24	19	18	15	16	21	15
Sn	114	57	50	56	63	53	72	49	59	152

W	36	32	51	60	48	35	349	8	23	35
Rare earth elements (ppm)										
La	17.4	25.7	15.7	23.2	20.7	19.0	17.4	12.4	26.2	23.3
Ce	36.7	80.7	34.6	76.1	46.7	39.4	38.4	27.6	82.3	73.6
Pr	4.1	6.3	3.9	5.8	5.1	4.6	4.1	3.0	6.4	5.6
Nd	14.7	22.3	14.2	20.9	18.2	16.5	15.2	11.1	23.3	20.1
Sm	2.5	4.0	2.5	3.7	3.2	3.0	2.6	2.1	4.2	3.6
Eu	0.2	0.2	0.2	0.2	0.2	0.2	0.2	0.1	0.1	0.2
Gd	1.4	2.4	1.4	2.1	1.9	1.7	1.4	1.2	2.5	2.0
Tb	0.0	0.1	0.0	0.1	0.1	n.d	n.d	n.d	0.1	0.1
Dy	0.3	0.6	0.4	0.6	0.5	0.5	0.3	0.4	0.7	0.5
Ho	0.1	0.1	0.1	0.1	0.1	0.1	0.1	0.1	0.1	0.1
Er	0.0	0.2	n.d	0.1	0.1	0.1	n.d	n.d	0.1	0.1
Tm	0.1	0.1	0.1	0.1	0.1	0.1	0.1	0.1	0.1	0.1
Yb	0.2	0.3	0.2	0.2	0.3	0.2	0.2	0.2	0.3	0.2
Lu	0.1	0.1	0.1	0.1	0.1	0.1	0.1	0.1	0.1	0.1
Total REE	77.8	143.1	73.4	133.3	97.3	85.5	80.1	58.4	146.5	129.6

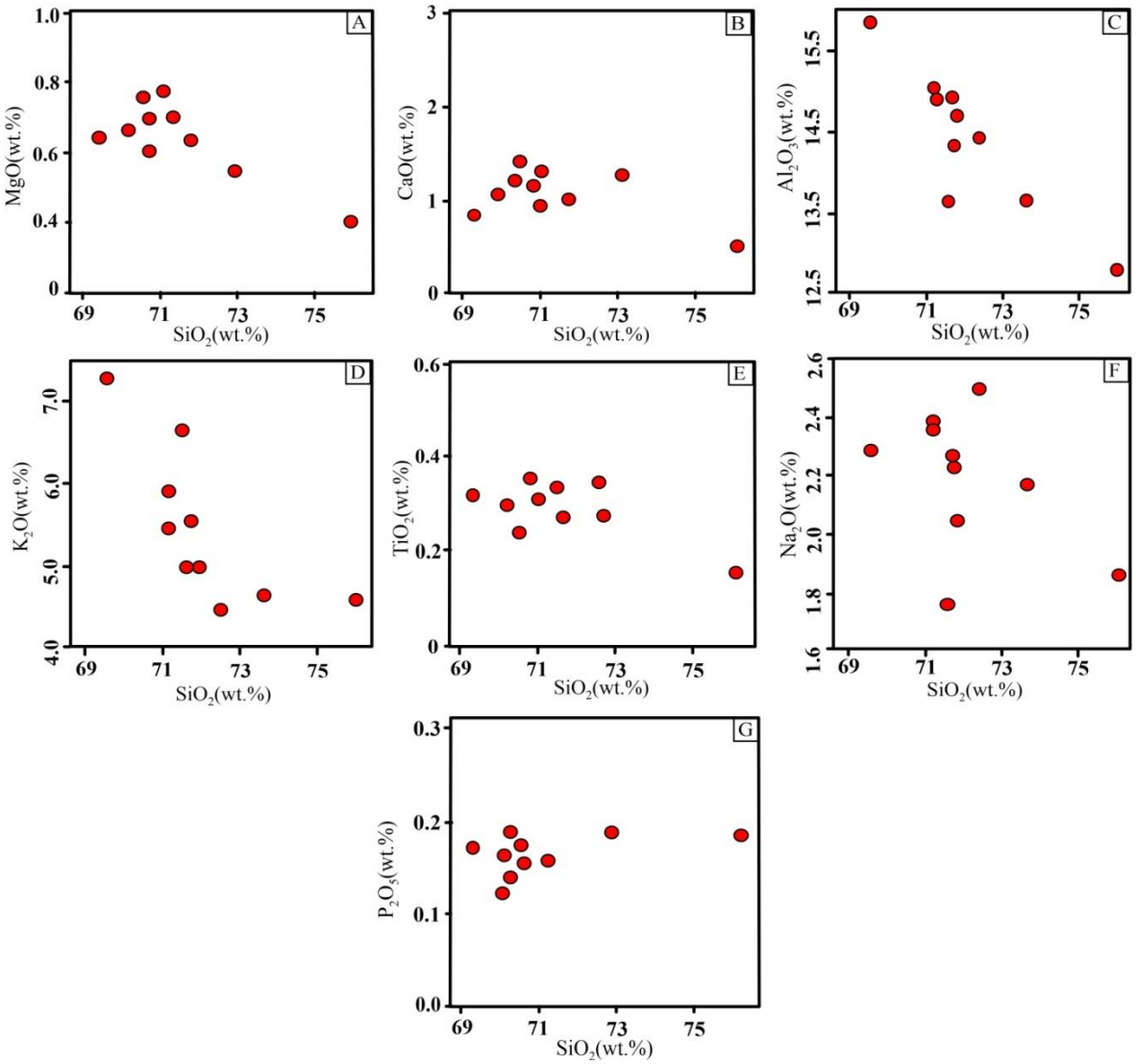

Figure 4.4. Harker variation diagrams; range of major oxides (in wt.%) plotted against silica (SiO_2 wt.%) for the granites of the Tagu area. A. MgO vs SiO_2; B. CaO vs SiO_2; C. Al_2O_3 vs SiO_2; D. K_2O vs SiO_2; E. TiO_2 vs SiO_2; F. Na_2O vs SiO_2 and G. P_2O_5 vs SiO_2.

Almost all granite samples from the Tagu area fall in the high-potassium calc-alkaline series in the K_2O vs SiO_2 diagram (Figure 4.6) after Peccarillo and Taylor (1976). The alumina saturation index (ASI) defined by molecular ratio $Al_2O_3/(Na_2O+K_2O+CaO)$ is greater than unity (one) in all the rock samples ranging from 1.17 to 1.41 implying that the granitic rocks are peraluminous and S-type (Shand, 1943) (Figure 4.7).

The alkali-iron-magnesium (AFM) diagram [(Na_2O + K_2O) (A), (FeO + Fe_2O_3) (F), and MgO (M)] shows a calc-alkaline trend (Figure 4.8). The calcic to alkalic compositional trend in alkali-lime index indicates that potassium is probably abundant in the nature of the magma (Figure 4.9).

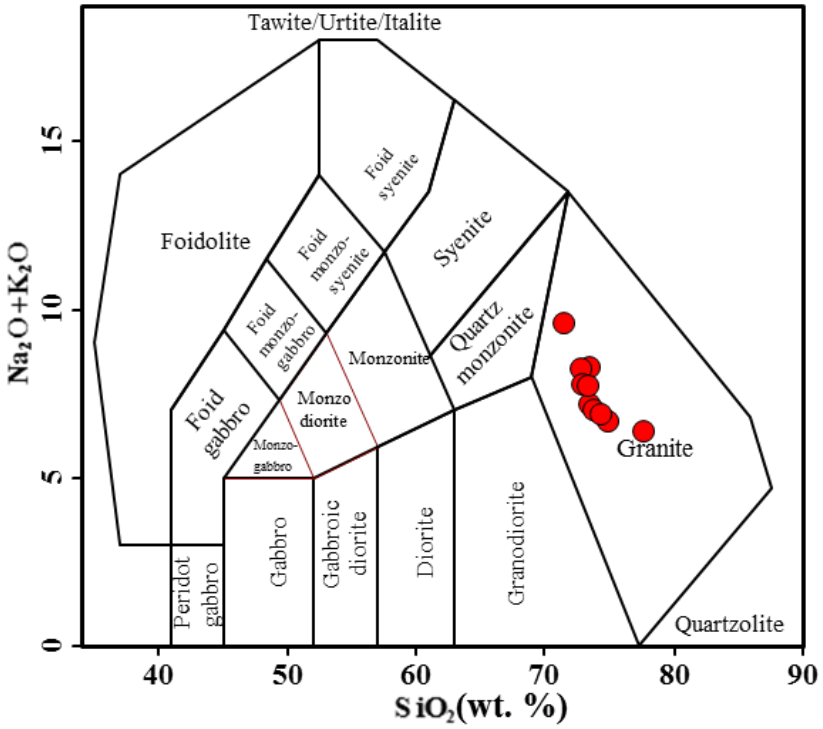

Figure 4.5. SiO_2 vs (Na_2O+K_2O) binary diagram shows majority of samples fall in granitoid field (Middlemost, 1994).

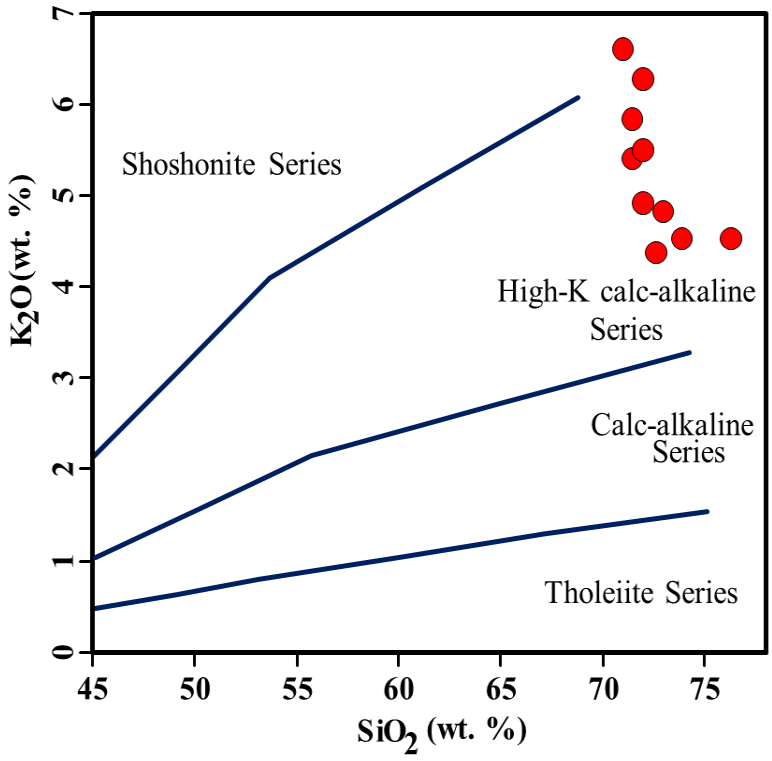

Figure 4.6. K_2O wt% vs SiO_2 wt%; the subdivisions are by Peccarillo and Taylor (1976).

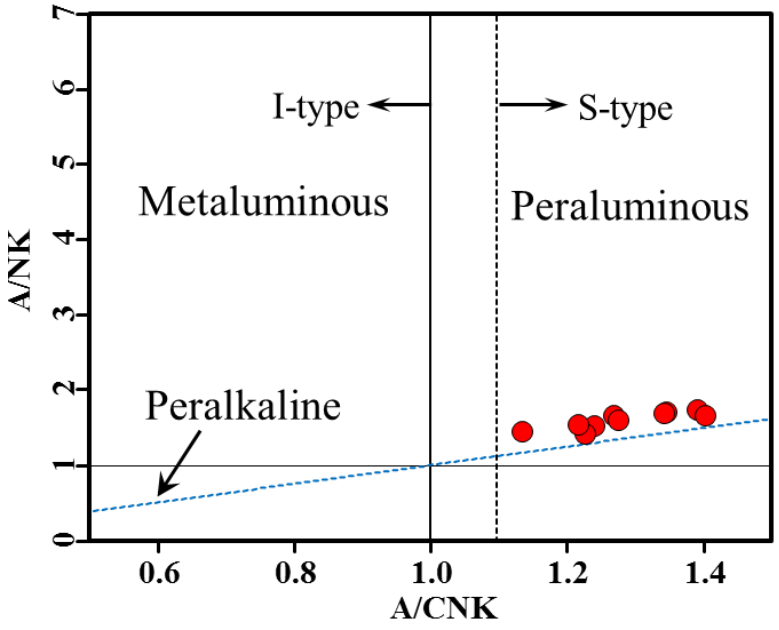

Figure 4.7 Alumina saturation index diagram, A/CNK ratio is greater than 1.1 and it can be assumed that the granite is peraluminous and S-type (Shand, 1943).

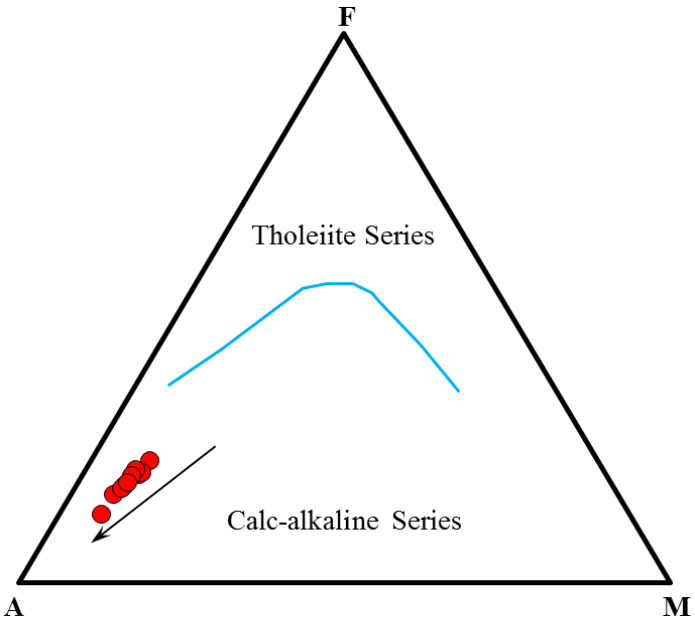

Figure 4.8 AFM triangular diagram for granitoids after Irvine and Baragar (1971). A = (Na_2O + K_2O) wt%, F = (FeO+Fe_2O_3) wt % and M = MgO wt%.

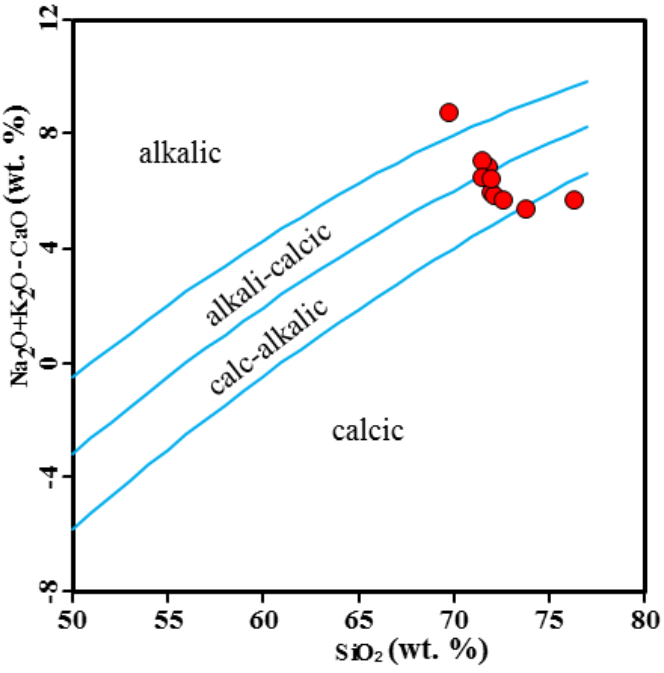

Figure 4.9 Na_2O+K_2O-CaO vs SiO_2 plot (after Frost et al., 2001).

4.2.2 Trace elements

Trace elements concentrations of the granite rocks from the Tagu area are listed in Table 4.1 which shows the concentration of large ion lithophile elements (LILE) such as Ba (159-437ppm), Rb (621-911ppm), Sr (25-49 ppm) and Pb (31-109 ppm) and high field strength elements (HFSE) such as Zr (154-217ppm), Nb (23-36ppm), Y (28-35ppm), Th (44-61ppm) and U (13-44ppm). The ternary diagram Rb-Ba-Sr is applied for classification of genetic types of plutonic rocks (El Bouseily and El Sokkary, 1975) (Figure 4.10).

Trace-element discrimination (Y+Nb) vs. Rb diagrams (Pearce et al., 1984) indicates that the granites of the Tagu area fall in a syn-collisional setting (Figure 4.11). The concentrations of light rare earth elements (LREE) of granitic rocks are generally elevated (La; 12.4-26.2ppm, Ce; 27.6 - 82ppm, Nd; 11.1-23.3ppm, and Sm; 2.1-4.2ppm) in contrast to the depleted heavy rare earth elements (HREE). The chondrite normalized REE pattern of granites (Figure 4.12) shows a significant negative Eu anomaly. The primitive mantle-normalized spider diagram of Sun and Mcdonough (1989) of the granitic rocks (Figure 4.13) reveals enrichment of LILE such as Rb, Pb and K exhibiting and distinct negative anomalies of HFSE such as Ti and Nb. Negative anomalies of Ba and Sr from Rb are remarkable.

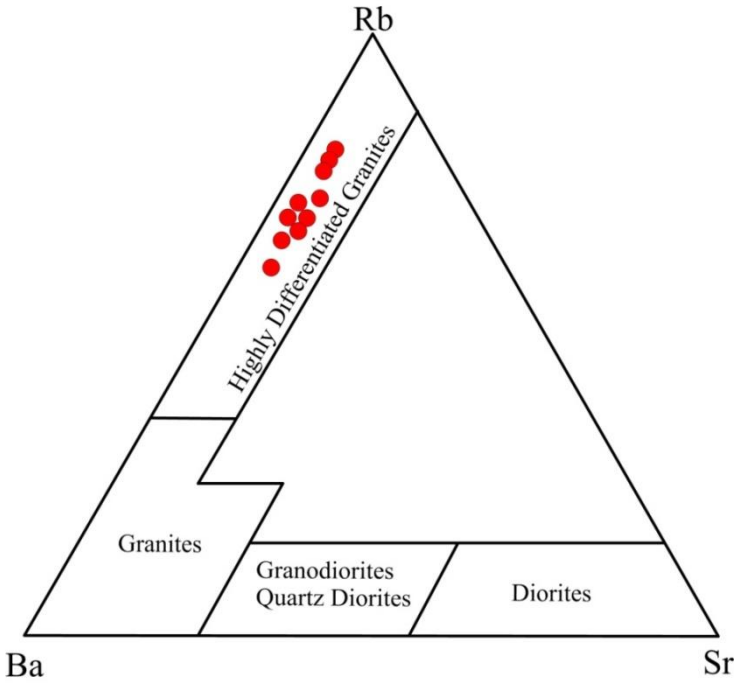

Figure 4.10 Rb-Sr-Ba triangular plot pointing the genetic aspect of the Tagu Granitoid (El Bouseily and El Sokkary, 1975).

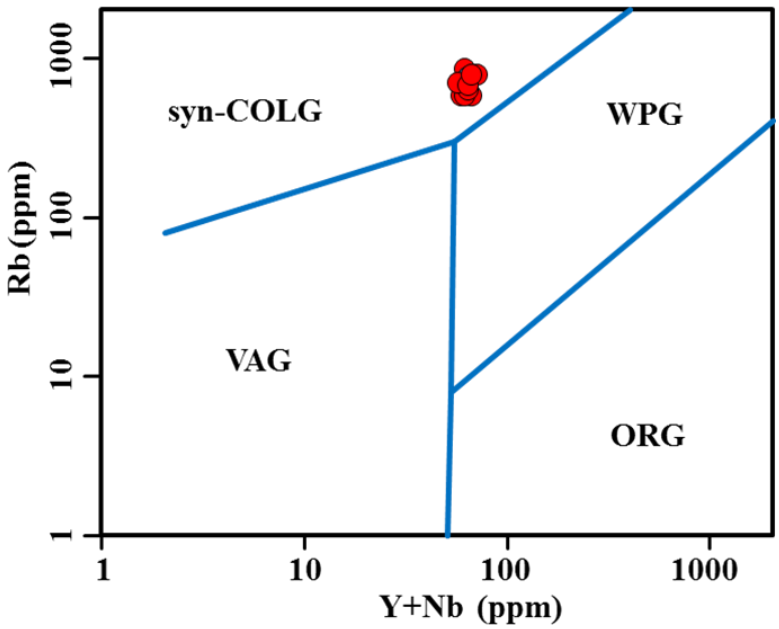

Figure 4.11. (Y +Nb) vs Rb diagram showing the tectonic setting (after Pearce et al., 1984) of the Tagu Granitic rocks.

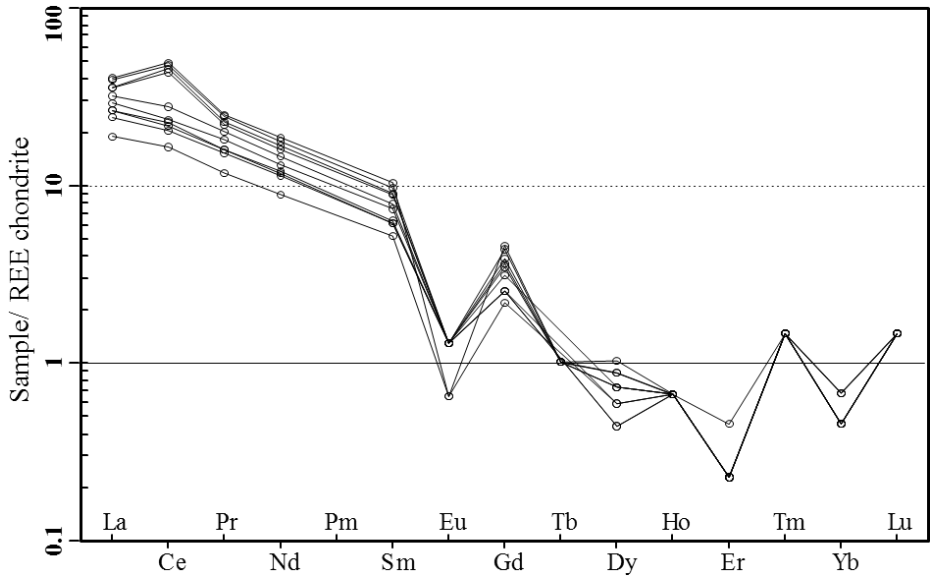

Figure 4.12 Chondrite normalized rare earth elements (REE) diagram of the Tagu Granite (normalizing values from Sun and McDonough, 1989).

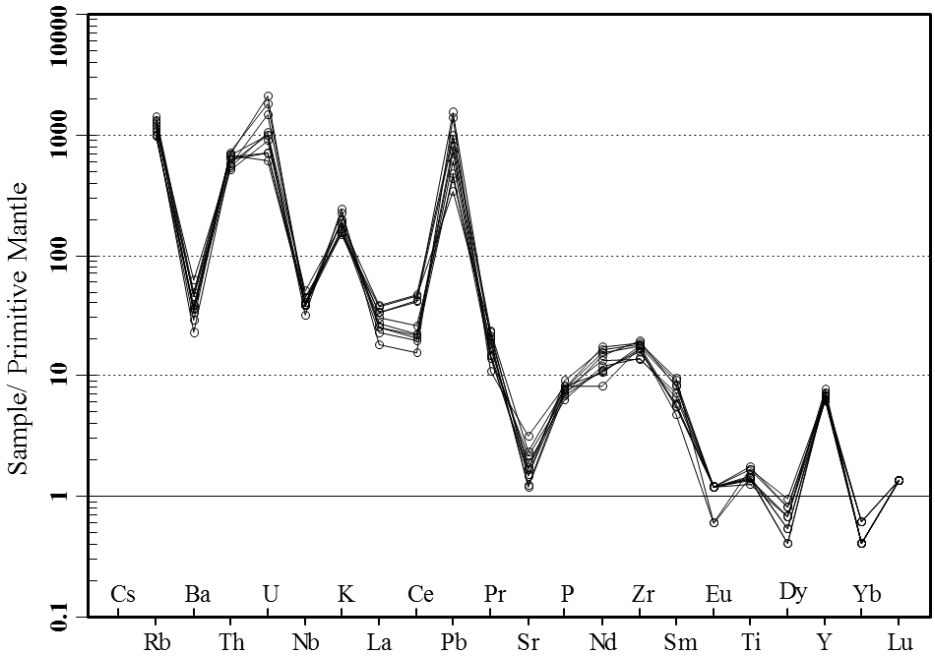

Figure 4.13 Primitive mantle-normalized trace element diagram of the Tagu Granite (normalizing values from Sun and McDonough, 1989).

CHAPTER V. ORE MINERALOGY AND FLUID INCLUSIONS

5.1 Mineralogy of Sn-W mineralization

At the Tagu tin-tungsten deposit, three ore formation stages are recognized; Oxide ore stage; Sulfide stage; and Supergene stage. Early formed minerals are characterized by oxide ore minerals such as cassiterite and wolframite, followed by sulfide minerals. In the Oxide ore stage, deposition of wolframite appeares somewhat later than cassiterite. Cassiterite occurs as idiomorphic crystals as well as aggregated with wolframite (Figures 5.1A). Most cassiterite is deformed and replaced by wolframite and sulfide minerals such as sphalerite and chalcopyrite (Figures 5.1B).

Most sulfide minerals from the sulfide-bearing vein coexist with mutual intergrowth (Figures 5.1C and D). Covellite from the sulfide-bearing vein replaced the rims of chalcopyrite along the grain boundaries (Figures 5.1E and F). Some sulfide minerals fill the fractures of cassiterite and wolframite. This suggests that cassiterites and wolframite were formed earlier than other sulfide minerals (Figures 5.2 A, B and C). Pyrite is associated with chalcopyrite and arsenopyrite and oxide ore minerals. It has mutual intergrowth with other sulfide minerals such as chalcopyrite, sphalerite, and molybdenite. Pyrite is most commonly found as massive aggregates but sometimes as veinlets within massive wolframite.

Sphalerite is found as anhedral, disseminated grains or associated with pyrite, chalcopyrite and molybdenite (Figure 5.2 D). Chalcopyrite which has covellite rims on its margin fills the fractures of wolframite (Figure 5.2E). Cassiterite and wolframite are closely associated with sphalerite in the quartz veins both in the granite and metasedimentary rocks. Sphalerite occurred as replacement minerals along the grain boundaries of cassiterite and

wolframite crystals. Sometimes it encloses chalcopyrite blebs (Figure 5.2F). Consequently, it is inferred that sphalerite occured contemporaneously with chalcopyrite. According to ore microscopic studies, paragenetic sequence representing only the tin-tungsten vein mineralization at the Tagu deposit is shown in Figures 5.3.

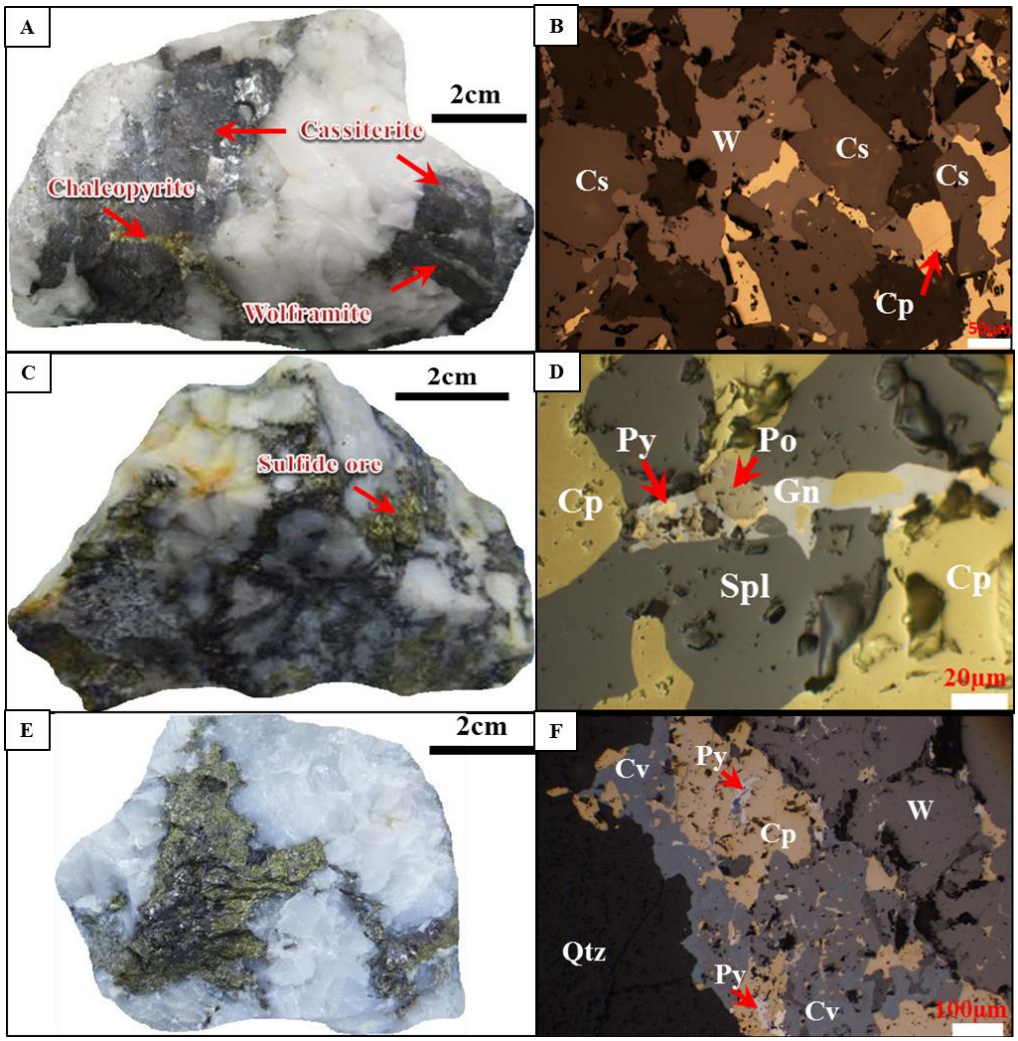

Figure 5.1 Photograph and photomicrographs of Sn-W ore specimen. A. Cassiterite and wolframite mineralized quartz vein (GV-1). B. Cassiterite replaced by wolframite which has fracture filling by chalcopyrite (GV-1). C. Sulfide bearing quartz vein (MV-28). D. Sulfide ores with mutual intergrowth each other (MV-28). E. Sulfide-bearing quartz vein (MV-23). F. Covellite is observed at rims replacing chalcopyrite. Abbreviations: Cs=cassiterite,

W=wolframite, Py=pyrite, Cp=chalcopyrite, Po=pyrrhotite, Spl=sphalerite, Gn=galena, Cv=covellite.

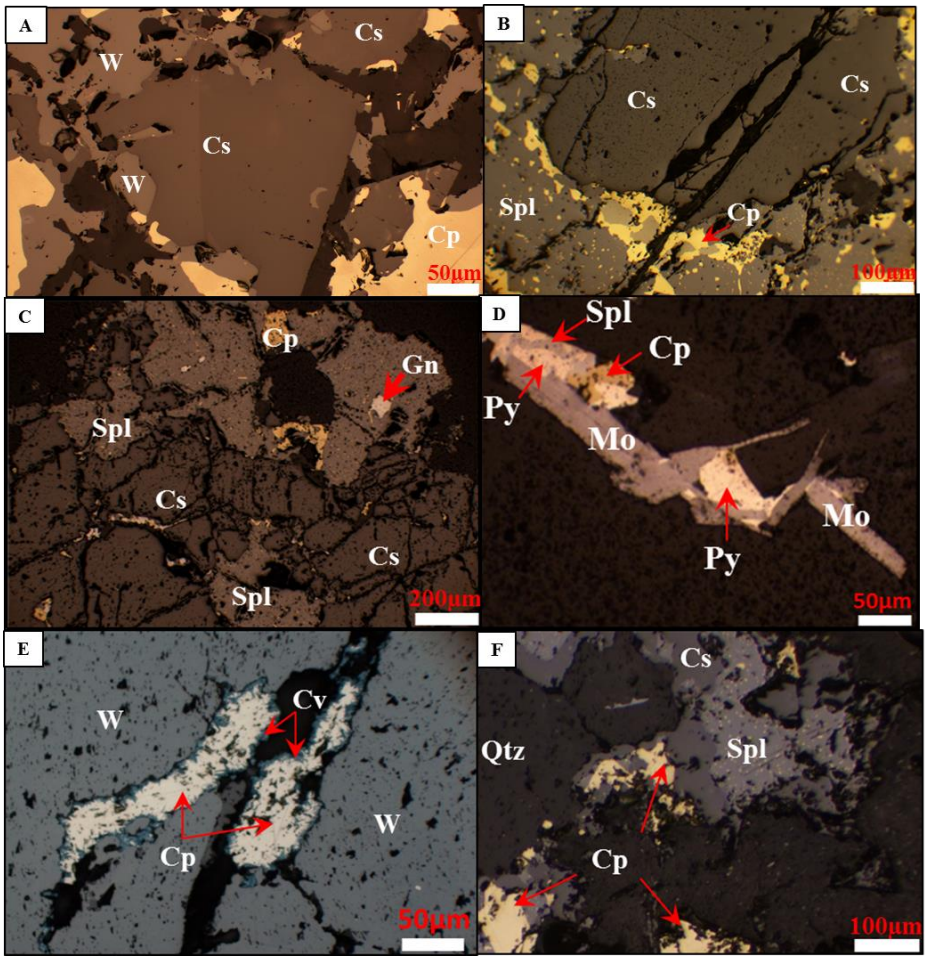

Figure 5.2 Photomicrographs of Sn-W ore specimen. A. Cassiterite replaced by wolframite associated with chalcopyrite (GV-2). B. Cassiterite replaced by sphalerite with chalcopyrite blebs (GV-3). C. Sphalerite with chalcopyrite blebs replacing between the fracture of cassiterite (GV-1). D. Molybdenite associated with other sulfide minerals (Gr-1). E. Chalcopyrite with covellite rims as fracture filling between the fracture of wolframite (MV-23). F. Cassiterite replaced by sphalerite and chalcopyrite (GV-4). Abbreviations:

Qtz=quartz, Cs=cassiterite, W=wolframite, Py=pyrite, Cp=chalcopyrite, Spl=sphalerite, Gn=galena, Cv=covellite, Mo=molybdenite.

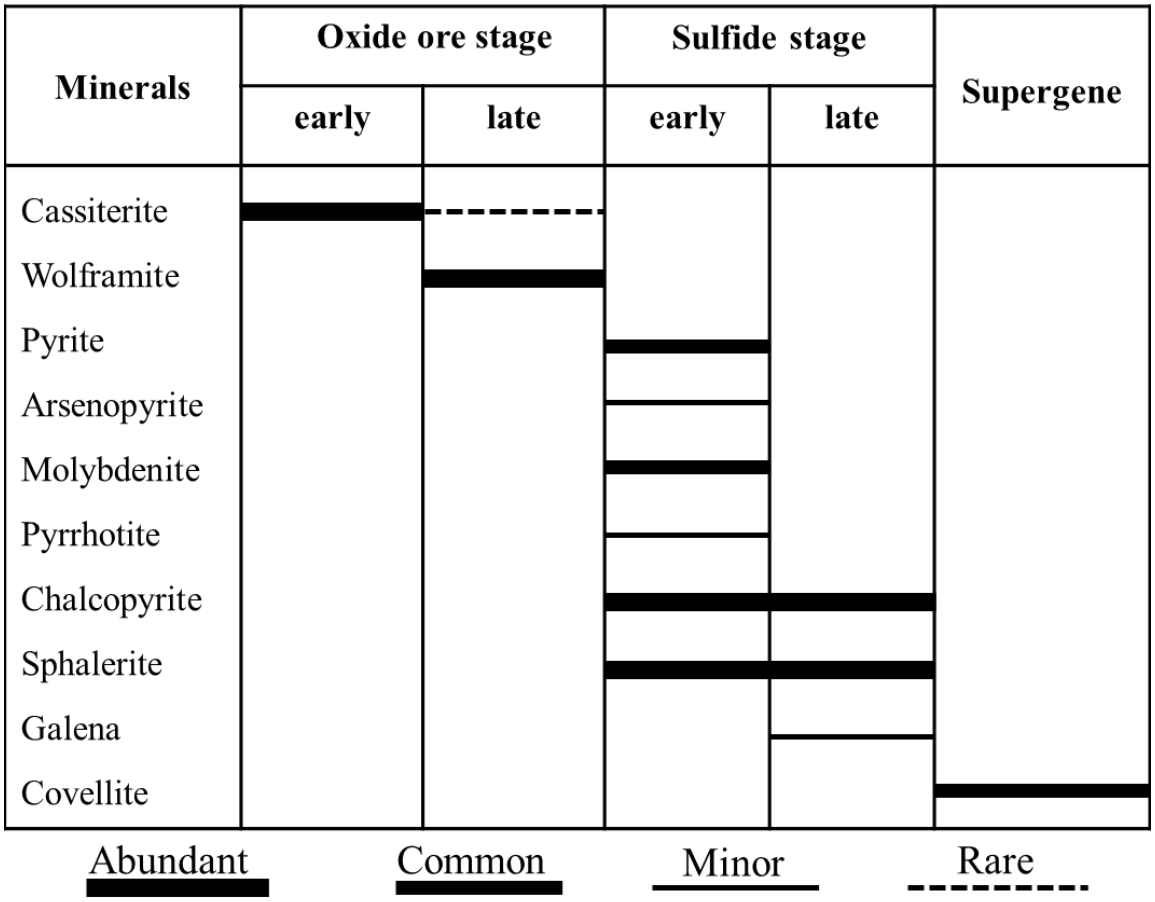

Figure 5.3. Paragenetic sequence of ore mineralization of the Tagu Sn-W deposit, southern Myanmar.

5.2 Fluid inclusion studies

The homogenization temperatures of 295 fluid inclusions, in seven vein quartz samples, were determined in the present study. Detailed microthermometric data is presented mainly for fluid inclusions in the veins quartz in granite and metasedimentary rocks.

5.2.1 Fluid inclusion petrography

The distribution pattern, shape, size, and phase content of fluid inclusions within the quartz crystals were examined to determine the fluid inclusion types and to distinguish primary and secondary inclusions as described by Roedder (1984). The fluid inclusions are commonly distributed in clusters, in isolation and along growth zones, and are considered to be primary in origin (Figures 5.4 A and 5.5 A). The shapes of fluid inclusions are variable, and they are spheroidal, irregular, polygonal, rounded, sub-rounded and elongated (Figure 5.4 B, C and 5.5 B, C). The size of fluid inclusions ranges from 5 μm to 30 μm in diameter. According to the phase relations observed at room temperature, fluid inclusions from the Tagu tin-tungsten deposit can be classified into three types.

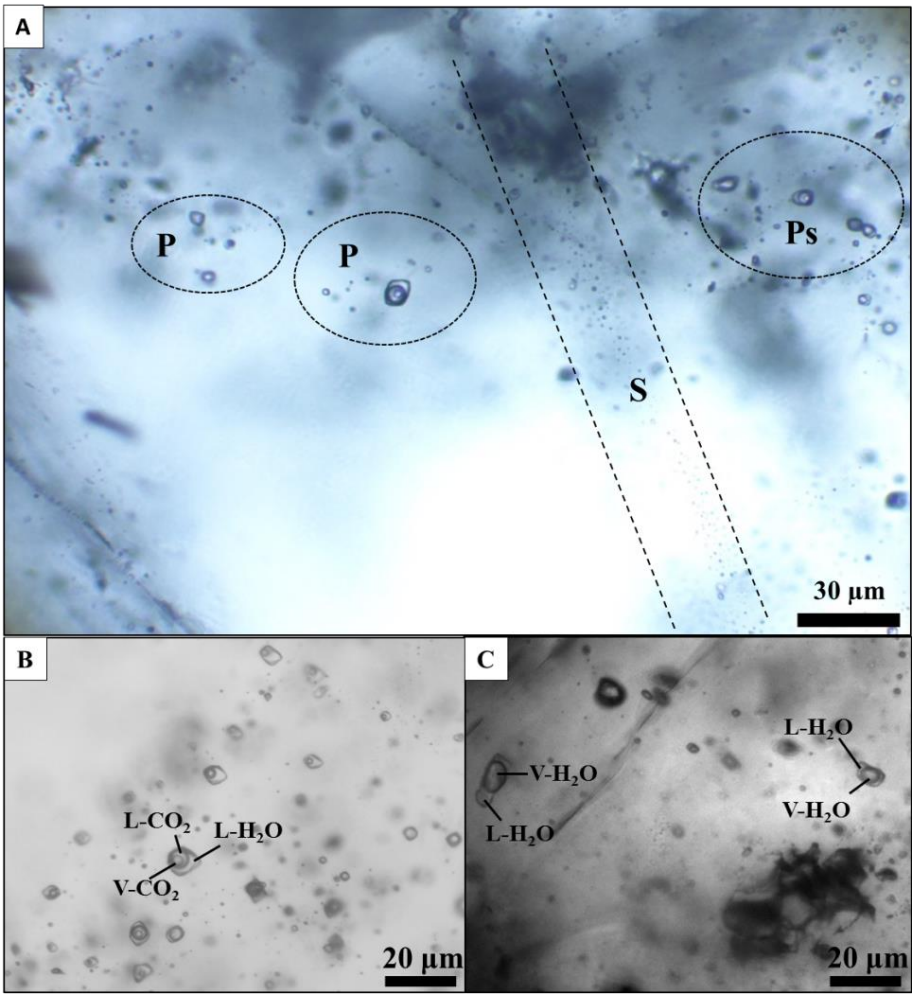

Figure 5.4. Fluid inclusion petrography of mineralized quartz veins at the Tagu tin-tungsten deposit. A. Fluid inclusions are distributed in clusters, in isolation and along growth zones as a primary and fluid inclusions are in healed fractures as a secondary fluid in granitic rock (GV-1). B. Three phase fluid inclusions are found as rounded and sub-rounded inclusions in the mineralized quartz in granitic rocks (GV-2). C. Two phase fluid inclusions are observed as tabular, elongated, rounded and sub-rounded inclusions in the mineralized quartz in granitic rocks (GV-1). Abbreviations: P= primary, S= secondary, Ps= pseudosecondary.

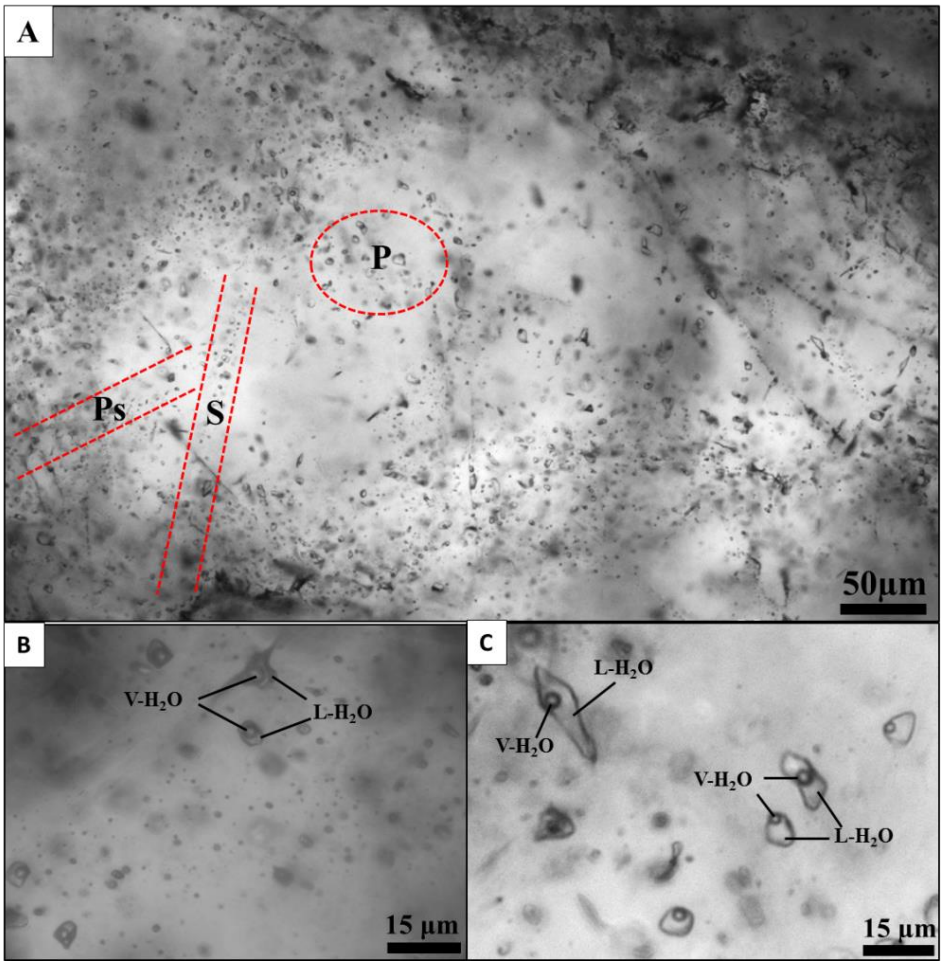

Figure 5.5 Fluid inclusion petrography of mineralized quartz veins at the Tagu tin-tungsten deposit. A. Primary fluid inclusions are distributed in clusters, in isolation and along growth zones, and fluid inclusions of healed fractures are present as secondary inclusions in metasedimentary rock (MV-28). B. Two phase fluid inclusions are found as a rounded and sub-rounded inclusions in the mineralized quartz in metasedimentary rocks (MV-29). C. Two phase fluid inclusions are observed as tabular, rounded and sub-rounded inclusions in the mineralized quartz in metasedimentary rocks (MV-28). Abbreviations: P= primary, S= secondary, Ps= pseudosecondary.

Type-A: Fluid inclusions are liquid-dominated two phase (L+V) at room temperature, occurring as isolated inclusions, clusters and planes of inclusions in milky quartz of tin-tungsten mineralized veins (Figures 5.6B and C). They range in size from 5 to 20 μm and are rounded, sub-rounded, elongated and irregular shapes. They are commonly found in tin-tungsten mineralized vein quartz of metasedimentary rocks and granite.

Type B: Vapor-dominated, two phase (V+L) inclusions at room temperature, occurring as isolated inclusions, clusters and planes of inclusions in milky quartz of tin-tungsten mineralized veins in granite (Figure. 5.6D). They range in size from 5 to 25 μm and are spheroidal, irregular polygonal and irregular shapes. They are the most common inclusion type in quartz of tin-tungsten mineralized quartz veins in granite.

Type-C: At room temperature these fluid inclusions consist of three phases, aqueous liquid + liquid CO_2+ vapor CO_2, with the volume of the CO_2 phase (liquid) varying widely from 60 vol % to 85 vol % (Figures 5.6F and 5.7B). They occur in planes of growth zones in vein quartz. This fluid inclusion is significantly different from other types. They range in size from 10 to 30 μm and are in spheroidal, irregular polygonal and irregular shapes. They were observed only in quartz of the tin-tungsten mineralized veins in granite. However, type-C fluid inclusions with varying volume proportions of the CO_2 phase (liquid), coexisting with type-A and type-B inclusions in groups, without showing any crosscutting relationships are common (Figure. 5.7D).

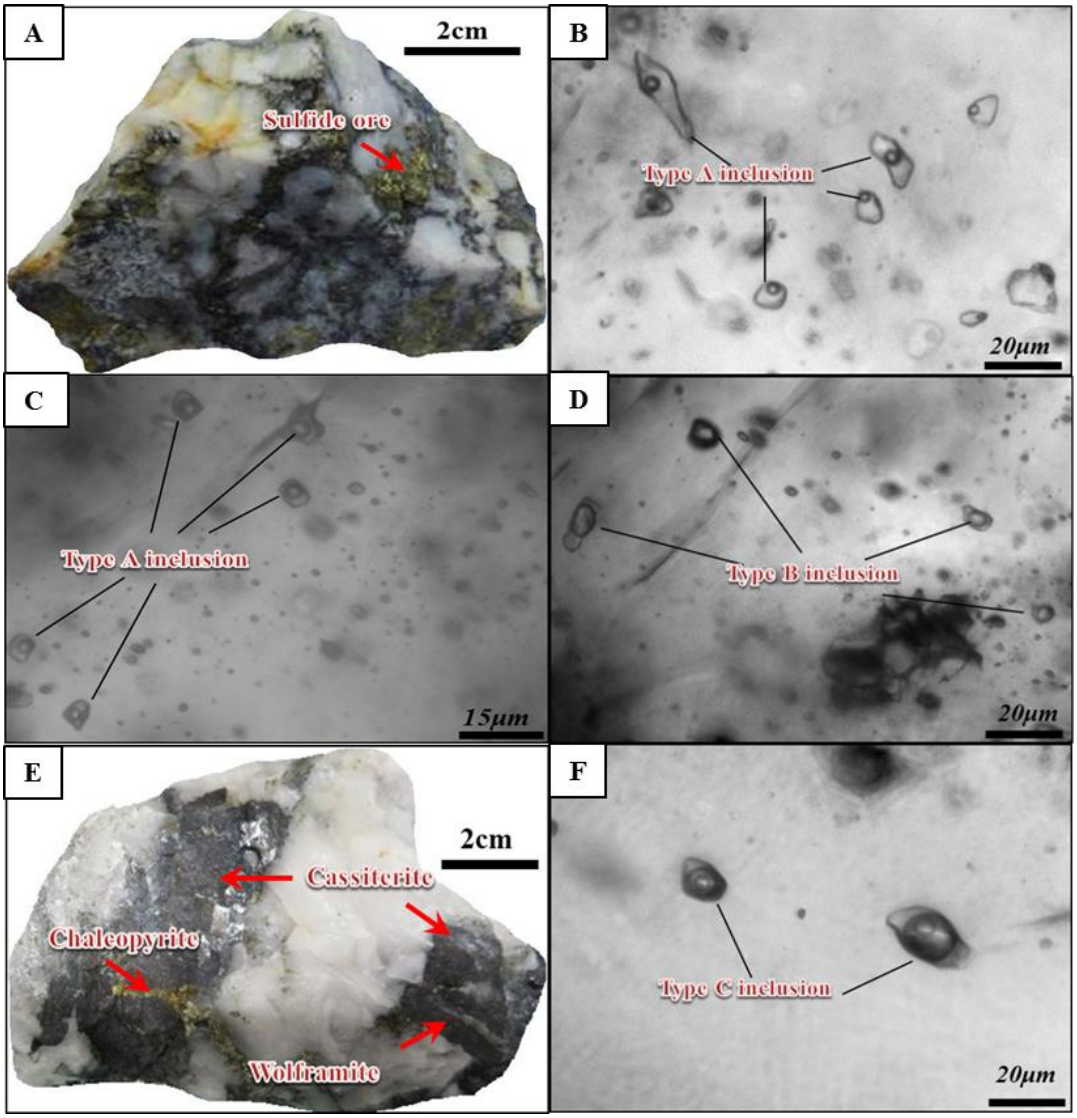

Figure 5.6 Photographs of mineralized quartz veins and photomicrographs of fluid inclusion types of the Tagu Sn-W deposit. A. Sulfide-bearing quartz vein in metasedimentary rock (MV-28). B. Type A fluid inclusions in metasedimentary hosted quartz (MV-28). C. Type A fluid inclusions in quartz vein hosted by metasedimentary rock (MV-29). D. Type B fluid inclusions in quartz vein hosted by granitic rock (GV-3). E. Sn-W bearing quartz vein in granitic rock (GV-1). F. Type C fluid inclusions in quartz vein hosted by granitic rock (GV-1).

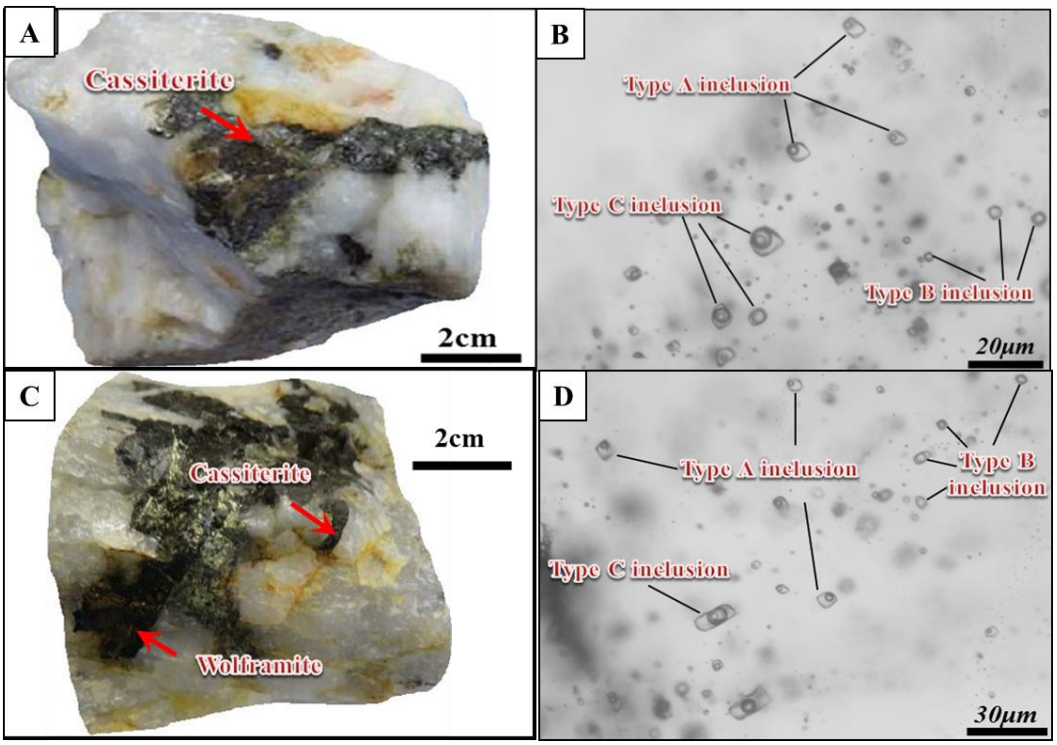

Figure 5.7 Photographs of mineralized quartz veins and photomicrographs of fluid inclusion types of the Tagu Sn-W deposit. A. Sn-W bearing quartz vein in granitic rock (GV-2). B. Type A, B and C fluid inclusions coexisting together within a small area in quartz vein hosted by granitic rock (GV-2). C. Cassiterite and wolframite bearing quartz veins in granite (GV-3). D. Type A, B and C fluid inclusions coexisting together within a small area of the quartz in granite (GV-3).

5.2.2 Microthermometric measurements

The microthermometric data of type-A, type-B and type-C inclusions are listed in Table 5.1. For type-A inclusions, final ice melting temperatures (Tice) vary from -0.6 to -5.2°C, -1.8 to -4.5 °C and -1.9 to -6.1°C for the vein MV-28, MV-23 and MV-4 respectively, and -2.0 to -7.1°C, -1.7 to -6.5°C, -2.6 to -5.9 °C and -1.8 to 5.3°C for vein GV-1, GV-2, GV-3 and GV-4 respectively, with corresponding salinities from 1.1 to 8.1, 3.1

to 7.2 and 3.2 to 9.3 wt. % NaCl equivalent and 2.0 to 7.1, 2.9 to 9.9, 4.3 to 9.1 and 3.1 to 8.3 wt. % NaCl equivalent, respectively (Figures 5.8 B, D, F, H, J, L and N).

The homogenization temperatures of type-A fluid inclusions vary from 140°C to 250°C, 190 to 270°C and 210 to 330°C for the vein MV-28, MV-23 and MV-4, respectively and from 230 to 370°C, 230 to 340°C, 230 to 330°C and 180 to 300°C for veins GV-1, GV-2, GV-3 and GV-4, respectively (Figures 5.8A, C, E, G, I, K and M).

For type-B vapor-rich fluid inclusions, these inclusions homogenized to the liquid phase from 320 to 350°C, 310 to 390°C and 350 to 380°C for vein GV-1, GV-2 and GV-3, respectively and their Tice range from -5.0 to -7.4°C, -4.2 to -8.4°C and -5.1 to -7.5°C , which corresponds to salinities from 7.9 to 11.0, 6.7 to 12.2 and 8.0 to 11.1 wt. % NaCl equivalent, respectively (Figures 5.8I, J, K, L, M and N).

The CO_2 melting temperatures (Tm-CO_2) of CO_2-bearing inclusions mineralized quartz veins in granite range from -59.5°C to -56.8°C, -59.1°C to 57.2 and -58.8°C to -56.9°C for the vein GV-1, GV-2 and GV-3, respectively suggesting that the carbonic phase is dominated by CO_2 with only minor components of other volatiles such as CH_4 and N_2 (Zhichao Zou, 2017). The partial homogenization temperatures (Th-CO_2) of the CO_2 phase into the liquid phase range from 25.1°C to 31.1°C, 25.8°C to 30.8°C and 26.3°C to 30.9°C for the vein GV-1, GV-2 and GV-3, respectively (Table 5.1).

The Th-tot range from 330°C to 405°C, 310°C to 350°C and 270°C to 350°C for vein GV-1, GV-2 and GV-3, respectively. The clathrate melting temperatures (Tm-clath) of type-C fluid inclusions vary from 7.3°C to 9.1°C, 7.1°C to 8.9°C and 7.1°C to 8.6°C for vein GV-1, GV-2 and GV-3, respectively corresponding to salinities ranging from 1.8 to 5.2, 2.2

to 5.6 and 2.8 to 5.6 wt. % NaCl equivalent, respectively (Figures 5.8I, J, K, L, M and N). The type-C, CO_2-bearing inclusions are marked by relatively high Th-tot and lower salinities, than the type-A liquid-rich inclusions and type-B, vapor-rich inclusions (Figure 5.9).

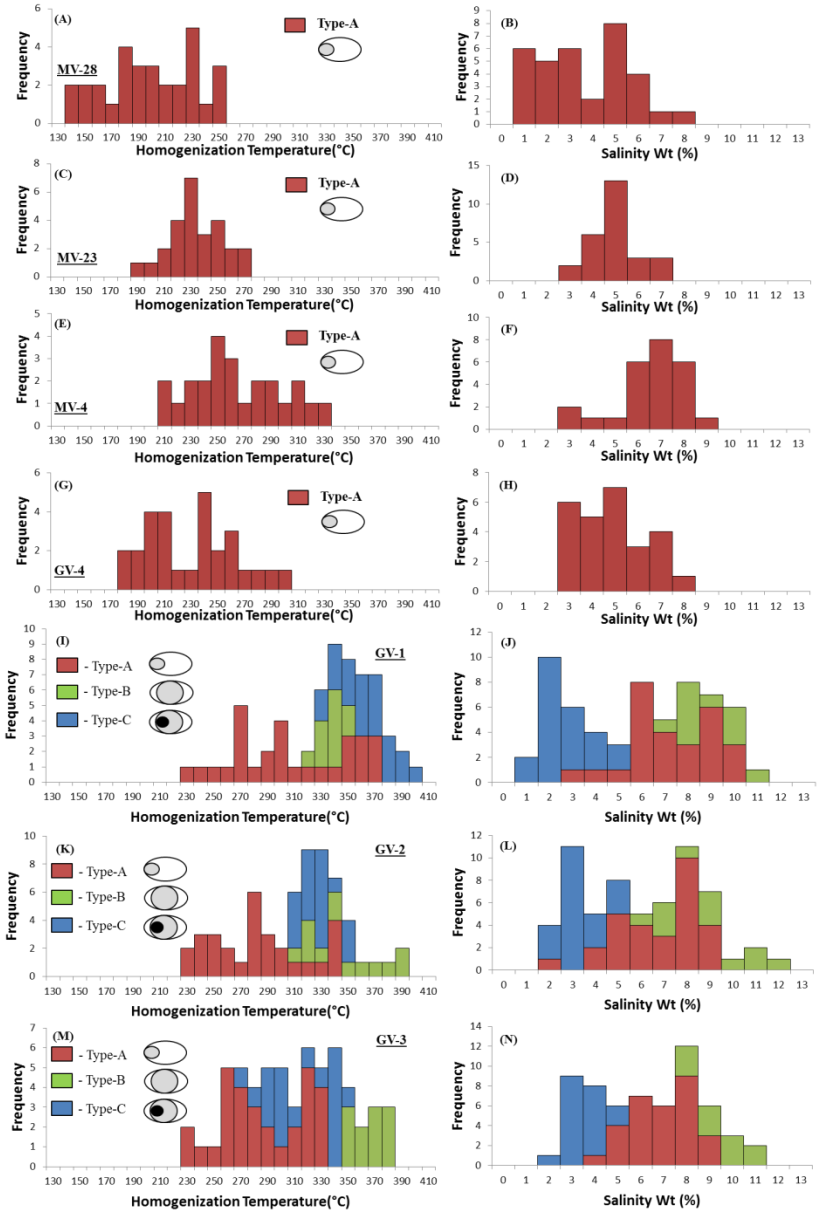

Figure 5.8. Histograms of fluid inclusion microthermometric data of the Tagu Sn-W deposit. (A). Homogenization temperature of type-A fluid inclusions in quartz vein in

metasedimentary rocks from MV-28 and; (B). Salinity of type-A fluid inclusions in quartz vein in metasedimentary rock from MV-28; (C). Homogenization temperature of type-A fluid inclusions in quartz vein in metasedimentary rock from MV-23; (D). Salinity of type-A fluid inclusions in quartz vein in metasedimentary rock from MV-23; (E). Homogenization temperature of type-A fluid inclusions in quartz vein in metasedimentary rock from MV-4; (F). Salinity of type-A fluid inclusions in quartz vein in metasedimentary rock from MV-4; (G) Homogenization temperature of type-A fluid inclusions in quartz vein in granitic rock from GV-4; (H) Salinity of type-A fluid inclusions in quartz vein in granitic rock from GV-4; (I) Homogenization temperature of type-A, type-B and type-C fluid inclusions in quartz vein in granitic rock from GV-1; (J) Salinity of type-A, type-B and type-C fluid inclusions in quartz vein in granitic rock from GV-1; (K) Homogenization temperature of type-A, type-B and type-C fluid inclusions in quartz vein in granitic rock from GV-2; (L) Salinity of type-A, type-B and type-C fluid inclusions in quartz vein in granitic rock from GV-2; (M) Homogenization temperature of type-A, type-B and type-C fluid inclusions in quartz vein in granitic rock from GV-3; (N) Salinity of type-A, type-B and type-C fluid inclusions in quartz vein in granitic rock from GV-3.

Table 5.1. Summary of fluid inclusion types and microthermometric data of the Tagu Sn-W deposit, Southern Myanmar.

Samples	Ore/mineral/ rock type	Type	Tm,CO_2 (°C)	Tm, clath (°C)	Th,CO_2 (°C)	Th (°C)	Tice (°C)	FI (N)	Salinity (wt.% NaCleqv.)
MV-28	Sulfide rich quartz in metasedimentary rock	Type-A				140~250	-0.6~-5.2	33	1.1~8.1
MV-23	Oxide and Sulfide bearing quartz in metasedimentary rock	Type-A				190~270	-1.8~-4.5	27	3.1~7.2
MV-4	Sulfide rich quartz in metasedimentary rock	Type-A				210~330	-1.9~-6.1	25	3.2~9.3
GV-1	Oxide ore rich quartz in granitic rock	Type-A				230~370	-2.0~-7.1	27	3.4~10.6
		Type-B				320~350	-5.0~-7.4	11	7.9~11.0
		Type-C	-59.5~-56.8	7.3~9.1	25.1~31.1	330~400		22	1.8~5.2
GV-2	Oxide ore rich quartz in granitic rock	Type-A				230~340	-1.7~-6.5	30	2.9~9.9
		Type-B				310~390	-4.2~-8.4	12	6.7~12.2
		Type-C	-59.1~-57.2	7.1~8.9	25.8~30.8	310~350		20	2.2~5.6
GV-3	Oxide ore rich quartz in granitic rock	Type-A				230~330	-2.6~-5.9	30	4.3~9.1
		Type-B				350~380	-5.1~-7.5	11	8.0~11.1
		Type-C	-58.8~-56.9	7.1~8.6	26.3~30.9	270~350		19	2.8~5.6
GV-4	Oxide and Sulfide bearing quartz in metasedimentary rock	Type-A				180~300	-1.8~-5.3	28	3.1~8.3

Tm,CO_2—final melting temperature of CO_2; Tm,cla—final melting temperature of CO_2 clathrate; Th,CO_2—partial homogenization temperature of CO_2 inclusions;Th—total homogenization temperature of inclusions; Tice—final ice melting temperature, FI(N)—fluid inclusion number

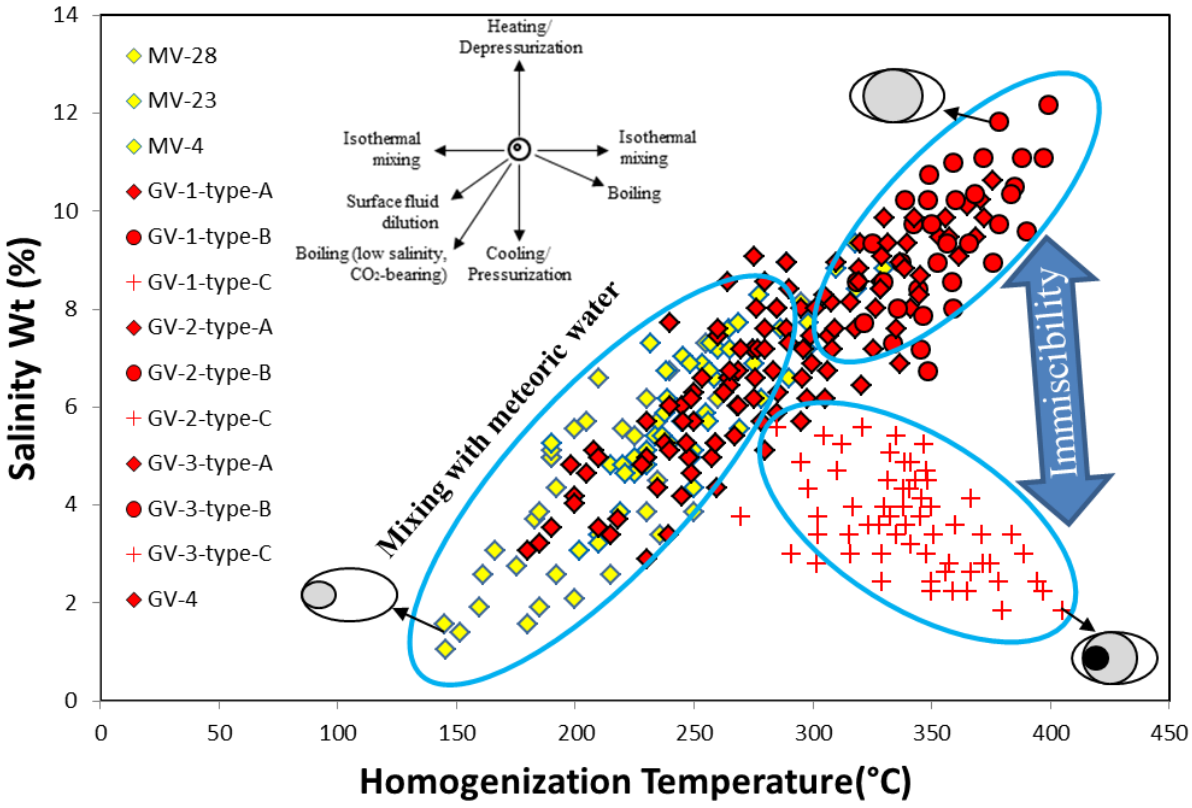

Figure 5.9. Plot of homogenization temperature (Th) vs. salinity of fluid inclusion data from the Tagu Sn-W deposit with typical trends of fluid evolution patterns of Wilkinson (2001).

CHAPTER VI. DISSCUSION AND CONCLUSION

6.1 Disscusions

6.1.1 Petrogenesis of granitic rocks

Strongly peraluminous S-type granite formed from the partial melting of peraluminous clastic sediments are common in the continental collisional zones, even during the Neoarchean time (Yang et al., 2018). The granites of the Tagu tin-tungsten deposit are characterized by the A/CNK [molar Al_2O_3/ ($CaO+Na_2O+K_2O$)] value ranging from 1.17 to 1.41 (Figure. 4.7). The SiO_2 is negatively correlated with Na_2O, MgO, TiO_2, Al_2O_3, K_2O and CaO except for P_2O_5 (Figure. 4.4).

The content of P_2O_5 in highly fractionated S-type granites is high compared to I-type granites (Chappel and White, 1992; Champion and Bultitude, 2013). In the Tagu tin-tungsten deposit, P_2O_5 of biotite granite is slightly increased with SiO_2 contents. It reveals a highly fractionated S-type granitic magma (Figure 4.4G). The Rb-Ba-Sr relationship also exhibits that highly differentiated granite (Figure 4.10). The granites at Tagu are characterized by generally elevated REE contents and LREE enriched pattern with a negative anomaly of Eu (Figure 4.12) which can be produced by either partial melting of a plagioclase-rich source or fractionation of plagioclase, or a combination of both (Cullers and Graf, 1984).

According to the primitive mantle-normalized spider diagram of Sun and Macdonough (1989), the granite at Tagu (Figure 4.13) reveal an enrichment of LILEs such as Rb, K and Pb exhibiting distinct negative anomalies for HFSEs such as Nb, P and Ti. Most of these features such as negative anomaly of Ba, Sr, Nb and Ti and positive anomaly

of Rb, Th and La abundances are compatible to those of typical crustal melt, e.g. S-type granites in North Queensland (Champion and Bultitude, 2013) and Himalayan leucogranite (Harris et. al., 1986). Enrichment of Rb, Th and Y are also consistent with crustal derivation. Thus, parental magma of the granites at Tagu may have been derived from the crustal source.

6.1.2 Tectonic implication

The tin granites of WGP of Southeast Asia were derived from the partial melting of the crust (Gardiner et al., 2016; Aung Zaw Myint et al., 2017a and b) and the emplacement of these granites has been variously related to the Cretaceous–Paleogene subduction and Himalayan orogeny-related collision (Gardiner et al., 2015b), back-arc extension, or post-collisional or syncollisional extension related granitic magmatism (Chen et al., 2015; Jiang et al., 2017; Aung Zaw Myint et al., 2017a; Chen et al., 2018).

Gardiner et al. (2016a) considered that tin-tungsten mineralized granites of the MMM Belt intruded the Slate Belt (e.g. at Hermyingyi, Mawchi and Yadanabon). They recorded zircon U-Pb ages of both mineralized and presumed coeval non-mineralized granites within the MMM Belt are largely of Palaeogene age. Their zircon U-Pb ages of 75–50 Ma from granites within the southern MMM Belt suggest that the collsion occurred during Late Cretaceous. Mlynarczyk and Williams-Jones (2005) also noted similar collisional setting at in the metallogeny of the Central Andean Tin Belt.

Mitchell et al. (2012) have proposed that the Slate Belt represents a separate continental fragment which was derived from the Gondwana margin and was accreted onto the western Sibumasu margin, probably during the Jurassic (Mitchell et al., 2015; Ridd,

2016). There is an agreement that by the Early Cretaceous the subduction of the Mesotethys Ocean beneath the western margin of the Slate Belt–Sibumasu Block was responsible for the growth of a continental-margin plutonic arc. This plutonic arc was described by Cobbing et al. (1992) as the 'Western Granite Province of Southeast Asia' and involved emplacement of both I- and S-type granites during the Early and Late Cretaceous–Eocene. The S-type granites occur in various settings that are generally related to plate convergence. Perhaps the best constrained are the S-type granites that clearly formed because of the collision of India and Asia (Christiansen and Keith, 1996). Moreover, many S-types are synkinematic. These suggest that S-type granites are syn-collisional granites (Christiansen and Keith, 1996), as in the geochemical classification of Pearce et al. (1984).

The granite of the Tagu deposit is characterized as highly fractionated, peraluminous, and exhibiting a tectonic signature of syn-collisional granites, which confirms that they were emplaced during the collision following the westward subduction of West Myanmar Terrane beneath Sibumasu during the Cretaceous to Paleogene (Khin Zaw, 1990, 2017; Schwartz et al., 1995; Mitchell et al., 2012; Gardiner et al., 2016a).

6.1.3 Comparison with other tin-bearing granites

The granites at Tagu fall within the field of tin-bearing granites of Stemprok and Sulcek, (1969) (Figure 6.1). Generally, geochemical characteristics of the granites at Tagu are similar with other tin-bearing granite throughout the world, for instance, Hatapang granite of Sumatra (Clark and Stephens, 1987) and Canadian granites (Liverton, 1990). These tin-tungsten granites are also highly differentiated and S-type affinity. The negative anomalies of Ba, Sr and Ti are also the characteristics of Canadian granites (Liverton, 1990).

The Rb/Sr-Sr variation diagram demonstrates that the granite at Tagu lies in the tin-bearing zone and it is similar to that of granites at Hermyingyi, Mawchi and Pilok. In this diagram the distribution pattern of tin-barren I-type granites of Loei and Chanthaburi, tin-barren S-type granite of Rayong and Thai-Myanmar border range and tin-bearing granies of Pilok, Hermyingyi, Mawchi and Tagu (Lehmann and Mahawat, 1989; Aung Zaw Myint, 2017a; Kyaw Thu Htun, 2019) are plotted (Figure 6.2) and it defines a general fractionation pattern of the different magma series. Moreover the diagram shows that the population of hydrothermally overprinted tin-bearing granites extends the general trend of magmatic differentiation to extreme levels and it also indicates that Rb-Sr system has not been disturbed by fluid from external sources. Furthermore, it also reveals that tin-mineralization is associated with the most fractionated granitic rocks.

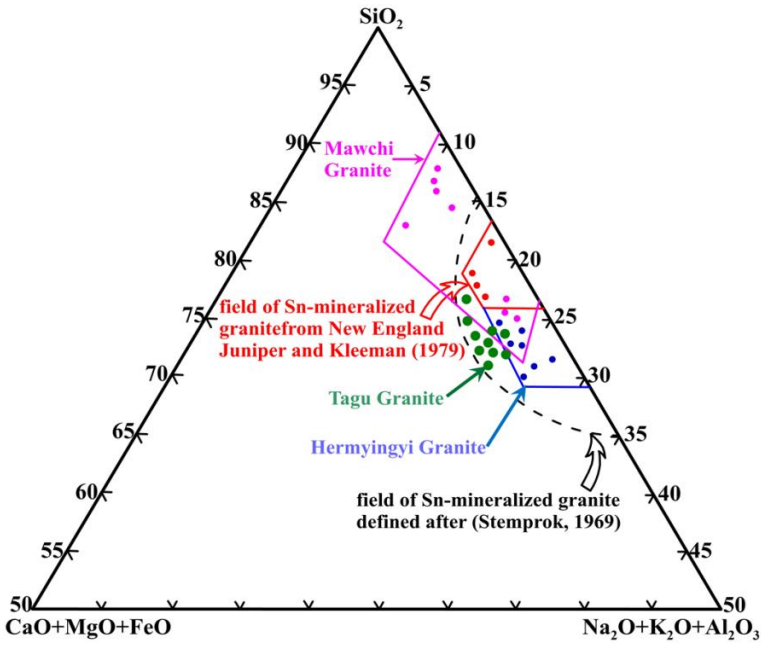

Figure 6.1 Triangular plot showing the Sn-mineralizing granite. The solid red line indicates field of Sn-mineralizing granitoids from New England (Juniper and Kleeman 1979). The dashed line indicates Sn-mineralizing granitoids defined after Stemprok and Sulcek (1969).

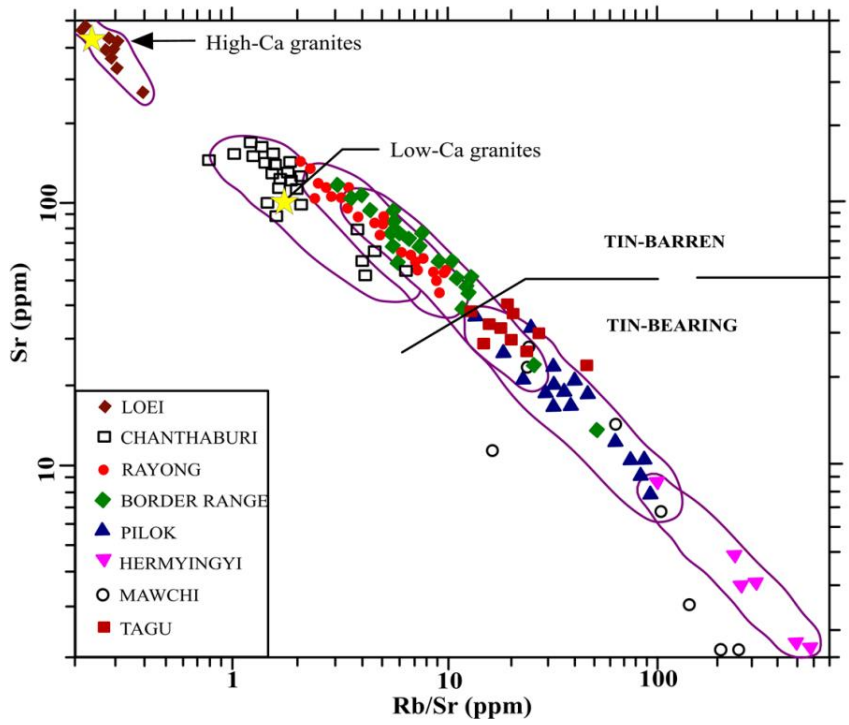

Figure 6.2 Rb/Sr-Sr variation diagram showing the distribution of the granite at Tagu, Hermyingyi, Mawchi and the central Thailand (modified after Lehmann and Mahawat, 1989).

6.1.4 Mechanism of ore formation

In the Tagu tin-tungsten deposit, the two-phase liquid-rich fluid inclusions, vapor-rich fluid inclusions as well as three-phases H_2O-CO_2-NaCl inclusions are the main fluid inclusion types observed in the studied samples. CO_2-bearing inclusions coexisting with vapor-rich and liquid-rich inclusions in groups are generally interpreted as evidence for fluid immiscibility (Roedder, 1984). Khin Zaw (1984) mentioned that tin-tungsten deposits in Myanmar were formed at less than 360°C with a formation temperature of 250°C.

In comparison, the homogenization temperature of the Tagu tin-tungsten deposit ranges from 140 to 405°C. Furthermore, the fluid inclusion assemblage of the Tagu tin-

tungsten deposit is different from those of other well-known world class tin-tungsten deposits in Myanmar such as Mawchi and Hermyingyi (Khin Zaw, 1978; Khin Zaw and Khin Myo Thet, 1983). Aung Zaw Mynit et al. (2018) also indicated that homogenization temperatures range from 175° to 340°C for the Mawchi vein system, in which liquid-rich two-phase (liquid and vapor) primary fluid inclusions are dominant, and H_2O-CO_2 fluid inclusions are absent. Khin Zaw (1984) also reported detailed fluid inclusion studies of the vein quartz and fluorite from the Hermyingyi deposit (Nilar Shwe, 1980) and other deposits. Khin Zaw (1984) shown that majority of inclusions homogenized about 250°C some filling temperatures of vapor-rich inclusions are up to 360 °C. Table 6.1 shows the correlation of mineralogical assemblages, deposit types and fluid inclusion systems between Tagu tin-tungsten deposit and other well-known tin-tungsten deposits in Myanmar such as Mawchi, Hermyingyi and Yadanabon.

In contrast, the temperature and fluid inclusion assemblages of the Tagu tin-tungsten deposit are somewhat different from those of other tin-tungsten deposits which were mentioned above. According to fluid inclusion studies of the above research, no H_2O-CO_2 fluid inclusions were found in granite related tin-tungsten deposits in Myanmar except granite related tin-tungsten deposition of the Tagu area by the present study. The fluid inclusions at the Tagu deposit are characterized by three types of fluid inclusions which are two-phase vapor-rich and two-phase liquid-rich fluid inclusions and three-phase H_2O-CO_2-NaCl fluid inclusions.

According to Wilkinson (2001), Figure 5.9 shows typical fluid evolutions between fluid inclusion types. It is considered that the parent and original hydrothermal fluid at Tagu was probably CO_2-bearing fluid which evolved to two-phase vapor-rich fluid by fluid

immiscibility or phase separation of fluids. Temperature and salinities of two-phase liquid-rich fluid decreased by mixing with meteoric water at the later stage. The ore-forming fluid of the Tagu tin-tungsten deposit most likely underwent fluid immiscibility process during early stage which is characterized by the similar homogenization temperatures and different salinities in a range (Figure 5.9).

The salinities of the vapor-rich inclusions are higher than those of the CO_2-rich inclusions, which may have resulted from CO_2 separation from the fluid as the temperature and pressure decreased. The escape of gases can lead to an increase in the salinity of the residual fluid (Wang et al., 2012). Eventually, the later stage ore fluid was produced by mixing of meteoric water circulated through adjacent metasedimentary rocks (Figure 6.3).

Table 6.1. Comparison of most important W-Sn deposits in southern Myanmar.

No	Deposit	Location (N, E)	Deposit type	Terrane/ fold belt	Host rocks/(ages)	Intrusions/(ages)	Fluid system	Ore mineralogy	References
1.	Mawchi (Sn–W) (mine)	18° 45′ 97° 10	Vein-type	Mogok–Mandalay–Mergui Metamorphic Belt	Meta-Sediments of Mawchi Formation equivalent to Mergui Group	Quartz veins and stockworks in both tourmalinized biotite granite (LA-MC-ICP-MS zircon 42–45 Ma)	H_2O-NaCl	Cassiterite, wolframite,scheelite, pyrite,chalcopyrite, arsenopyrite, molybdenite, galena bismuthinite,sphalerite	Aung Zaw Myint et al. (2017, 2018) Than Htun et al. (2017b)
2.	Hermyingyi (Sn–W) (mine)	14° 15′ 98° 35	Vein-type	Southern Mogok–Mandalay–Mergui Metamorphic Belt	Meta-sedimentary rocks of Mergui Group	Megacrystic biotite granite(U–Pb SHRIMP zircon age of 61.7 ±1.3 Ma; LA-ICP- MS zircon ages of 70.5 ±0.8 Ma and 68.9 ±1.8 Ma)	H_2O-NaCl	Wolframite, cassiterite, molybdenite, pyrite, sphalerite, chalcopyrite, galena, bismuth, bismuthinite	Nilar Shwe (1980), Than Htun et al. (2017b)
3.	Yadanabon (Sn–W) (mine)	11° 17′ 05″ 99° 17′	Vein-type, alluvial	Southern Mogok–Mandalay–Mergui Metamorphic Belt	Meta-sedimentary rocks of Mergui Group	Coarse-grained biotite granite (U–Pb zircon age of 50.3 ± 0.6 Ma)	No data	Wolframite, cassiterite, molybdenite, bismuth, pyrite, bismuthinite, chalcopyrite	Gardiner et al. (2016), Than Htun etal.(2017b)
4.	Tagu (Sn-W) (mine)	12° 14′ 05″ 98° 59′54″	Vein-type	Southern Mogok–Mandalay–Mergui Metamorphic Belt	Meta-sedimentary rocks of Mergui Group	Pophyritic biotite granite	H_2O-CO_2-NaCl	Cassiterite, wolframite,pyrite, arsenopyrite, galena pyrrhotite,molybdenite ,native bismuth, sphalerite,chalcopyrite,	This study

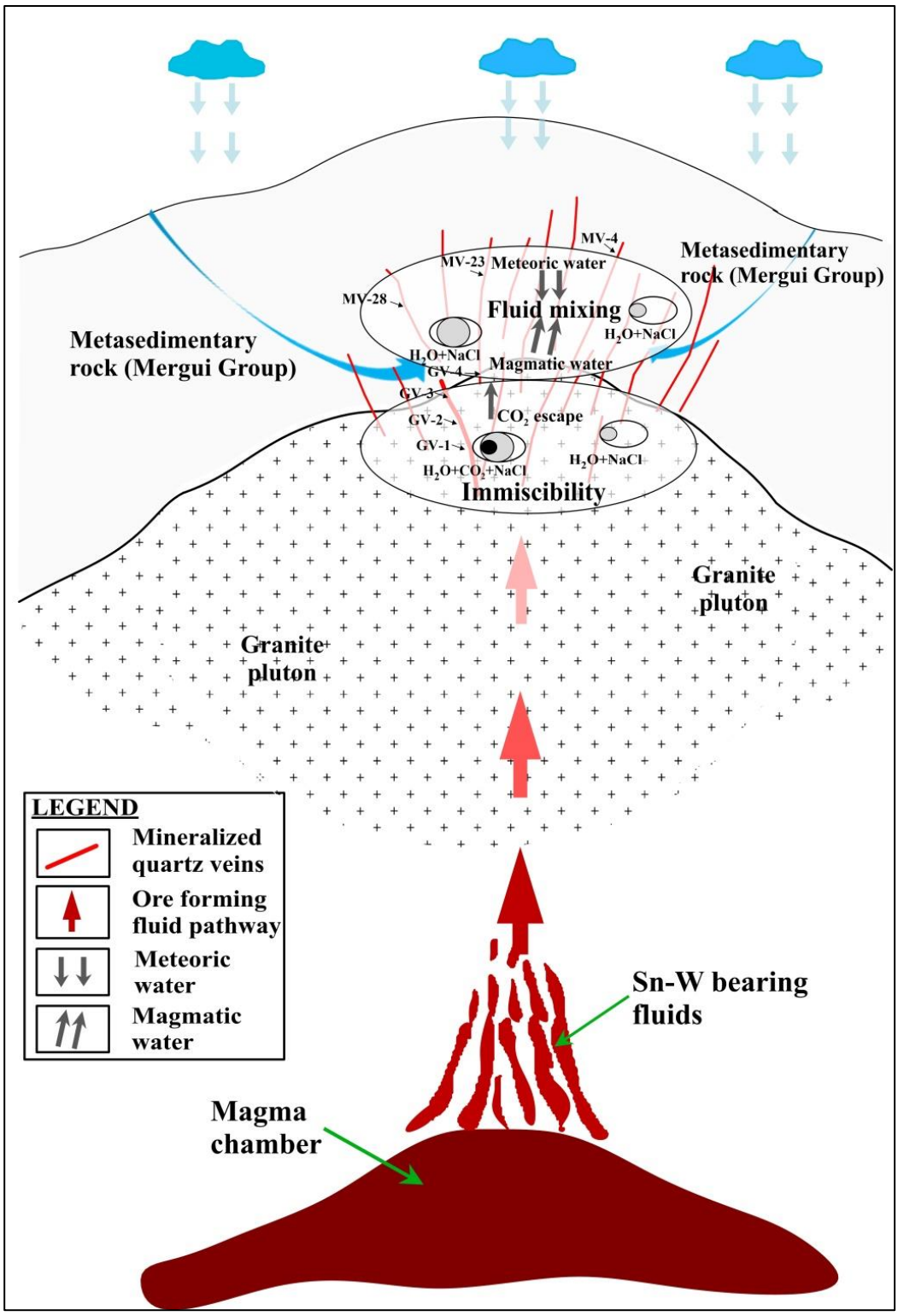

Figure 6.3. Schematic model of ore forming mechanism for the Tagu Sn-W deposit

6.2 Conclusions

The tin-tungsten mineralization in the Western Granite Province (WGP) of Southeast Asia occurred as cassiterite and wolframite bearing pegmatites and greisen-bordered quartz veins in the Dawei (Tavoy) and Myeik (Mergui). These are hosted both by the granites, and also by metasedimentary country rocks (Mergui Group). The majority of tin-tungsten deposits are situated in the Tanintharyi (Tennanserim) region, especially in the Dawei (Tavoy) and Myeik (Mergui) districts, except the largest deposit at Mawchi (Kayah State). The Dawei district has the largest and more important tin–tungsten vein mines, whereas more tin-rich tin–tungsten vein mines, tin vein mines and alluvial tin deposits occur in the Myeik district.

The Tagu tin-tungsten deposit is located in the middle region of the WGP at the southern part of Myanmar. It is one of the largest tin-tungsten deposits in the Mergui district and lies about 59 km southeast of Myeik and 62 km west of the Burma-Thailand border. The mineralized quartz veins are found in the metasedimentary rocks (Carboniferous to Early Permian) and the granitic rocks (Cretaceous to Eocene), and trend NEE-SWW and E-W steeply dipping to the south. More than 30 mineralized quartz veinlets parallel each other are found in metasedimentary rocks, whereas massive mineralized quartz veins are observed in granite. Some mineralized quartz veins are found as a pinch and swell structure and some are broken by the faults during tectonic events in the country rocks of metasedimentary rocks (Mergui Group).

The granites within the WGP of the Southeast Asia are mostly S-type and I-type granites which are related to collision following the westward subduction of the West

Myanmar Terrane beneath Sibumasu during the Cretaceous to Tertiary. Tin-tungsten mineralization in the Central Granitoid Belt of Myanmar occurs dominantly as near-vertical and parallel, greisen bordered, quartz vein-type deposits at the cusps of small granitoid plutons or along the granitoid metasedimentary rocks contact or exclusively in the adjacent metasedimentary country rocks.

The granitic rocks of the Tagu tin-tungsten deposit are mainly composed of quartz, feldspar (plagioclase, orthoclase, and microcline), and mica (muscovite and biotite). They are strongly peraluminous and highly fractionated S-type granites formed in a syn-collisional setting. The granites at Tagu are characterized by generally LREE enriched REE pattern with negative Eu anomaly which can be produced by either partial melting of a plagioclase-rich source or fraction of plagioclase, or a combination of both.

The granitic rocks of the Tagu area show enrichment of LILEs such as Rb, K and Pb and exhibits distinct negative anomalies for HFSEs such as Nb, P and Ti indicating derivation of magma from the lower continental crust. More than that, enrichment of Rb, Th and Y are also consistent with crustal derivation. Thus, S-type granites of Tagu area were produced through partial melting of the metasedimentary rocks and parental magma may have been derived from a crustal source.

Mineralogically, three ore formation stages are recognized as; Oxide ore stage (early); Sulfide stage (late); and Supergene stage. The major tin-tungsten ores are composed of cassiterite and wolframite. They are associated with sulfide minerals such as arsenopyrite, pyrite, chalcopyrite, sphalerite, molybdenite, galena and covellite. Early formed minerals are characterized by cassiterite and wolframite, followed by sulfide minerals. Deposition of

these two major oxide ore minerals may be overlapped, however wolframite appears to be somewhat later than cassiterite. Some sulfide minerals fill the fractures of cassiterite and wolframite. This suggests that cassiterites and wolframite were formed earlier than other sulfide minerals.

Three main types of fluid inclusions were distinguished from the mineralized quartz veins hosted by granite and metasedimentary rocks: type-A: two phases, liquid (L) + vapor (V) aqueous inclusions; type-B: two phases, vapor (V) + liquid (L) vapor-rich inclusions and type-C: three phases, liquid + CO_2-liquid + CO_2-vapor inclusions. Quartz in the veins hosted in granite corresponding with earlier stage mineralization contains type-A, type-B and type-C fluid inclusions, whereas those in the veins hosted in metasedimentary rocks corresponding with later stage mineralization contains only type-A fluid inclusions. The original ascending ore fluid was probably CO_2-bearing fluid which evolved into two phase fluid by immiscibility due to pressure drop in the mineralization channels. The ore-forming fluid of the Tagu tin-tungsten deposit probably underwent a fluid immiscibility process during early stage which is characterized by the similar homogenization temperature and different salinities. They have similar homogenization temperatures and are most likely derived from a magmatic to post-magmatic hydrothermal fluids.

The salinities of the vapor-rich fluid are higher than those of the CO_2-rich fluid, which may have resulted from CO_2 separation from the fluid as the temperature and pressure declined. The escape of gases can lead to an increase in the salinity of the residual fluid (e.g., Collins, 1979). Subsequently, ore fluid that was derived from magmatic water was probably mixed with meteoric water in the later stage which have circulated through the adjacent metasedimentary rocks. The present study strongly suggests that the ore-forming

mechanisms of the Tagu tin-tungsten mineralization is characterized by fluid immiscibility during an early stage and fluid mixing with meteoric water in a subsequent stage at lower temperature.

REFERENCES

1. Ahad, D., 1980. Mineralogical and petrological studies of metamorphic and igneous rocks of the salingi area, Salingi township, MSc thesis, Department of Geology, Rangoon University, Rangoon, Burma (Myanmar).

2. Aung Zaw Myint, Watanabe, K., Yonezu, K., 2013. Relationship between granitoid types and tin mineralization: A review of Tertiary granitoids in central granitoid belt. Myanmar. Proc. Internat. Conf. Georesources and Geological Engineering, Yogyakarta, Indonesia, 13–21.

3. Aung Zaw Myint., Suzaki, R., Yonezu, K., Watanabe, K., Ya, K.Z., 2014. Geology of Dawei Sn-W District, Myanmar. Proc. Internat. Symp. Earth Science and Technology 2014, Fukuoka, Japan, 244–246.

4. Aung Zaw Myint., Yonezu, K., Watanabe, K., 2016. Sn-W mineralization in central granitoid belt of Myanmar. Oral presentation at the annual meeting of Resource Geology Society, Japan.

5. Aung Zaw Myint., Khin Zaw, Ye Myint Swe, Yonezu, K., Cai, Y., Manaka, T., Watanabe, K., 2017a. Geochemistry and geochronology of granites hosting the Mawchi Sn–W deposit, Myanmar: implications for tectonic setting and granite emplacement: In: Barber, A.J., Khin Zaw, Crow, M.J. (Eds.), Myanmar: Geology, Resources and Tectonics. Geological Society of London, Memoir 48, 385–400.

6. Aung Zaw Myint., Yonezu, K., Watanabe, K., 2017b. The tin and tungsten deposits of the Dawei region, with an emphasis on the Wagone and Bawapin deposits. In: Mineral Deposits of Myanmar (Burma) 54. SEG Guide Book, 22–27.

7. Aung Zaw Myint., Yonezu, K., Boyce, A, J., Selby, D., Scherstén, A., Tindell, T., Watanabe, K., Ye Myint Swe., 2018. Stable isotope and geochronological study of the Mawchi Sn-W deposit, Myanmar: Implications for timing of mineralization and ore genesis, Ore Geol. Rev., 95, 663–679.

8. Aye Ko Aung, 2012. The Palaeozoic stratigraphy of Shan Plateau,Myanmar — an up-dated version. J. Myanmar Geosci. Soc. 5, 1–73.

9. Barber, A. J., Crow, M. J., 2003. An Evaluation of Plate Tectonic Models for the Development of Sumatra. Gondwana Research, 6(1), 1-28.

10. Barley, M. E., A. L. Pickard, K. Zaw, P. Rak, and M. G. Doyle., 2003. Jurassic to Miocene magmatism and metamorphism in the Mogok metamorphic belt and the India-Eurasia collision in Myanmar, Tectonics, 22(3), 1019, doi:10.1029/2002TC001398.

11. Barr, S.M., Jamieson, R.A., and Raeside, R.P., 1985. Igneous and metamorphic geology of the Cape Breton Highlands; Geological Association of Canada/Mineralogical Association of Canada 1985 Excursion 10, Guidebook, 48 p.

12. Barr, S.M., Macdonald, A.S., 1991. Toward a late Paleozoic-early Mesozoic tectonic model for Thailand. Thail. J. Geosci. 1, 11–22.

13. Beckinsale, R.D., 1979. Granite magmatism in the tin belt of Southeast Asia, in Atherton, M.P., and Tarney, J., eds., Origin of Granite Batholiths: Geochemical Evidence: Orpington, UK, Shiva Publishing, p. 34–44.

14. Bender, F., (1983) Geology of Burma. Gebruder Borntraeger, Berlin, Stuttgart, 293p.

15. Bignell, J.D. & Snelling, N.J., 1977. Geochronology of Malaysian granites. Overseas Geology and Mineral Resources 47: 70. Institute of Geological Sciences.

16. Bodnar, R. J. (1993) Revised equation and table for determining the freezing point depression of H2O-NaCl solutions. Geochim. Cosmochim. Acta., 57, 683–684.

17. Bozzo A. T., Chen H-S., Kass J. R., and Barduhn A. J. (1973) The properties of the hydrates of chlorine and carbon dioxide. In The Fourth International Symposium on Fresh Water from the Sea, Vol. 3 (eds. A. Delyannis and E. Delyannis), 437-451.

18. Brook, M. and Snelling, N.J., 1976. K/Ar and Rb/Sr age determinations on rocks and minerals from Burma. Inst. Geol. Sci., London, Rep. No. 76/12 (unpublished).

19. Brown, J.C., Heron, A., 1923. The Geology and Ore Deposits of the Tavoy District. Geological Survey of India, 44, 167–354.

20. Brunnschweiler, R.O., 1966. On the geology of the Indoburman ranges. J. Geol. Soc. Aust. 13, 137–194.

21. Chakkaphak, K. R. and Veeraburus, M., 1982. 1:1,000,000 Geological map of Thailand. Dept. Miner. Resource.

22. Champion, D.C., Bultitude, R.J., 2013. The geochemical and Sr–Nd isotopic characteristics of Paleozoic fractionated S-types granites of north Queensland: implications for S-type granite petrogenesis. Lithos, 162–163, 37–56.

23. Chappell, B.W., White, A.J.R., 1992. I- and S-type granites in the Lachlan Fold Belt. Trans. R. Soc. Edinburgh: Earth Sci., 83, 1–26.

24. Chen, J., Niemeijer, A.R., Spiers, C.J., 2017. Microphysically derived expressions for rate-and-state friction parameters, a, b, and Dc . J. Geophys. Res. 122, 9627–9657.

25. Chen, X.C., Zhao, C.H., Zhu, J.J., Wang, X.S., Cui, T., 2018. He, Ar, and S isotopic constraints on the relationship between A-type granites and tin mineralization: A case study of tin deposits in the Tengchong-Lianghe tin belt, southwest China. Ore Geol. Rev., 92, 416–429.

26. Chhibber, H. L., 1934. Geology of Burma, Macmillan and Co., London. 620p.

27. Christiansen, E.H., Keith, J.D., 1996. Trace element systematics in silicic magmas: a metallogenic perspective, in Wyman, D.A., ed., Trace Element Geochemistry of Volcanic Rocks: Applications for Massive Sulphide Exploration: Geological Association of Canada, Short Coures Notes, 12, 115-151.

28. Clarke, M. C G., Beddoe-Stephens, B., 1987. Geochemistry, mineralogy and plate tectonic setting of a late Cretaceous Sn-W granite from Sumatra, Indonesia. Miner. Mag. 51, 371-387.

29. Clegg, E.L.G., 1944. Notes on tin and wolfram in Burma and India. Records of the Geological Survey of India, 76, Economic Bulletin, 15, 1–68.

30. Cobbing, E. J., 2005. Granites. Chapter 5 in Barber, A.J.; Crow, M. J. and Milsom, J. S. (eds.) Sumatra: geology, resources and tectonic evolution. Geological Society of London, memoir 31, 54-62.

31. Cobbing, E.J., 2011. Granitic rocks. In: Ridd, M.F., Barber, A.J., Crow, M.J. (Eds.), The Geology of Thailand. Geological Society of London, pp. 441–457.

32. Cobbing, E.J., Pitfield, P.E.J., Darbyshire, D.P.F., Mallick, D.I.J., 1992. The granites of the South-East Asian tin belt. Overseas Memoir 10, British Geological Survey, London., p. 369.

33. Cobbing, E.J., Mallick, D.I.J., Pitfield, P.E.J., Teoh, L.H., 1986. The granites of the southeast Asian tin belt. J. Geol. Soc. London 143, 537–550.

34. Collins P. L. F., 1979. Gas hydrates in CO_2-bearing fluid inclusions and the use of freezing data for estimation of salinity. Econ. Geol. 74, 1435-1444.

35. Cullers, R.L. and Graf, J.L., 1984. Rare Earth Elements in Igneous Rocks of the Continental Crust: Intermediate and Silicic Rocks-Ore Petrogenesis. In: Henderson, P., Ed., Rare Earth Element Geochemistry, Elsevier, Amsterdam., 275-316.

36. El Bouseily, A.M. and El Sokkary, A.A.,1975. The Relation between Rb, Ba and Sr in Granitic Rocks. Chem. Geol., 16, 207-219.

37. Frost B.R., Arculus R.J., Barnes C.G., Collins W.J., Ellis D.J., Frost C.D., 2001. A geochemical classification of granitic rocks. J Petrol., 42, 2033-2048.

38. Gardiner, N.J., Robb, L.J., Searle, M.P., 2014. The metallogenic provinces of Myanmar. Applied Earth Science 123, 25–38.

39. Gardiner, N.J., Searle, M.P., Morley, C.K., Whitehouse, M.P., Spencer, C.J., Robb, L.J., 2015a. The closure of Palaeo-Tethys in Eastern Myanmar and Northern Thailand: new insights from zircon U–Pb and Hf isotope data. Gondwana Res. http://dx.doi.org/10.1016/j.gr.2015.03.001.

40. Gardiner, N.J., Searle, M.P., Robb, L.J., Morley, C.K., 2015b. Neo-Tethyan magmatism and metallogeny in Myanmar – an Andean analogue? Journal of Asian Earth Sciences. 106, 197–215.

41. Gardiner, N.J., Robb, L.J., Morley, C.K., Searle, M.P., Cawood, P.A., Whitehouse, M.J., Kirkland, C.L., Roberts, N.M.W., Tin Aung Myint., 2016a. The tectonic and

metallogenic framework of Myanmar: a Tethyan mineral system, Ore Geol. Rev., 79, 26–45.

42. Gardiner, N.J., Roberts, N.M.W., Morley, C.K., Searle, M.P., Whitehouse, M.J., 2016b. Did Oligocene crustal thickening precede basin development in northern Thailand? A geochronological reassessment of Doi Inthanon and Doi Suthep, Lithos 240–243, 69–83.

43. Ghose, N.C., Chatterjee, N., Fareeduddin, 2014. A Petrographic Atlas of Ophiolite, An Example From the Eastern India-Asia Collision Zone. Springer, India.

44. Hall, R., 2012. Late Jurassic–Cenozoic reconstructions of the Indonesian region and the Indian Ocean. Tectonophysics, 570–571, 1–41.

45. Hall, R., and Spakman, W., 2015. Mantle structure and tectonic history of SE Asia: Tectonophysics, v. 658, p. 14–45.

46. Hammarstrom, J.M., Bookstrom, A.A. et al. 2013. Porphyry Copper Assessment of Southeast Asia and Melanesia. US Geological Survey, Scientific Investigations Report 2010-5090-D.

47. Harris, N.B.W., Pearce, J.A., Tindle, A.G., 1986. Geochemical characteristics of collision-zone magmatism. In: M.P. Coward and A.C. Ries (Editors), Collision Tectonics. Special Publication, Geological Society., London, 67–81.

48. Hobson, G. V., 1941. A geological survey in parts of Karenni and the Southern Shan States. Geol. Surv. India Mem., 74 (2), 103-105.

49. Hou, Z. Q. and Zhang, H. R., 2015. Geodynamics and Metallogeny of the Eastern Tethyan Metallogenic Domain. Ore Geology Reviews, 70, 346-384.

50. Htun Linn., 2013. Geology and Tin-Tungsten Occurrences at the Eastern Thabawleik Area, Tanintharyi Township, Tanintharyi Region. 68p.

51. Hutchison, C. S., 2007. Geological Evolution of South-east Asia. Geological Society of Malaysia, 407p.

52. Hutchison, C. S., 1973. Tectonic evolution of Sundaland: a Phanerozoic synthesis. Geological Society of Malaysia Bulletin 6, 61-86.

53. Hutchison, C. S., 1975. Ophiolite in Southeast Asia. Geological Society of America Bulletin 86, 797-806.

54. Hutchison, C. S., 1977. Granite emplacement and tectonic subdivision of Peninsular Malaysia. Geological Society of Malaysia Bulletin 9, 187-207.

55. Hutchison, C. S., 1978. Southeast Asian tin granitoids of contrasting tectonic setting. Journal of the Physics of the Earth 26, supplement, S221-S232.

56. Hutchison, C.S., Taylor, D., 1978. Metallogenesis in SE Asia. J. Geol. Soc. Lond. 135, 407–428.

57. Hutchison, C. S., 1983. Multiple Mesozoic Sn-W-Sb granitoids of Southeast Asia. Roddick, J. A. (ed.) Circum-Pacific plutonic terranes. Geological Society of America memoir 159, 35-60.

58. Imai, N.; Terashima, S.; Itoh, S.; Ando, A. 1994 compilation of analytical data for minor and trace elements in seventeen GSJ geochemical reference samples, "Igneous rock series". Geostand. Newsl. 1995, 19, 135–213.

59. Irvine, T.N.,and Baragar., 1971. W.R.A. A guide chemical classification of the common volcanic rock.Canada, J. Earth Sci, 8, 523–548.

60. Jiang, H., Li, W.Q., Jiang, S.Y., Wang, H., Wei, X.P., 2017. Geochronological, geochemical and Sr Nd-Hf isotopic constraints on the petrogenesis of Late Cretaceous A-type granites from the Sibumasu Block, Southern Myanmar, SE Asia. Lithos. 268, 32–47.

61. Juniper, D. N and Kleeman, J. D., 1979. Geochemical characterization of some tin-mineralizing granites of New South Wales. J Geochem Explor. 11, 321-333.

62. Khin Zaw., 1978. Fluid inclusion studies on the Hermyingyi W-Sn deposit, southern Burma: Regional Conf. Geology Mineral Resources Southeast Asia, 3rd, Bangkok 1978, Proc., p. 393-397.

63. Khin Zaw., 1984. Geology and geothermometry of vein-type W-Sn deposits at Pennaichaung and Yetkanzintaung Prospects, Tavoy Township, Tennasserim Division, Southern Burma. Min., Deposita 19, 138-144.

64. Khin Zaw, Khin Myo Thet., 1983. A note on a fluid inclusion study of tin-tungsten mineralization at Mawchi Mine, Kayah State, Burma. Econ Geol., 8, 530–534.

65. Khin Zaw., 1990. Geological, petrological and geochemical characteristics of granitoid rocks in Burma; with special reference to the associated W-Sn mineralization and their tectonic setting, J. Southeast Asian Earth Sci., 4, 293-335.

66. Khin Zaw., Meffre, S., Lai, C. k., et al., 2014. Tectonics and Metallogeny of Mainland Southeast Asia- A Review and Contribution. Gondwana Research, 26(1), 5-30.

67. Khin Zaw., 2017. Overview of mineralization styles and tectonic–metallogenic setting in Myanmar: In: Barber, A.J., Khin Zaw, Crow, M.J. (Eds.), Myanmar: Geology, Resources and Tectonics. J Geol Soc, London, Memoir, 48, 532–556.

68. Kyaw Thu and Khin Zaw, 2017. Gem deposits of Myanmar. In: BARBER, A.J., KHIN ZAW & CROW, M.J. (eds) Myanmar: Geology, Resources and Tectonics. Geological Society, London, Memoirs, 48, 497–529,

69. Kyaw Thu Htun, Yonezu, K., Aung Zaw Myint, Tindell, T., Watanabe, K., 2019. Petrogenesis, Ore Mineralogy, and Fluid Inclusion Studies of the Tagu Sn–W Deposit, Myeik, Southern Myanmar. Minerals, 9, 654.

70. La Touche, T.H.D., 1913. Geology of the Northern Shan State, Mem. Geol. Surv. India, 39:1-379.

71. Lehmann, B., Mahawat, C., 1989. Metallogeny of tin in central Thailand. a genetic concept Geology 17, 426-429.

72. Li, H., Aung Zaw Myint, Yonezu, K., Watanabe, K., Tindle, T.J. Algeo, Jing-Hua Wu., 2018. Geochemistry and U–Pb geochronology of the Wagone and Hermyingyi A type granites, southern Myanmar: Implications for tectonic setting, magma evolution and Sn–W mineralization, Ore Geol. Rev., 95, 575–592.

73. Liew, T.-C., 1983. Petrogenesis of the Peninsular Malaysian Granitoid Batholiths [Ph.D. thesis]: Canberra, Australian National University, 291 p.

74. Liu, C. Z., Chung, S. L., Wu, F. Y., et al., 2016. Tethyan Suturing in Southeast Asia: Zircon U-Pb and Hf-O Isotopic Constraints from Myanmar Ophiolites. Geology, 44(4), 344-314.

75. Liu, S. S., Yang, Y. F., Guo, L. N. et al., 2018. Tectonic Characteristics and Metallogeny in Southeast Asia. Geology in China, 45 (5): 863-889.

76. Liverton, T., 1990. Tin-bearing skarns of the ThirtymileRange, NTS sheet 105 C/9: A progress report. In: Yukon Geology, Volume 3, Exploration and Geological Services Division, Yukon Region, Indian and Northern Affairs Canada, p. 52-70.

77. Makoundi, C., Khin Zaw., Large, R. R., Meffre, S., Lai, Chun-kit., Hoe, T. G., 2014. Geology, Geochemistry and Metallogenesis of the Selinsing Gold Deposit, Central Malaysia. Gondwana Research, 26(1), 241-261.

78. Metcalfe, I., 1988. Origin and assembly of Southeast Asian continental terranes. In: Audley-Charles, M. G. & Hallam, A. (eds) Gondwana and Tethys. Geological Society, London, Special Publications, 37, 101–118.

79. Metcalfe, I., 2000. The Bentong — Raub Suture Zone. J. Asian Earth Sci. 18, 691–712.

80. Metcalfe, I., 2002. Permian tectonic framework and palaeogeography of SE Asia. J. Asian Earth Sci. 20, 551–566. http://dx.doi.org/10.1016/S 1367-9120(02)00022-6.

81. Metacalfe, I., 2011. Tectonic Framework and Phanerozoic Evolution of Sundaland. Gondwana Research. 19(1), 3-21.

82. Metcalfe, I., 2012. Cold Gondwana to warm Tethys: Late Palaeozoic–Mesozoic evolution of Tibetan and SE Asian continental blocks. 2012 IAGR Annual Convention and 9th International Symposium on Gondwana to Asia, Adelaide, Australia.

83. Metcalfe, I., 2013. Gondwana Dispersion and Asian Accretion: Tectonic and Palaeogeographic Evolution of Eastern Tethys. Journal of Asian Earth Sciences, 66, 1-33.

84. Metcalfe, I., 2017. Tectonic evolution of Sundaland. Bulletin of the Geological Society of Malaysia, Volume 63, June 2017, pp. 27 – 60.

85. MGS 2013. Geological Map of Myanmar, Myanmar Geosciences Society, Yangon

86. Middlemost, E.A.K., 1994. Naming Materials in the Magma/ Igneous Rock System. Earth-Science Reviews, 37, 215- 244.

87. Mitchell, A.H.G., 1977. Tectonic settings for the emplacement of Southeast Asian tin granites. Geol. Soc. Malaysia Bull. 9, 123–140.

88. Mitchell, A.H.G., 1981. Phanerozoic plate boundaries in mainland SE Asia, the Himalaya and Tibet. Journal of Geological Society of London 138, 109-122.

89. Mitchell, A.H.G., 1993. Cretaceous-Cenozoic tectonic events in the western Myanmar (Burma)-Assam region. J. Geol. Soc. Lond. 150, 1089–1102.

90. Mitchell, A.H.G., 2017. Geological Belts, Plate Boundaries, and Mineral Deposits in Myanmar. Elsevier 524p.

91. Mitchell, A.H.G., McKerrow,W.S., 1975. Analogous evolution of the Burma Orogen and the Scottish Caledonides. Bull. Geol. Soc. Am. 86, 305–315.

92. Mitchell, A.H.G., Nyunt Htay, Ausa, C., Deiparine, L., Aung Khine, Sein Po, 1999. Geological Settings of Gold Districts in Myanmar. Semin, Pacrim Berli.

93. Mitchell, A.H.G., Ausa, C.A., Deiparine, L., Tin Hlaing, Nyunt Htay, Khine, A., 2004. The Modi Taung–Nankwe gold district, Slate belt, central Myanmar: mesothermal veins in a Mesozoic orogen. J. Asian Earth Sci. 23, 321–341.

94. Mitchell, A. H. G.,Win Myint, Kyi Lynn, Myint Thein Htay, Maw Oo, and Thein Zaw, 2011. Geology of the High Sulfidation Copper Deposits, Monywa Mine, Monywa, Resour. Geol., 61, 1–29.

95. Mitchell, A.H.G., Chung, S.L., Thura, O., Lin, T.H., Hung, C.H., 2012. Zircon U-Pb ages in Myanmar: magmatic–metamorphic events and the closure of a Neo-Tethys ocean? J. Asian Earth Sci. 56, 1–23.

96. Mitchell, A.H.G., Myint Thein Htay, Kyaw Min Htun., 2015. The Medial Myanmar Suture Zone and the Western Myanmar–Mogok foreland. J. Myan. Geosci. Soc., 6, 73–88.

97. Mlynarczyk, Williams-Jones, A.E., 2005. The role of collisional tectonics in the metallogeny of the Central Andean tin belt. Earth Planet Sclet., 240, 656–667.

98. Morley, C. K., 2012. Late Cretaceous-Early Palaeogene Tectonic Development of SE Asia. Earth-Science Reviews. 115(1/2), 37-75.

99. Ng, S.W.P., Chung, S.-L., Robb, L.J., Searle,M.P., Ghani, A.A.,Whitehouse, M.J., Oliver, G.J.H., Sone, M., Gardiner, N.J., Roselee, M.H., 2015. Petrogenesis of Malaysian granitoids in the Southeast Asian tin belt: part 1. Geochemical and Sr–Nd isotopic characteristics. Geol. Soc. Am. Bull. 1–29.

100. Nilar Shwe., 1980. Mineralogical studies of the tin–tungsten deposit of the Hermyingyi Mine, Tavoy. MSc thesis, Department of Geology, Yangon University, Yangon, Myanmar.

101. Passcoe, E.H., 1959. A Manual of Geology of India and Burma: vol. 2, 3rd ed., Govt. of India Press, .Calcutta, p. 485-1343.

102. Pearce J.A., Harris N.B.W., Tindle, A.G., 1984. Trace element discrimination diagrams for the tectonic interpretation of granitic rocks. J Petrol., 25, 956–983

103. Peccerillo A., Taylor S.R., 1976. Geochemistry of Eocene calc-alkaline volcanic rocks from the Kastamonu area, Northern Turkey. Contributions to Mineralogy and Petrology 58, 63–81.

104. Pitcher, W. S. 1983. Granite Type and Tectonic Environment. In: Hsu, K. (Ed.), Mountuin Building Processes. Academic Prcss, London. 19-40.

105. Rao, S.R., 1930. Geology of the Mergui District. Memoirs of the Geological Survey of India, 55, 273–313.

106. Ridd, M.F., 2016. Should Sibumasu be renamed Sibuma? The case for a discrete Gondwana-derived block embracing western Myanmar, upper Peninsular Thailand and NE Sumatra. J. Geol. Soc, London 173, 249–264.

107. Roedder, E., 1984. Fluid inclusions. Rev. Miner., 12, 644p.

108. Schwartz, M.O., Rajah, S.S., Askury, A.K., Putthapiban, P., Djaswadi, S., 1995. The Southeast Asian tin belt. Earth-Science Reviews 38, 95-293.

109. Searle, D. L., and B. T. Haq., 1964. The Mogok belt of Burma and its relationship to the Himalayan orogeny, Proc. Int. Geol. Congr.,22, 132 – 161.

110. Searle, M.P., Whitehouse, M.J., Robb, L.J., Ghani, A.A., Hutchison, C.S., Sone, M., Ng, S.W.-P., Roselee, M.H., Chung, S.-L., Oliver, G.J.H., 2012. Tectonic evolution of the Sibumasu–Indochina terrane collision zone in Thailand and Malaysia: constraints from new U–Pb zircon chronology of SE Asian tin granitoids. Journal of the Geological Society 169, 489–500.

111. Searle,M.P., Morley, C.K., Waters, D.J., Gardiner, N.J., Kyi Htun, Robb, L.J., 2016. Tectonics of the Mogok Metamorphic Belt, Myanmar (Burma) and its correlations from the East Himalayan Syntaxis to the Malay Peninsula. In: Barber, A.J., Khin Zaw, Crow, M.J., Rangin, C. (Eds.), Myanmar: Geology, Resources and Tectonics. The Geological Society, London.

112. Sengör, A. M. C., 1987. Tectonics of the Tethysides: Orogenic Collage Development in a Collisional Setting. Annual Review of Earth and Planetary Sciences, 15(1), 213-244.

113. Sethu Rama Rao, S., 1930. The geology of the Mergui district. Mem. Geol. Sum. India 55, 1-62.

114. Shand, S.J., 1943. The eruptive rocks: 2nd edition, John Wiley, New York, 444 p.

115. Simons, W. J. F., et al., 2007. A decade of GPS in Southeast Asia: Resolving Sundaland motion and boundaries, J. Geophys. Res., 112, B06420.

116. Sone, M., Metcalfe, I., 2008. Parallel Tethyan sutures in mainland Southeast Asia: new insights for Palaeo-Tethys closure and implications for the Indosinian orogeny. Comptes Rendus Geosci. 340, 166–179.

117. Stauffer, P. H.,1983. Unraveling the mosaic of Paleozoic crustal blocks in Southeast Asia. Geologische Rundschau 72, 1061-1080.

118. Stauffer, P. H. and Lee Chai Peng., 1986. Late Paleozoic glacial marine facies in Southeast Asia and its implications. Geological society of Malaysia bulletin 20 363-397.

119. Stemprok, M. and Sulcek, Z., 1969. Geochemical profile through an ore-bearing lithium granite Econ. Geol. 64, 392-404.

120. S.-s. Sun., W.F. McDonough., 1989. Chemical and isotopic systematics of oceanic basalts: implications for mantle composition and processes. Geological Society, London, Special Publications. 42, 313-345.

121. Teggin, D.E., 1975. The granites of northern Thailand. Unpub. Ph.D. thesis, Univ. Manchester.

122. Than Htun, Than Htay, Khin Zaw., 2017. Tin–tungsten deposits of Myanmar. In: Barber, A.J., Khin Zaw, Crow, M.J. (Eds.), Myanmar: Geology, Resources and Tectonics. J. Geol. Soc, London, Memoirs, 48, 625–647.

123. Tin Aye and Kyaw Nyein., 1966. Review of tin and tungsten deposits of Burma. First Burma Research Congress, Rangoon, Burma, 39–73.

124. UNDP, 1978. Geology and Exploration Geochemistry of the Pinlebu-Banmauk Area, Sagaing Division, Northern Burma. United Nations Geological Survey and Exploration Project, New York.

125. Wang, X.D., Ni, P., Yuan, S.D., Wu, S.H., 2012. Fluid inclusion studies of the Huangsha quartz–vein type tungsten deposit, Jiangxi Province. Acta Petrol. Sinica 28, 122–132.

126. Wilkinson, J.J., 2001. Fluid inclusions in hydrothermal ore deposits. Lithos 55, 229–272

127. Yang, X.M., Drayson, D., and Polat, A., 2018. S-type granites in the western Superior Province: a marker of Archean collision zones. Canadian Journal of Earth Sciences. 1-28.

128. Zhichao Zou., Zhang, J. R., Hu, R. Z., 2017. Geology, fluid inclusions, and isotopic geochemistry of the Jinman sediment-hosted copper deposit in the Lanping Basin, China. Resource Geology 67, 384-398.

129. Zi, J.W., Cawood, P.A., Fan, W.M.,Wang, Y.J., Tohver, E., McCuaig, T.C., Peng, T.P., 2012. Triassic collision in the Paleo-Tethys Ocean constrained by volcanic activity in SWChina. Lithos 144-145, 145–160.